Section 5 Time Dependent Processes

Chapter 14

The interaction of a molecular species with electromagnetic fields can cause transitions to occur among the available molecular energy levels (electronic, vibrational, rotational, and nuclear spin). Collisions among molecular species likewise can cause transitions to occur. Time-dependent perturbation theory and the methods of molecular dynamics can be employed to treat such transitions.

I. The Perturbation Describing Interactions With Electromagnetic Radiation

The full N-electron non-relativistic Hamiltonian H discussed earlier in this text involves the kinetic energies of the electrons and of the nuclei and the mutual coulombic interactions among these particles

$$H = \Sigma_{a=1,M} (- \hbar^2/2m_a) \quad {}_a{}^2 + \Sigma_j \ [(- \hbar^2/2m_e) \quad {}_j{}^2 - \Sigma_a \ Z_a e^2/r_{j,a}]$$

$$+ \Sigma_{j<k} \ e^2/r_{j,k} \ + \Sigma_{a<b} \ Z_a \ Z_b \ e^2/R_{a,b}.$$

When an electromagnetic field is present, this is not the correct Hamiltonian, but it can be modified straightforwardly to obtain the proper H.

A. The Time-Dependent Vector **A(r**,t**)** Potential

The only changes required to achieve the Hamiltonian that describes the same system in the presence of an electromagnetic field are to replace the momentum operators $\mathbf{P}_a$ and $\mathbf{p}_j$ for the nuclei and electrons, respectively, by ($\mathbf{P}_a$ - Z_a e/c $\mathbf{A}(R_a,t)$) and ($\mathbf{p}_j$ - e/c $\mathbf{A}(r_j,t)$). Here Z_a e is the charge on the a^{th} nucleus, -e is the charge of the electron, and c is the speed of light.

The vector potential **A** depends on time t and on the spatial location **r** of the particle in the following manner:

$$\mathbf{A}(\mathbf{r},t) = 2 \ \mathbf{A}_o \cos (\omega t - \mathbf{k} \cdot \mathbf{r}).$$

The circular frequency of the radiation ω (radians per second) and the wave vector **k** (the magnitude of **k** is $|\mathbf{k}| = 2\pi/\lambda$, where λ is the wavelength of the light) control the temporal

and spatial oscillations of the photons. The vector $\mathbf{A}_o$ characterizes the strength (through the magnitude of $\mathbf{A}_o$) of the field as well as the direction of the **A** potential; the direction of propagation of the photons is given by the unit vector $\mathbf{k}/|\mathbf{k}|$. The factor of 2 in the definition of **A** allows one to think of $\mathbf{A}_0$ as measuring the strength of both $\exp(i(\omega t - \mathbf{k}\cdot\mathbf{r}))$ and $\exp(-i(\omega t - \mathbf{k}\cdot\mathbf{r}))$ components of the $\cos(\omega t - \mathbf{k}\cdot\mathbf{r})$ function.

B. The Electric $\mathbf{E}(\mathbf{r},t)$ and Magnetic $\mathbf{H}(\mathbf{r},t)$ Fields

The electric $\mathbf{E}(\mathbf{r},t)$ and magnetic $\mathbf{H}(\mathbf{r},t)$ fields of the photons are expressed in terms of the vector potential **A** as

$$\mathbf{E}(\mathbf{r},t) = -\,1/c\;\partial\mathbf{A}/\partial t = \omega/c\;2\,\mathbf{A}_o \sin(\omega t - \mathbf{k}\cdot\mathbf{r})$$

$$\mathbf{H}(\mathbf{r},t) = \quad \mathbf{x}\;\mathbf{A} = \mathbf{k}\;\mathbf{x}\;\mathbf{A}_o\;2\sin(\omega t - \mathbf{k}\cdot\mathbf{r}).$$

The **E** field lies parallel to the $\mathbf{A}_o$ vector, and the **H** field is perpendicular to $\mathbf{A}_o$; both are perpendicular to the direction of propagation of the light $\mathbf{k}/|\mathbf{k}|$. **E** and **H** have the same phase because they both vary with time and spatial location as $\sin(\omega t - \mathbf{k}\cdot\mathbf{r})$. The relative orientations of these vectors are shown below.

C. The Resulting Hamiltonian

Replacing the nuclear and electronic momenta by the modifications shown above in the kinetic energy terms of the full electronic and nuclear-motion hamiltonian results in the following additional factors appearing in H:

$$H_{int} = \Sigma_j \{ (ie\hbar/m_e c)\,\mathbf{A}(r_j,t)\cdot \nabla_j + (e^2/2m_e c^2)\,|\mathbf{A}(r_j,t)|^2 \}$$

$$+ \Sigma_a \{ (iZ_a e\hbar/m_a c)\,\mathbf{A}(R_a,t)\cdot \nabla_a + (Z_a^2 e^2/2m_a c^2)\,|\mathbf{A}(R_a,t)|^2 \}.$$

These so-called interaction perturbations H_{int} are what induces transitions among the various electronic/vibrational/rotational states of a molecule. The one-electron additive nature of H_{int} plays an important role in determining the kind of transitions that H_{int} can induce. For example, it causes the most intense electronic transitions to involve excitation of a single electron from one orbital to another (recall the Slater-Condon rules).

II. Time-Dependent Perturbation Theory

A. The Time-Dependent Schrödinger Equation

The mathematical machinery needed to compute the rates of transitions among molecular states induced by such a time-dependent perturbation is contained in time-dependent perturbation theory (TDPT). The development of this theory proceeds as follows. One first assumes that one has in-hand all of the eigenfunctions $\{\Phi_k\}$ and eigenvalues $\{E_k^0\}$ that characterize the Hamiltonian H^0 of the molecule in the absence of the external perturbation:

$$H^0\,\Phi_k = E_k^0\,\Phi_k.$$

One then writes the time-dependent Schrödinger equation

$$i\hbar\,\partial\Psi/\partial t = (H^0 + H_{int})\,\Psi$$

in which the full Hamiltonian is explicitly divided into a part that governs the system in the absence of the radiation field and H_{int} which describes the interaction with the field.

B. Perturbative Solution

By treating H^0 as of zeroth order (in the field strength $|\mathbf{A}_0|$), expanding Ψ order-by-order in the field-strength parameter:

$$\Psi = \Psi^0 + \Psi^1 + \Psi^2 + \Psi^3 + \ldots,$$

realizing that H_{int} contains terms that are both first- and second- order in $|\mathbf{A}_0|$

$$H^1_{int} = \Sigma_j \{ (ie\hbar/m_e c)\, \mathbf{A}(r_j,t) \cdot \quad _j \}$$

$$+ \Sigma_a \{ (i Z_a e\hbar/m_a c)\, \mathbf{A}(R_a,t) \cdot \quad _a \},$$

$$H^2_{int} = \Sigma_j \{ (e^2/2m_e c^2)\, |\mathbf{A}(r_j,t)|^2 \}$$

$$+ \Sigma_a \{ (Z_a^2 e^2/2m_a c^2)\, |\mathbf{A}(R_a,t)|^2 \},$$

and then collecting together all terms of like power of $|\mathbf{A}_0|$, one obtains the set of time-dependent perturbation theory equations. The lowest order such equations read:

$$i\hbar\, \partial\Psi^0/\partial t = H^0\, \Psi^0$$

$$i\hbar\, \partial\Psi^1/\partial t = (H^0\, \Psi^1 + H^1_{int}\, \Psi^0)$$

$$i\hbar\, \partial\Psi^2/\partial t = (H^0\, \Psi^2 + H^2_{int}\, \Psi^0 + H^1_{int}\, \Psi^1).$$

The zeroth order equations can easily be solved because H^0 is independent of time. Assuming that at $t = -\infty$, $\Psi = \psi_i$ (we use the index i to denote the initial state), this solution is:

$$\Psi^0 = \Phi_i \exp(-i E_i^0 t/\hbar).$$

The first-order correction to Ψ^0, Ψ^1 can be found by (i) expanding Ψ^1 in the complete set of zeroth-order states $\{\Phi_f\}$:

$$\Psi^1 = \Sigma_f\, \Phi_f <\Phi_f|\Psi^1> = \Sigma_f\, \Phi_f\, C_f^1,$$

(ii) using the fact that

$$H^0\, \Phi_f = E_f^0\, \Phi_f,$$

and (iii) substituting all of this into the equation that Ψ^1 obeys. The resultant equation for the coefficients that appear in the first-order equation can be written as

$$i \hbar \partial C_f^1/\partial t = \Sigma_k \{E_k^0 C_k^1 \delta_{f,k} \} + \langle \Phi_f | H^1_{int} | \Phi_i \rangle \exp(- i E_i^0 t / \hbar),$$

or

$$i \hbar \partial C_f^1/\partial t = E_f^0 C_f^1 + \langle \Phi_f | H^1_{int} | \Phi_i \rangle \exp(- i E_i^0 t / \hbar).$$

Defining

$$C_f^1 (t) = D_f^1(t) \exp (- i E_f^0 t / \hbar),$$

this equation can be cast in terms of an easy-to-solve equation for the D_f^1 coefficients:

$$i \hbar \partial D_f^1/\partial t = \langle \Phi_f | H^1_{int} | \Phi_i \rangle \exp(i [E_f^0 - E_i^0] t / \hbar).$$

Assuming that the electromagnetic field $\mathbf{A}(\mathbf{r},t)$ is turned on at t=0, and remains on until t = T, this equation for D_f^1 can be integrated to yield:

$$D_f^1(t) = (i \hbar)^{-1} \int_0^T \langle \Phi_f | H^1_{int} | \Phi_i \rangle \exp(i [E_f^0 - E_i^0] t' / \hbar) \, dt' .$$

C. Application to Electromagnetic Perturbations

1. First-Order Fermi-Wentzel "Golden Rule"

Using the earlier expressions for H^1_{int} and for $\mathbf{A}(\mathbf{r},t)$

$$H^1_{int} = \Sigma_j \{ (ie \hbar /m_e c) \mathbf{A}(r_j,t) \cdot \quad _j \}$$

$$+ \Sigma_a \{ (i Z_a e \hbar /m_a c) \mathbf{A}(R_a,t) \cdot \quad _a \}$$

and

$$2\,\mathbf{A}_o \cos(\omega t - \mathbf{k}\cdot\mathbf{r}) = \mathbf{A}_o \{ \exp[i(\omega t - \mathbf{k}\cdot\mathbf{r})] + \exp[-i(\omega t - \mathbf{k}\cdot\mathbf{r})] \},$$

it is relatively straightforward to carry out the above time integration to achieve a final expression for $D_f^1(t)$, which can then be substituted into $C_f^1(t) = D_f^1(t) \exp(-i E_f^0 t / \hbar)$ to obtain the final expression for the first-order estimate of the probability amplitude for the molecule appearing in the state $\Phi_f \exp(-i E_f^0 t / \hbar)$ after being subjected to electromagnetic radiation from t = 0 until t = T. This final expression reads:

$$C_f^1(T) = (i\hbar)^{-1} \exp(-i E_f^0 T / \hbar) \{ \langle \Phi_f | \Sigma_j \{ (ie\hbar / m_e c) \exp[-i\mathbf{k}\cdot\mathbf{r}_j] \mathbf{A}_0 \cdot \quad_j$$

$$+ \Sigma_a (i Z_a e \hbar / m_a c) \exp[-i\mathbf{k}\cdot\mathbf{R}_a] \mathbf{A}_0 \cdot \quad_a | \Phi_i \rangle \} \quad \frac{\exp(i(\omega + \omega_{f,i}) T) - 1}{i(\omega+\omega_{f,i})}$$

$$+ (i\hbar)^{-1} \exp(-i E_f^0 T / \hbar) \{ \langle \Phi_f | \Sigma_j \{ (ie\hbar / m_e c) \exp[i\mathbf{k}\cdot\mathbf{r}_j] \mathbf{A}_0 \cdot \quad_j$$

$$+ \Sigma_a (i Z_a e \hbar / m_a c) \exp[i\mathbf{k}\cdot\mathbf{R}_a] \mathbf{A}_0 \cdot \quad_a | \Phi_i \rangle \} \quad \frac{\exp(i(-\omega + \omega_{f,i}) T) - 1}{i(-\omega+\omega_{f,i})},$$

where

$$\omega_{f,i} = [E_f^0 - E_i^0] / \hbar$$

is the resonance frequency for the transition between "initial" state Φ_i and "final" state Φ_f.

Defining the time-independent parts of the above expression as

$$\alpha_{f,i} = \langle \Phi_f | \Sigma_j \{ (e / m_e c) \exp[-i\mathbf{k}\cdot\mathbf{r}_j] \mathbf{A}_0 \cdot \quad_j$$

$$+ \Sigma_a (Z_a e / m_a c) \exp[-i\mathbf{k}\cdot\mathbf{R}_a] \mathbf{A}_0 \cdot \quad_a | \Phi_i \rangle,$$

this result can be written as

$$C_f^1(T) = \exp(-i E_f^0 T / \hbar) \{ \alpha_{f,i} \frac{\exp(i(\omega + \omega_{f,i}) T) - 1}{i(\omega+\omega_{f,i})}$$

$$+ \alpha_{f,i} \frac{\exp(-i(\omega - \omega_{f,i}) T) - 1}{-i(\omega-\omega_{f,i})} \} .$$

The modulus squared $|C_f^1(T)|^2$ gives the probability of finding the molecule in the final state Φ_f at time T, given that it was in Φ_i at time t = 0. If the light's frequency ω is tuned close to the transition frequency $\omega_{f,i}$ of a particular transition, the term whose denominator contains $(\omega - \omega_{f,i})$ will dominate the term with $(\omega + \omega_{f,i})$ in its denominator. Within this "near-resonance" condition, the above probability reduces to:

$$|C_f^1(T)|^2 = 2\,|\alpha_{f,i}|^2\,\frac{(1 - \cos((\omega - \omega_{f,i})T))}{(\omega - \omega_{f,i})^2}$$

$$= 4\,|\alpha_{f,i}|^2\,\frac{\sin^2(1/2(\omega - \omega_{f,i})T)}{(\omega - \omega_{f,i})^2} \quad .$$

This is the final result of the first-order time-dependent perturbation theory treatment of light-induced transitions between states Φ_i and Φ_f.

The so-called sinc- function

$$\frac{\sin^2(1/2(\omega - \omega_{f,i})T)}{(\omega - \omega_{f,i})^2}$$

as shown in the figure below is strongly peaked near $\omega = \omega_{f,i}$, and displays secondary maxima (of decreasing amplitudes) near $\omega = \omega_{f,i} + 2\,n\,\pi/T$, n = 1, 2, ... In the $T \rightarrow \infty$ limit, this function becomes narrower and narrower, and the area under it

$$\int_{-\infty}^{\infty} \frac{\sin^2(1/2(\omega - \omega_{f,i})T)}{(\omega - \omega_{f,i})^2}\,d\omega \quad = T/2 \int_{-\infty}^{\infty} \frac{\sin^2(1/2(\omega - \omega_{f,i})T)}{1/4T^2(\omega - \omega_{f,i})^2}\,d\omega T/2$$

$$= T/2 \int_{-\infty}^{\infty} \frac{\sin^2(x)}{x^2}\,dx \quad = \pi\,T/2$$

grows with T. Physically, this means that when the molecules are exposed to the light source for long times (large T), the sinc function emphasizes ω values near $\omega_{f,i}$ (i.e., the on-resonance ω values). These properties of the sinc function will play important roles in what follows.

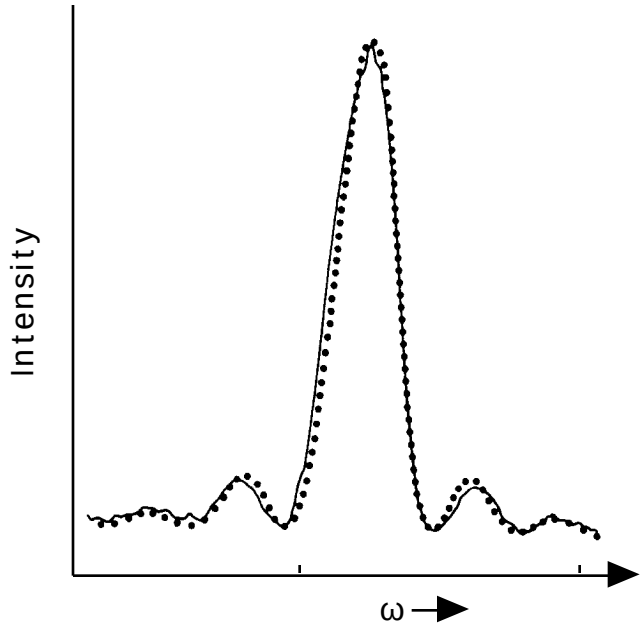

In most experiments, light sources have a "spread" of frequencies associated with them; that is, they provide photons of various frequencies. To characterize such sources, it is common to introduce the spectral source function $g(\omega)\, d\omega$ which gives the probability that the photons from this source have frequency somewhere between ω and $\omega+d\omega$. For narrow-band lasers, $g(\omega)$ is a sharply peaked function about some "nominal" frequency ω_o; broader band light sources have much broader $g(\omega)$ functions.

When such non-monochromatic light sources are used, it is necessary to average the above formula for $|C_f^1(T)|^2$ over the $g(\omega)\, d\omega$ probability function in computing the probability of finding the molecule in state Φ_f after time T, given that it was in Φ_i up until t = 0, when the light source was turned on. In particular, the proper expression becomes:

$$|C_f^1(T)|^2_{ave} = 4\,|\alpha_{f,i}|^2 \int_0^\infty g(\omega)\, \frac{\sin^2(1/2(\omega - \omega_{f,i})T)}{(\omega - \omega_{f,i})^2}\, d\omega$$

$$= 2\,|\alpha_{f,i}|^2\,T \int_{-\infty}^{\infty} g(\omega)\,\frac{\sin^2(1/2(\omega - \omega_{f,i})T)}{1/4T^2(\omega - \omega_{f,i})^2}\,d\omega T/2\ .$$

If the light-source function is "tuned" to peak near $\omega = \omega_{f,i}$, and if $g(\omega)$ is much broader (in ω-space) than the $\frac{\sin^2(1/2(\omega - \omega_{f,i})T)}{(\omega - \omega_{f,i})^2}$ function, $g(\omega)$ can be replaced by its value at the peak of the $\frac{\sin^2(1/2(\omega - \omega_{f,i})T)}{(\omega - \omega_{f,i})^2}$ function, yielding:

$$|C_f^1(T)|^2_{ave} = 2\,g(\omega_{f,i})\,|\alpha_{f,i}|^2\,T \int_{-\infty}^{\infty} \frac{\sin^2(1/2(\omega - \omega_{f,i})T)}{1/4T^2(\omega - \omega_{f,i})^2}\,d\omega T/2$$

$$= 2\,g(\omega_{f,i})\,|\alpha_{f,i}|^2\,T \int_{-\infty}^{\infty} \frac{\sin^2(x)}{x^2}\,dx = 2\,\pi\,g(\omega_{f,i})\,|\alpha_{f,i}|^2\,T.$$

The fact that the probability of excitation from Φ_i to Φ_f grows linearly with the time T over which the light source is turned on implies that the rate of transitions between these two states is constant and given by:

$$R_{i,f} = 2\,\pi\,g(\omega_{f,i})\,|\alpha_{f,i}|^2\ ;$$

this is the so-called first-order Fermi-Wentzel "**golden rule**" expression for such transition rates. It gives the rate as the square of a transition matrix element between the two states involved, of the first order perturbation multiplied by the light source function $g(\omega)$ evaluated at the transition frequency $\omega_{f,i}$.

2. Higher Order Results

Solution of the second-order time-dependent perturbation equations,

$$i\,\hbar\,\partial\Psi^2/\partial t = (H^0\,\Psi^2 + H^2_{int}\,\Psi^0 + H^1_{int}\,\Psi^1)$$

which will not be treated in detail here, gives rise to two distinct types of contributions to the transition probabilities between Φ_i and Φ_f:

i. There will be matrix elements of the form

$$<\Phi_f | \Sigma_j \{ (e^2/2m_ec^2) |\mathbf{A}(r_j,t)|^2 \} + \Sigma_a \{ (Z_a^2e^2/2m_ac^2) |\mathbf{A}(R_a,t)|^2 \} |\Phi_i>$$

arising when H^2_{int} couples Φ_i to Φ_f.

ii. There will be matrix elements of the form

$$\Sigma_k <\Phi_f | \Sigma_j \{ (ie\hbar/m_ec) \mathbf{A}(r_j,t) \cdot \quad_j \} + \Sigma_a \{ (i Z_ae\hbar/m_ac) \mathbf{A}(R_a,t) \cdot \quad_a \} |\Phi_k>$$

$$<\Phi_k | \Sigma_j \{ (ie\hbar/m_ec) \mathbf{A}(r_j,t) \cdot \quad_j \} + \Sigma_a \{ (i Z_ae\hbar/m_ac) \mathbf{A}(R_a,t) \cdot \quad_a \} |\Phi_i>$$

arising from expanding $H^1_{int}\ \Psi^1 = \Sigma_k\ C_k^1\ H^1_{int}|\Phi_k>$ and using the earlier result for the first-order amplitudes C_k^1. Because both types of second-order terms vary quadratically with the $\mathbf{A}(\mathbf{r},t)$ potential, and because $\mathbf{A}$ has time dependence of the form $\cos(\omega t - \mathbf{k}\cdot\mathbf{r})$, these terms contain portions that vary with time as $\cos(2\omega t)$. As a result, transitions between initial and final states Φ_i and Φ_f whose transition frequency is $\omega_{f,i}$ can be induced when $2\omega = \omega_{f,i}$; in this case, one speaks of coherent two-photon induced transitions in which the electromagnetic field produces a perturbation that has twice the frequency of the "nominal" light source frequency ω.

D. The "Long-Wavelength" Approximation

To make progress in further analyzing the first-order results obtained above, it is useful to consider the wavelength λ of the light used in most visible/ultraviolet, infrared, or microwave spectroscopic experiments. Even the shortest such wavelengths (ultraviolet) are considerably longer than the spatial extent of all but the largest molecules (i.e., polymers and biomolecules for which the approximations we introduce next are not appropriate).

In the definition of the essential coupling matrix element $\alpha_{f,i}$

$$\alpha_{f,i} = <\Phi_f | \Sigma_j \ (e/m_ec) \exp[-i\mathbf{k}\cdot\mathbf{r}_j] \mathbf{A}_0 \cdot \quad_j$$

$$+ \Sigma_a \ (Z_ae/m_ac) \ \exp[-i\mathbf{k}\cdot\mathbf{R}_a] \mathbf{A}_0 \cdot \quad_a \ | \Phi_i>,$$

the factors exp [-i$\mathbf{k}\cdot\mathbf{r}_j$] and exp[-i $\mathbf{k}\cdot\mathbf{R}_a$] can be expanded as:

$$\exp[-i\mathbf{k}\cdot\mathbf{r}_j] = 1 + (-i\mathbf{k}\cdot\mathbf{r}_j) + 1/2\,(-i\mathbf{k}\cdot\mathbf{r}_j)^2 + \ldots$$

$$\exp[-i\,\mathbf{k}\cdot\mathbf{R}_a] = 1 + (-i\,\mathbf{k}\cdot\mathbf{R}_a) + 1/2\,(-i\,\mathbf{k}\cdot\mathbf{R}_a)^2 + \ldots \ .$$

Because $|\mathbf{k}| = 2\pi/\lambda$, and the scales of $\mathbf{r}_j$ and $\mathbf{R}_a$ are of the dimension of the molecule, $\mathbf{k}\cdot\mathbf{r}_j$ and $\mathbf{k}\cdot\mathbf{R}_a$ are less than unity in magnitude, within this so-called "long-wavelength" approximation.

1. Electric Dipole Transitions

Introducing these expansions into the expression for $\alpha_{f,i}$ gives rise to terms of various powers in $1/\lambda$. The lowest order terms are:

$$\alpha_{f,i}(E1) = \langle\Phi_f \mid \Sigma_j\,(e/m_e c)\,\mathbf{A}_0\cdot\ \ _j + \Sigma_a\,(Z_a e/m_a c)\,\mathbf{A}_0\cdot\ \ _a \mid \Phi_i\rangle$$

and are called "electric dipole" terms, and are denoted E1. To see why these matrix elements are termed E1, we use the following identity (see Chapter 1) between the momentum operator - i $\hbar$ and the corresponding position operator **r**:

$$_j = -\,(m_e/\hbar^2)\,[\,H,\,\mathbf{r}_j\,]$$

$$_a = -\,(m_a/\hbar^2)\,[\,H,\,\mathbf{R}_a\,].$$

This derives from the fact that H contains $_j$ and $_a$ in its kinetic energy operators (as ^2_a and ^2_j).

Substituting these expressions into the above $\alpha_{f,i}$(E1) equation and using H $\Phi_{i\text{ or }f}$ = $E^0_{i\text{ or }f}\,\Phi_{i\text{ or }f}$, one obtains:

$$\alpha_{f,i}(E1) = (E^0_f - E^0_i)\,\mathbf{A}_0\cdot\ \langle\Phi_f \mid \Sigma_j\ (e/\hbar^2 c)\,\mathbf{r}_j\ + \Sigma_a\,(Z_a e/\hbar^2 c)\ \mathbf{R}_a\ \mid \Phi_i\rangle$$

$$= \omega_{f,i}\ \mathbf{A}_0\cdot\ \langle\Phi_f \mid \Sigma_j\ (e/\hbar c)\,\mathbf{r}_j\ + \Sigma_a\,(Z_a e/\hbar c)\ \mathbf{R}_a\ \mid \Phi_i\rangle$$

$$= (\omega_{f,i}/\hbar c)\,\mathbf{A}_0\cdot\ \langle\Phi_f \mid \mu \mid \Phi_i\rangle,$$

where μ is the electric dipole moment operator for the electrons and nuclei:

$$\mu = \Sigma_j \; e \; \mathbf{r}_j \; + \Sigma_a \; Z_a \, e \;\; \mathbf{R}_a \, .$$

The fact that the E1 approximation to $\alpha_{f,i}$ contains matrix elements of the electric dipole operator between the initial and final states makes it clear why this is called the electric dipole contribution to $\alpha_{f,i}$; within the E1 notation, the E stands for electric moment and the 1 stands for the first such moment (i.e., the dipole moment).

Within this approximation, the overall rate of transitions is given by:

$$R_{i,f} = 2 \, \pi \, g(\omega_{f,i}) \, |\alpha_{f,i}|^2$$

$$= 2 \, \pi \, g(\omega_{f,i}) \, (\omega_{f,i} / \hbar c)^2 \, |\mathbf{A}_0 \cdot \; <\Phi_f \, | \, \mu \, | \, \Phi_i> \, |^2 .$$

Recalling that $\mathbf{E}(\mathbf{r},t) = - \, 1/c \; \partial \mathbf{A}/\partial t = \omega/c \; \mathbf{A}_o \sin (\omega t - \mathbf{k} \cdot \mathbf{r})$, the magnitude of $\mathbf{A}_0$ can be replaced by that of $\mathbf{E}$, and this rate expression becomes

$$R_{i,f} \; = (2\pi/\hbar^2) \, g(\omega_{f,i}) \, | \, \mathbf{E}_0 \cdot \; <\Phi_f \, | \, \mu \, | \, \Phi_i> \, |^2 .$$

This expresses the widely used E1 approximation to the Fermi-Wentzel golden rule.

2. Magnetic Dipole and Electric Quadrupole Transitions

When E1 predictions for the rates of transitions between states vanish (e.g., for symmetry reasons as discussed below), it is essential to examine higher order contributions to $\alpha_{f,i}$. The next terms in the above long-wavelength expansion vary as $1/\lambda$ and have the form:

$$\alpha_{f,i}(E2+M1) \; = <\Phi_f \, | \, \Sigma_j \;\; (e \, / m_e c) \, [-i \mathbf{k} \cdot \mathbf{r}_j] \, \mathbf{A}_0 \cdot \quad _j$$

$$+ \, \Sigma_a \, (\, Z_a e \, / m_a c) \, [-i \mathbf{k} \cdot \mathbf{R}_a] \, \mathbf{A}_0 \cdot \quad _a \; | \, \Phi_i> .$$

For reasons soon to be shown, they are called electric quadrupole (E2) and magnetic dipole (M1) terms. Clearly, higher and higher order terms can be so generated. Within the long-wavelength regime, however, successive terms should decrease in magnitude because of the successively higher powers of $1/\lambda$ that they contain.

To further analyze the above E2 + M1 factors, let us label the propagation direction of the light as the z-axis (the axis along which **k** lies) and the direction of $\mathbf{A}_0$ as the x-axis. These axes are so-called "lab-fixed" axes because their orientation is determined by the direction of the light source and the direction of polarization of the light source's **E** field, both of which are specified by laboratory conditions. The molecule being subjected to this light can be oriented at arbitrary angles relative to these lab axes.

With the x, y, and z axes so defined, the above expression for $\alpha_{f,i}$ (E2+M1) becomes

$$\alpha_{f,i}(E2+M1) = - i (A_0 2\pi/\lambda) \langle \Phi_f | \Sigma_j (e/m_e c) z_j \partial/\partial x_j + \Sigma_a (Z_a e/m_a c) z_a \partial/\partial x_a | \Phi_i \rangle .$$

Now writing (for both z_j and z_a)

$$z \partial/\partial x = 1/2 (z \partial/\partial x - x \partial/\partial z + z \partial/\partial x + x \partial/\partial z),$$

and using

$$_j = - (m_e/\hbar^2) [H, \mathbf{r}_j]$$

$$_a = - (m_a/\hbar^2) [H, \mathbf{R}_a],$$

the contributions of $1/2 (z \partial/\partial x + x \partial/\partial z)$ to $\alpha_{f,i}$ (E2+M1) can be rewritten as

$$\alpha_{f,i}(E2) = - i \frac{(A_0 \, e 2\pi \, \omega_{f,i})}{c\lambda\hbar} \langle \Phi_f | \Sigma_j z_j x_j + \Sigma_a Z_a z_a x_a | \Phi_i \rangle .$$

The operator $\Sigma_i z_i x_j + \Sigma_a Z_a z_a x_a$ that appears above is the z,x element of the electric quadrupole moment operator $Q_{z,x}$; it is for this reason that this particular component is labeled E2 and denoted the electric quadrupole contribution.

The remaining $1/2 (z \partial/\partial x - x \partial/\partial z)$ contribution to $\alpha_{f,i}$ (E2+M1) can be rewritten in a form that makes its content more clear by first noting that

$$1/2 (z \partial/\partial x - x \partial/\partial z) = (i/2\hbar) (z p_x - x p_z) = (i/2\hbar) L_y$$

contains the y-component of the angular momentum operator. Hence, the following contribution to $\alpha_{f,i}$ (E2+M1) arises:

$$\alpha_{f,i}\,(M1) = \frac{A_0 2\pi\, e}{2\lambda c\hbar} \;\; \langle \Phi_f \,|\, \Sigma_j \, L_{y_j}/m_e + \Sigma_a \;\; Z_a \, L_{y_a}/m_a \;\; |\, \Phi_i \rangle .$$

The magnetic dipole moment of the electrons about the y axis is

$$\mu_{y\,,electrons} = \Sigma_j \; (e/2m_e c) \;\; L_{y_j} \; ;$$

that of the nuclei is

$$\mu_{y\,,nuclei} = \Sigma_a \; (Z_a e/2m_a c) \;\; L_{y_a} .$$

The $\alpha_{f,i}$ (M1) term thus describes the interaction of the magnetic dipole moments of the electrons and nuclei with the magnetic field (of strength $|H| = A_0\, k$) of the light (which lies along the y axis):

$$\alpha_{f,i}\,(M1) = \frac{|H|}{\hbar} \;\; \langle \Phi_f \,|\, \mu_{y\,,electrons} + \mu_{y\,,nuclei} \;\; |\, \Phi_i \rangle .$$

The total rate of transitions from Φ_i to Φ_f is given, through first-order in perturbation theory, by

$$R_{i,f} = 2\,\pi\, g(\omega_{f,i})\, |\alpha_{f,i}|^2 ,$$

where $\alpha_{f,i}$ is a sum of its E1, E2, M1, etc. pieces. In the next chapter, molecular symmetry will be shown to be of use in analyzing these various pieces. It should be kept in mind that the contributions caused by E1 terms will dominate, within the long-wavelength approximation, unless symmetry causes these terms to vanish. It is primarily under such circumstances that consideration of M1 and E2 transitions is needed.

III. The Kinetics of Photon Absorption and Emission

A. The Phenomenological Rate Laws

Before closing this chapter, it is important to emphasize the context in which the transition rate expressions obtained here are most commonly used. The perturbative approach used in the above development gives rise to various contributions to the overall rate coefficient for transitions from an initial state Φ_i to a final state Φ_f; these contributions include the electric dipole, magnetic dipole, and electric quadrupole first order terms as well contributions arising from second (and higher) order terms in the perturbation solution.

In principle, once the rate expression

$$R_{i,f} = 2\,\pi\, g(\omega_{f,i})\, |\alpha_{f,i}|^2$$

has been evaluated through some order in perturbation theory and including the dominant electromagnetic interactions, one can make use of these state-to-state rates, which are computed on a per-molecule basis, to describe the time evolution of the populations of the various energy levels of the molecule under the influence of the light source's electromagnetic fields.

For example, given two states, denoted i and f, between which transitions can be induced by photons of frequency $\omega_{f,i}$, the following kinetic model is often used to describe the time evolution of the numbers of molecules n_i and n_f in the respective states:

$$\frac{dn_i}{dt} = - R_{i,f}\, n_i + R_{f,i}\, n_f$$

$$\frac{dn_f}{dt} = - R_{f,i}\, n_f + R_{i,f} n_i \; .$$

Here, $R_{i,f}$ and $R_{f,i}$ are the rates (per molecule) of transitions for the i ==> f and f ==> i transitions respectively. As noted above, these rates are proportional to the intensity of the light source (i.e., the photon intensity) at the resonant frequency and to the square of a matrix element connecting the respective states. This matrix element square is $|\alpha_{i,f}|^2$ in the former case and $|\alpha_{f,i}|^2$ in the latter. Because the perturbation operator whose matrix elements are $\alpha_{i,f}$ and $\alpha_{f,i}$ is Hermitian (this is true through all orders of perturbation theory and for all terms in the long-wavelength expansion), these two quantities are complex conjugates of one another, and, hence $|\alpha_{i,f}|^2 = |\alpha_{f,i}|^2$, from which it follows that $R_{i,f} = R_{f,i}$. This means that the state-to-state absorption and stimulated emission rate coefficients (i.e., the rate per molecule undergoing the transition) are identical. This result is referred to as the principle of **microscopic reversibility**.

Quite often, the states between which transitions occur are members of levels that contain more than a single state. For example, in rotational spectroscopy a transition between a state in the J = 3 level of a diatomic molecule and a state in the J = 4 level involve such states; the respective levels are 2J+1 = 7 and 2J+1 = 9 fold degenerate, respectively.

To extend the above kinetic model to this more general case in which degenerate levels occur, one uses the number of molecules in each **level (**N_i and N_f for the two levels in the above example) as the time dependent variables. The kinetic equations then governing their time evolution can be obtained by summing the state-to-state equations over all states in each level

$$\sum_{\text{i in level I}} \left(\frac{dn_i}{dt}\right) = \frac{dN_I}{dt}$$

$$\sum_{\text{f in level F}} \left(\frac{dn_f}{dt}\right) = \frac{dN_F}{dt}$$

and realizing that each state within a given level can undergo transitions to all states within the other level (hence the total rates of production and consumption must be summed over all states to or from which transitions can occur). This generalization results in a set of rate laws for the populations of the respective levels:

$$\frac{dN_i}{dt} = - g_f R_{i,f} N_i + g_i R_{f,i} N_f$$

$$\frac{dN_f}{dt} = - g_i R_{f,i} N_f + g_f R_{i,f} N_i \ .$$

Here, g_i and g_f are the degeneracies of the two levels (i.e., the number of states in each level) and the $R_{i,f}$ and $R_{f,i}$, which are equal as described above, are the state-to-state rate coefficients introduced earlier.

B. Spontaneous and Stimulated Emission

It turns out (the development of this concept is beyond the scope of this text) that the rate at which an excited level can emit photons and decay to a lower energy level is dependent on two factors: (i) the rate of **stimulated** photon emission as covered above, and (ii) the rate of **spontaneous** photon emission. The former rate $g_f R_{i,f}$ (per molecule) is proportional to the light intensity $g(\omega_{f,i})$ at the resonance frequency. It is conventional to

separate out this intensity factor by defining an intensity independent rate coefficient $B_{i,f}$ for this process as:

$$g_f R_{i,f} = g(\omega_{f,i}) B_{i,f}.$$

Clearly, $B_{i,f}$ embodies the final-level degeneracy factor g_f, the perturbation matrix elements, and the 2π factor in the earlier expression for $R_{i,f}$. The spontaneous rate of transition from the excited to the lower level is found to be <u>independent</u> of photon intensity, because it deals with a process that does not require collision with a photon to occur, and is usually denoted $A_{i,f}$. The rate of photon-stimulated upward transitions from state f to state i ($g_i R_{f,i} = g_i R_{i,f}$ in the present case) is also proportional to $g(\omega_{f,i})$, so it is written by convention as:

$$g_i R_{f,i} = g(\omega_{f,i}) B_{f,i} .$$

An important relation between the $B_{i,f}$ and $B_{f,i}$ parameters exists and is based on the identity $R_{i,f} = R_{f,i}$ that connects the state-to-state rate coefficients:

$$\frac{(B_{i,f})}{(B_{f,i})} = \frac{(g_f R_{i,f})}{(g_i R_{f,i})} = \frac{g_f}{g_i} .$$

This relationship will prove useful in the following sections.

C. Saturated Transitions and Transparency

Returning to the kinetic equations that govern the time evolution of the populations of two levels connected by photon absorption and emission, and adding in the term needed for spontaneous emission, one finds (with the initial level being of the lower energy):

$$\frac{dN_i}{dt} = - \; gB_{i,f} N_i + (A_{f,i} + gB_{f,i})N_f$$

$$\frac{dN_f}{dt} = - (A_{f,i} + gB_{f,i})N_f + gB_{i,f} N_i$$

where $g = g(\omega)$ denotes the light intensity at the resonance frequency.

At steady state, the populations of these two levels are given by setting $\frac{dN_i}{dt} = \frac{dN_f}{dt} = 0$:

$$\frac{N_f}{N_i} = \frac{(gB_{i,f})}{(A_{f,i}+gB_{f,i})} .$$

When the light source's intensity is so large as to render $gB_{f,i} >> A_{f,i}$ (i.e., when the rate of spontaneous emission is small compared to the stimulated rate), this population ratio reaches $(B_{i,f}/B_{f,i})$, which was shown earlier to equal (g_f/g_i). In this case, one says that the populations have been **saturated** by the intense light source. Any further increase in light intensity will result in zero increase in the rate at which photons are being absorbed. Transitions that have had their populations saturated by the application of intense light sources are said to display optical **transparency** because they are unable to absorb (or emit) any further photons because of their state of saturation.

D. Equilibrium and Relations Between A and B Coefficients

When the molecules in the two levels being discussed reach equilibrium (at which time the $\frac{dN_i}{dt} = \frac{dN_f}{dt} = 0$ also holds) with a photon source that itself is in equilibrium characterized by a temperature T, we must have:

$$\frac{N_f}{N_i} = \frac{g_f}{g_i} \exp(-(E_f - E_i)/kT) = \frac{g_f}{g_i} \exp(-\hbar\omega/kT)$$

where g_f and g_i are the degeneracies of the states labeled f and i. The photon source that is characterized by an equilibrium temperature T is known as a **black body** radiator, whose intensity profile $g(\omega)$ (in erg cm^{-3} sec) is know to be of the form:

$$g(\omega) = \frac{2(\hbar\omega)^3}{\pi c^3 \hbar^2} (\exp(\hbar\omega/kT) - 1)^{-1}.$$

Equating the kinetic result that must hold at equilibrium:

$$\frac{N_f}{N_i} = \frac{(gB_{i,f})}{(A_{f,i}+gB_{f,i})}$$

to the thermodynamic result:

$$\frac{N_f}{N_i} = \frac{g_f}{g_i} \exp(-\hbar\omega/kT),$$

and using the above black body $g(\omega)$ expression and the identity

$$\frac{(B_{i,f})}{(B_{f,i})} = \frac{g_f}{g_i} ,$$

one can solve for the $A_{f,i}$ rate coefficient in terms of the $B_{f,i}$ coefficient. Doing so yields:

$$A_{f,i} = B_{f,i} \frac{2(\hbar\omega)^3}{\pi c^3 \hbar^2} .$$

E. Summary

In summary, the so-called **Einstein A and B rate coefficients** connecting a lower-energy initial state i and a final state f are related by the following conditions:

$$B_{i,f} = \frac{g_f}{g_i} B_{f,i}$$

and

$$A_{f,i} = \frac{2(\hbar\omega)^3}{\pi c^3 \hbar^2} B_{f,i}.$$

These phenomenological level-to-level rate coefficients are related to the state-to-state $R_{i,f}$ coefficients derived by applying perturbation theory to the electromagnetic perturbation through

$$g_f R_{i,f} = g(\omega_{f,i}) B_{i,f} .$$

The A and B coefficients can be used in a kinetic equation model to follow the time evolution of the populations of the corresponding levels:

$$\frac{dN_i}{dt} = - \; gB_{i,f} N_i + (A_{f,i} + gB_{f,i})N_f$$

$$\frac{dN_f}{dt} = - (A_{f,i} + gB_{f,i})N_f + gB_{i,f} N_i \; .$$

These equations possess steady state solutions

$$\frac{N_f}{N_i} = \frac{(gB_{i,f})}{(A_{f,i}+gB_{f,i})}$$

which, for large g(ω), produce saturation conditions:

$$\frac{N_f}{N_i} = \frac{(B_{i,f})}{(B_{f,i})} = \frac{g_f}{g_i} \; .$$

Chapter 15

The tools of time-dependent perturbation theory can be applied to transitions among electronic, vibrational, and rotational states of molecules.

I. Rotational Transitions

Within the approximation that the electronic, vibrational, and rotational states of a molecule can be treated as independent, the total molecular wavefunction of the "initial" state is a product

$$\Phi_i = \psi_{ei}\, \chi_{vi}\, \varphi_{ri}$$

of an electronic function ψ_{ei}, a vibrational function χ_{vi}, and a rotational function φ_{ri}. A similar product expression holds for the "final" wavefunction Φ_f.

In microwave spectroscopy, the energy of the radiation lies in the range of fractions of a cm^{-1} through several cm^{-1}; such energies are adequate to excite rotational motions of molecules but are not high enough to excite any but the weakest vibrations (e.g., those of weakly bound Van der Waals complexes). In rotational transitions, the electronic and vibrational states are thus left unchanged by the excitation process; hence $\psi_{ei} = \psi_{ef}$ and $\chi_{vi} = \chi_{vf}$.

Applying the first-order electric dipole transition rate expressions

$$R_{i,f} = 2\, \pi\, g(\omega_{f,i})\, |\alpha_{f,i}|^2$$

obtained in Chapter 14 to this case requires that the E1 approximation

$$R_{i,f} = (2\pi/\hbar^2)\, g(\omega_{f,i})\, |\, \mathbf{E}_0 \cdot \langle \Phi_f \,|\, \mu \,|\, \Phi_i \rangle\, |^2$$

be examined in further detail. Specifically, the electric dipole matrix elements $\langle \Phi_f \,|\, \mu \,|\, \Phi_i \rangle$ with $\mu = \Sigma_j\ e\ \mathbf{r}_j\ + \Sigma_a\ Z_a\, e\ \ \mathbf{R}_a$ must be analyzed for Φ_i and Φ_f being of the product form shown above.

The integrations over the electronic coordinates contained in $\langle \Phi_f \,|\, \mu \,|\, \Phi_i \rangle$, as well as the integrations over vibrational degrees of freedom yield "expectation values" of the electric dipole moment operator because the electronic and vibrational components of Φ_i and Φ_f are identical:

$$\langle \psi_{ei} \mid \mu \mid \psi_{ei} \rangle = \mu(\mathbf{R})$$

is the dipole moment of the initial electronic state (which is a function of the internal geometrical degrees of freedom of the molecule, denoted **R**); and

$$\langle \chi_{vi} \mid \mu(\mathbf{R}) \mid \chi_{vi} \rangle = \mu_{ave}$$

is the vibrationally averaged dipole moment for the particular vibrational state labeled χ_{vi}. The vector μ_{ave} has components along various directions and can be viewed as a vector "locked" to the molecule's internal coordinate axis (labeled a, b, c as below).

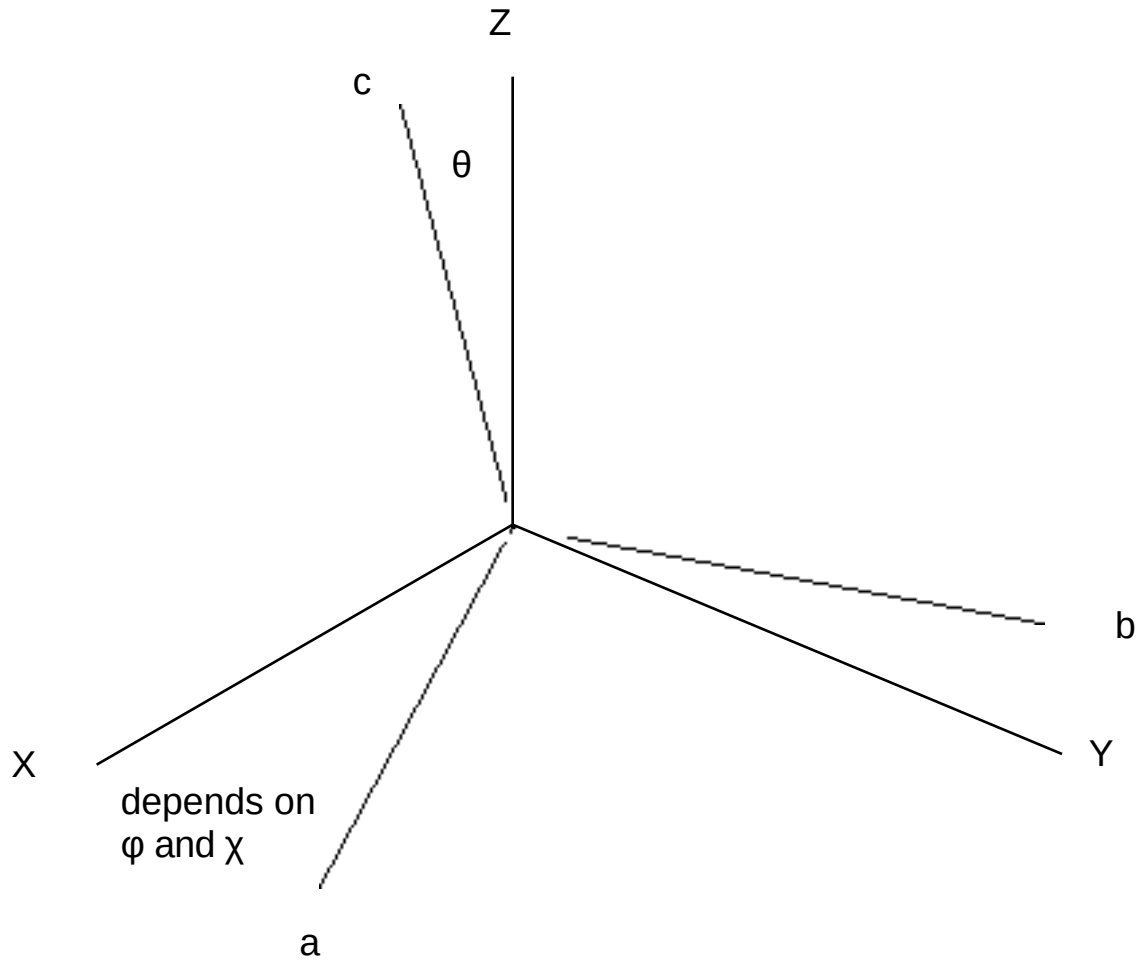

The rotational part of the $\langle \Phi_f | \mu | \Phi_i \rangle$ integral is not of the expectation value form because the initial rotational function φ_{ir} is not the same as the final φ_{fr}. This integral has the form:

$$\langle \varphi_{ir} | \mu_{ave} | \varphi_{fr} \rangle = \int (Y^*_{L,M}(\theta,\varphi) \quad \mu_{ave} \, Y_{L',M'}(\theta,\varphi) \sin\theta \, d\theta \, d\varphi)$$

for linear molecules whose initial and final rotational wavefunctions are $Y_{L,M}$ and $Y_{L',M'}$, respectively, and

$$\langle \varphi_{ir} | \mu_{ave} | \varphi_{fr} \rangle = \sqrt{\frac{2L+1}{8\pi^2}} \sqrt{\frac{2L'+1}{8\pi^2}}$$

$$\int (D_{L,M,K}(\theta,\varphi,\chi) \; \mu_{ave} \, D^*_{L',M',K'}(\theta,\varphi,\chi) \sin\theta \, d\theta \, d\varphi \, d\chi)$$

for spherical or symmetric top molecules (here, $\sqrt{\frac{2L+1}{8\pi^2}}$ $D^*_{L,M,K}(\theta,\varphi,\chi)$ are the normalized rotational wavefunctions described in Chapter 13 and in Appendix G). The angles θ, φ, and χ refer to how the molecule-fixed coordinate system is oriented with respect to the space-fixed X, Y, Z axis system.

A. Linear Molecules

For linear molecules, the vibrationally averaged dipole moment μ_{ave} lies along the molecular axis; hence its orientation in the lab-fixed coordinate system can be specified in terms of the same angles (θ and φ) that are used to describe the rotational functions $Y_{L,M}(\theta,\varphi)$. Therefore, the three components of the $\langle \varphi_{ir} | \mu_{ave} | \varphi_{fr} \rangle$ integral can be written as:

$$\langle \varphi_{ir} | \mu_{ave} | \varphi_{fr} \rangle_x = \mu \int (Y^*_{L,M}(\theta,\varphi) \sin\theta \cos\varphi \, Y_{L',M'}(\theta,\varphi) \sin\theta \, d\theta \, d\varphi)$$

$$\langle \varphi_{ir} | \mu_{ave} | \varphi_{fr} \rangle_y = \mu \int (Y^*_{L,M}(\theta,\varphi) \sin\theta \sin\varphi \, Y_{L',M'}(\theta,\varphi) \sin\theta \, d\theta \, d\varphi)$$

$$<\varphi_{ir} | \mu_{ave} | \varphi_{fr}>_z = \mu \int (Y^*_{L,M}(\theta,\varphi) \cos\theta\ Y_{L',M'}(\theta,\varphi) \sin\theta\ d\theta\ d\varphi),$$

where μ is the magnitude of the averaged dipole moment. **If the molecule has no dipole moment**, all of the above electric dipole integrals vanish and the **intensity** of E1 rotational transitions **is zero**.

The three E1 integrals can be further analyzed by noting that $\cos\theta \propto Y_{1,0}$; $\sin\theta \cos\varphi \propto Y_{1,1} + Y_{1,-1}$; and $\sin\theta \sin\varphi \propto Y_{1,1} - Y_{1,-1}$ and using the angular momentum coupling methods illustrated in Appendix G. In particular, the result given in that appendix:

$$D_{j,\,m,\,m'}\, D_{l,\,n,\,n'}$$

$$= \sum_{J,M,M'} <J,M|j,m;l,n> <j,m';\, l,n'|J,M'>\, D_{J,\,M,\,M'}$$

when multiplied by $D^*_{J,M,M'}$ and integrated over $\sin\theta\, d\theta\, d\varphi\, d\chi$, yields:

$$\int (D^*_{J,M,M'}\, D_{j,\,m,\,m'}\, D_{l,\,n,\,n'} \sin\theta\, d\theta\, d\varphi\, d\chi)$$

$$= \frac{8\pi^2}{2J+1} <J,M|j,m;l,n> <j,m';\, l,n'|J,M'>$$

$$= 8\pi^2 \begin{pmatrix} j & l & J \\ m & n & -M \end{pmatrix} \begin{pmatrix} j & l & J \\ m' & n' & -M' \end{pmatrix} (-1)^{M+M'}.$$

To use this result in the present linear-molecule case, we note that the $D_{J,M,K}$ functions and the $Y_{J,M}$ functions are related by:

$$Y_{J,M}(\theta,\varphi) = \sqrt{(2J+1)/4\pi}\ D^*_{J,M,0}(\theta,\varphi,\chi).$$

The normalization factor is now $\sqrt{(2J+1)/4\pi}$ rather than $\sqrt{(2J+1)/8\pi^2}$ because the $Y_{J,M}$ are no longer functions of χ, and thus the need to integrate over $0 \le \chi \le 2\pi$ disappears. Likewise, the χ-dependence of $D^*_{J,M,K}$ disappears for $K = 0$.

We now use these identities in the three E1 integrals of the form

$$\mu \int (Y^*_{L,M}(\theta,\varphi)\ Y_{1,m}(\theta,\varphi)\ Y_{L',M'}(\theta,\varphi) \sin\theta\ d\theta\ d\varphi),$$

with m = 0 being the Z- axis integral, and the Y- and X- axis integrals being combinations of the m = 1 and m = -1 results. Doing so yields:

$$\mu \int (Y^*_{L,M}(\theta,\varphi)\, Y_{1,m}(\theta,\varphi)\, Y_{L',M'}(\theta,\varphi)\, \sin\theta\, d\theta\, d\varphi)$$

$$= \mu \sqrt{\frac{2L+1}{4\pi}\,\frac{2L'+1}{4\pi}\,\frac{3}{4\pi}} \int (D_{L,M,0}\, D^*_{1,m,0}\, D^*_{L',M',0}\, \sin\theta\, d\theta\, d\varphi\, d\chi/2\pi) .$$

The last factor of $1/2\pi$ is inserted to cancel out the integration over $d\chi$ that, because all K-factors in the rotation matrices equal zero, trivially yields 2π. Now, using the result shown above expressing the integral over three rotation matrices, these E1 integrals for the linear-molecule case reduce to:

$$\mu \int (Y^*_{L,M}(\theta,\varphi)\, Y_{1,m}(\theta,\varphi)\, Y_{L',M'}(\theta,\varphi)\, \sin\theta\, d\theta\, d\varphi)$$

$$= \mu \sqrt{\frac{2L+1}{4\pi}\,\frac{2L'+1}{4\pi}\,\frac{3}{4\pi}\,\frac{8\pi^2}{2\pi}} \begin{pmatrix} L' & 1 & L \\ M' & m & -M \end{pmatrix} \begin{pmatrix} L' & 1 & L \\ 0 & 0 & -0 \end{pmatrix} (-1)^M$$

$$= \mu \sqrt{(2L+1)(2L'+1)\,\frac{3}{4\pi}} \begin{pmatrix} L' & 1 & L \\ M' & m & -M \end{pmatrix} \begin{pmatrix} L' & 1 & L \\ 0 & 0 & -0 \end{pmatrix} (-1)^M .$$

Applied to the z-axis integral (identifying m = 0), this result therefore vanishes unless:

$$M = M'$$

and

$$L = L' + 1 \text{ or } L' - 1.$$

Even though angular momentum coupling considerations would allow L = L' (because coupling two angular momenta with j = 1 and j = L' should give L'+1, L', and L'-1), the 3-j symbol $\begin{pmatrix} L' & 1 & L \\ 0 & 0 & -0 \end{pmatrix}$ vanishes for the L = L' case since 3-j symbols have the following symmetry

$$\begin{pmatrix} L' & 1 & L \\ M' & m & -M \end{pmatrix} = (-1)^{L+L'+1} \begin{pmatrix} L' & 1 & L \\ -M' & -m & M \end{pmatrix}$$

with respect to the M, M', and m indices. Applied to the $\begin{pmatrix} L' & 1 & L \\ 0 & 0 & -0 \end{pmatrix}$ 3-j symbol, this means that this particular 3-j element vanishes for L = L' since L + L' + 1 is odd and hence $(-1)^{L + L' + 1}$ is -1.

Applied to the x- and y- axis integrals, which contain m = ± 1 components, this same analysis yields:

$$\mu \sqrt{(2L+1)(2L'+1)\frac{3}{4\pi}} \begin{pmatrix} L' & 1 & L \\ M' & \pm 1 & -M \end{pmatrix} \begin{pmatrix} L' & 1 & L \\ 0 & 0 & -0 \end{pmatrix} (-1)^M$$

which then requires that

$$M = M' \pm 1$$

and

$$L = L' + 1, L' - 1,$$

with L = L' again being forbidden because of the second 3-j symbol.

These results provide so-called "**selection rules**" because they limit the L and M values of the final rotational state, given the L', M' values of the initial rotational state. In the figure shown below, the L = L' + 1 absorption spectrum of NO at 120 °K is given. The intensities of the various peaks are related to the populations of the lower-energy rotational states which are, in turn, proportional to $(2 L' + 1) \exp(- L'(L'+1) \hbar^2/8\pi^2 IkT)$. Also included in the intensities are so-called **line strength factors** that are proportional to the squares of the quantities:

$$\mu \sqrt{(2L+1)(2L'+1)\frac{3}{4\pi}} \begin{pmatrix} L' & 1 & L \\ M' & m & -M \end{pmatrix} \begin{pmatrix} L' & 1 & L \\ 0 & 0 & -0 \end{pmatrix} (-1)^M$$

which appear in the E1 integrals analyzed above (recall that the rate of photon absorption $R_{i,f} = (2\pi/\hbar^2)\, g(\omega_{f,i}) \,|\, \mathbf{E}_0 \cdot \langle \Phi_f \,|\, \mu \,|\, \Phi_i \rangle \,|^2$ involves the squares of these matrix elements). The book by Zare gives an excellent treatment of line strength factors' contributions to rotation, vibration, and electronic line intensities.

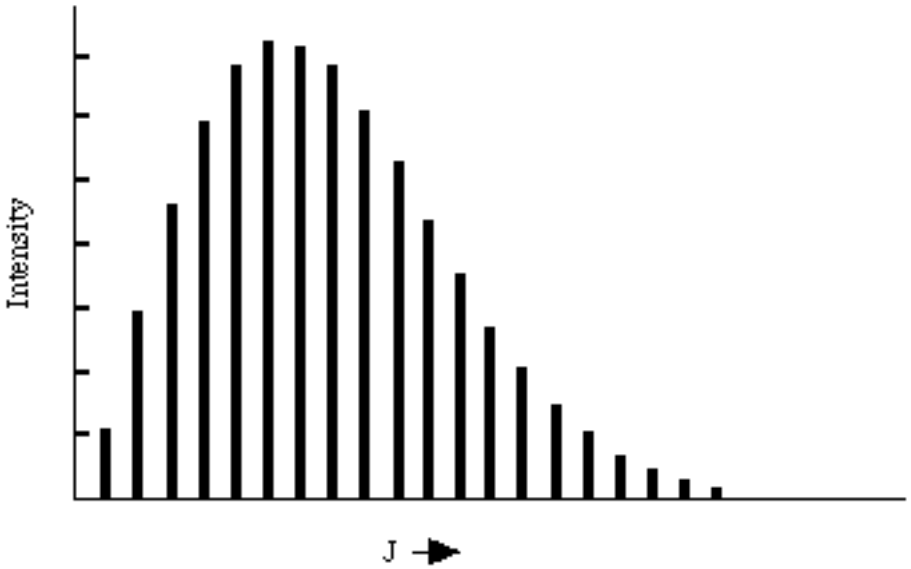

B. Non-Linear Molecules

For molecules that are non-linear and whose rotational wavefunctions are given in terms of the spherical or symmetric top functions $D^*_{L,M,K}$, the dipole moment μ_{ave} can have components along any or all three of the molecule's internal coordinates (e.g., the three molecule-fixed coordinates that describe the orientation of the principal axes of the moment of inertia tensor). For a spherical top molecule, $|\mu_{ave}|$ vanishes, so E1 transitions do not occur.

For symmetric top species, μ_{ave} lies along the symmetry axis of the molecule, so the orientation of μ_{ave} can again be described in terms of θ and φ, the angles used to locate the orientation of the molecule's symmetry axis relative to the lab-fixed coordinate system. As a result, the E1 integral again can be decomposed into three pieces:

$$\langle \varphi_{ir} | \mu_{ave} | \varphi_{fr} \rangle_x = \mu \int (D_{L,M,K}(\theta,\varphi,\chi) \cos\theta \cos\varphi D^*_{L',M',K'}(\theta,\varphi,\chi) \sin\theta \, d\theta \, d\varphi \, d\chi)$$

$$\langle \varphi_{ir} | \mu_{ave} | \varphi_{fr} \rangle_y = \mu \int (D_{L,M,K}(\theta,\varphi,\chi) \cos\theta \sin\varphi D^*_{L',M',K'}(\theta,\varphi,\chi) \sin\theta \, d\theta \, d\varphi \, d\chi)$$

$$\langle \varphi_{ir} | \mu_{ave} | \varphi_{fr} \rangle_z = \mu \int (D_{L,M,K}(\theta,\varphi,\chi) \cos\theta D^*_{L',M',K'}(\theta,\varphi,\chi) \sin\theta \, d\theta \, d\varphi \, d\chi) .$$

Using the fact that cosθ $D^*_{1,0,0}$; sinθ cosφ $D^*_{1,1,0} + D^*_{1,-1,0}$; and sinθ sinφ $D^*_{1,1,0} - D^*_{1,-1,0}$, and the tools of angular momentum coupling allows these integrals to be expressed, as above, in terms of products of the following 3-j symbols:

$$\begin{pmatrix} L' & 1 & L \\ M' & m & -M \end{pmatrix} \begin{pmatrix} L' & 1 & L \\ K' & 0 & -K \end{pmatrix},$$

from which the following selection rules are derived:

$L = L' + 1, L', L' - 1$ (but not $L = L' = 0$),

$K = K'$,

$M = M' + m$,

with m = 0 for the Z-axis integral and m = ± 1 for the X- and Y- axis integrals. In addition, if K = K' = 0, the L = L' transitions are also forbidden by the second 3-j symbol vanishing.

II. Vibration-Rotation Transitions

When the initial and final electronic states are identical but the respective vibrational and rotational states are not, one is dealing with transitions between vibration-rotation states of the molecule. These transitions are studied in infrared (IR) spectroscopy using light of energy in the 30 cm^{-1} (far IR) to 5000 cm^{-1} range. The electric dipole matrix element analysis still begins with the electronic dipole moment integral $\langle \psi_{ei} | \mu | \psi_{ei} \rangle = \mu(\mathbf{R})$, but the integration over internal vibrational coordinates no longer produces the vibrationally averaged dipole moment. Instead one forms the vibrational **transition dipole** integral:

$$\langle \chi_{vf} | \mu(\mathbf{R}) | \chi_{vi} \rangle = \mu_{f,i}$$

between the initial χ_i and final χ_f vibrational states.

A. The Dipole Moment Derivatives

Expressing $\mu(\mathbf{R})$ in a power series expansion about the equilibrium bond length position (denoted $\mathbf{R}_e$ collectively and $R_{a,e}$ individually):

$$\mu(\mathbf{R}) = \mu(\mathbf{R}_e) + \Sigma_a \, \partial\mu/\partial R_a \, (R_a - R_{a,e}) + \ldots,$$

substituting into the $\langle \chi_{vf} | \mu(\mathbf{R}) | \chi_{vi} \rangle$ integral, and using the fact that χ_i and χ_f are orthogonal (because they are eigenfunctions of vibrational motion on the same electronic surface and hence of the same vibrational Hamiltonian), one obtains:

$$\langle \chi_{vf} | \mu(\mathbf{R}) | \chi_{vi} \rangle = \mu(\mathbf{R}_e) \langle \chi_{vf} | \chi_{vi} \rangle + \Sigma_a \, \partial\mu/\partial R_a \langle \chi_{vf} | \, (R_a - R_{a,e}) | \chi_{vi} \rangle \; + \ldots$$

$$= \Sigma_a \, (\partial\mu/\partial R_a) \langle \chi_{vf} | \, (R_a - R_{a,e}) | \chi_{vi} \rangle \; + \ldots \; .$$

This result can be interpreted as follows:

i. Each independent vibrational mode of the molecule contributes to the $\mu_{f,i}$ vector an amount equal to $(\partial\mu/\partial R_a) \langle \chi_{vf} | \, (R_a - R_{a,e}) | \chi_{vi} \rangle \; + \ldots$.

ii. Each such contribution contains one part $(\partial\mu/\partial R_a)$ that depends on how the molecule's dipole moment function varies with vibration along that particular mode (labeled a),

iii. and a second part $\langle \chi_{vf} | \, (R_a - R_{a,e}) | \chi_{vi} \rangle$ that depends on the character of the initial and final vibrational wavefunctions.

If the vibration does not produce a **modulation of the dipole moment** (e.g., as with the symmetric stretch vibration of the CO_2 molecule), its infrared intensity vanishes because $(\partial\mu/\partial R_a) = 0$. One says that such transitions are infrared "inactive".

B. Selection Rules on the Vibrational Quantum Number in the Harmonic Approximation

If the vibrational functions are described within the harmonic oscillator approximation, it can be shown that the $\langle \chi_{vf} | \, (R_a - R_{a,e}) | \chi_{vi} \rangle$ integrals vanish unless vf = vi +1 , vi -1 (and that these integrals are proportional to $(vi +1)^{1/2}$ and $(vi)^{1/2}$ in the respective cases). Even when χ_{vf} and χ_{vi} are rather non-harmonic, it turns out that such $\Delta v = \pm 1$ transitions have the largest $\langle \chi_{vf} | \, (R_a - R_{a,e}) | \chi_{vi} \rangle$ integrals and therefore the highest infrared intensities. For these reasons, transitions that correspond to $\Delta v = \pm 1$ are called "**fundamental**"; those with $\Delta v = \pm 2$ are called "first **overtone**" transitions.

In summary then, vibrations for which the molecule's dipole moment is modulated as the vibration occurs (i.e., for which $(\partial\mu/\partial R_a)$ is non-zero) and for which $\Delta v = \pm 1$ tend to have large infrared intensities; overtones of such vibrations tend to have smaller intensities, and those for which $(\partial\mu/\partial R_a) = 0$ have no intensity.

C. Rotational Selection Rules for Vibrational Transitions

The result of all of the vibrational modes' contributions to $\Sigma_a (\partial\mu/\partial R_a) \langle\chi_{vf} | (R_a - R_{a,e}) | \chi_{vi}\rangle$ is a vector μ_{trans} that is termed the vibrational "transition dipole" moment. This is a vector with components along, in principle, all three of the internal axes of the molecule. For each particular vibrational transition (i.e., each particular χ_i and χ_f) its orientation in space depends only on the orientation of the molecule; it is thus said to be locked to the molecule's coordinate frame. As such, its orientation relative to the lab-fixed coordinates (which is needed to effect a derivation of rotational selection rules as was done earlier in this Chapter) can be described much as was done above for the vibrationally averaged dipole moment that arises in purely rotational transitions. There are, however, important differences in detail. In particular,

i. For a linear molecule μ_{trans} can have components either along (e.g., when stretching vibrations are excited; these cases are denoted σ-cases) or perpendicular to (e.g., when bending vibrations are excited; they are denoted π cases) the molecule's axis.

ii. For symmetric top species, μ_{trans} need not lie along the molecule's symmetry axis; it can have components either along or perpendicular to this axis.

iii. For spherical tops, μ_{trans} will vanish whenever the vibration does not induce a dipole moment in the molecule. Vibrations such as the totally symmetric a_1 C-H stretching motion in CH_4 do not induce a dipole moment, and are thus infrared inactive; non-totally-symmetric vibrations can also be inactive if they induce no dipole moment.

As a result of the above considerations, the angular integrals

$$\langle\varphi_{ir} | \mu_{trans} | \varphi_{fr}\rangle = \int (Y^*_{L,M}(\theta,\varphi)\ \mu_{trans}\ Y_{L',M'}(\theta,\varphi)\ \sin\theta\ d\theta\ d\varphi)$$

and

$$\langle \varphi_{ir} | \mu_{trans} | \varphi_{fr} \rangle = \int (D_{L,M,K}(\theta,\varphi,\chi)\ \mu_{trans}\ D^*_{L',M',K'}(\theta,\varphi,\chi)\ \sin\theta\ d\theta\ d\varphi\ d\chi)$$

that determine the rotational selection rules appropriate to vibrational transitions produce similar, but not identical, results as in the purely rotational transition case.

The derivation of these selection rules proceeds as before, with the following additional considerations. The transition dipole moment's μ_{trans} components along the lab-fixed axes must be related to its molecule-fixed coordinates (that are determined by the nature of the vibrational transition as discussed above). This transformation, as given in Zare's text, reads as follows:

$$(\mu_{trans})_m = \sum_k D^*_{1,m,k}(\theta,\varphi,\chi)\,(\mu_{trans})_k$$

where $(\mu_{trans})_m$ with m = 1, 0, -1 refer to the components along the lab-fixed (X, Y, Z) axes and $(\mu_{trans})_k$ with k = 1, 0, -1 refer to the components along the molecule- fixed (a, b, c) axes.

This relationship, when used, for example, in the symmetric or spherical top E1 integral:

$$\langle \varphi_{ir} | \mu_{trans} | \varphi_{fr} \rangle = \int (D_{L,M,K}(\theta,\varphi,\chi)\ \mu_{trans}\ D^*_{L',M',K'}(\theta,\varphi,\chi)\ \sin\theta\ d\theta\ d\varphi\ d\chi)$$

gives rise to products of 3-j symbols of the form:

$$\begin{pmatrix} L' & 1 & L \\ M' & m & -M \end{pmatrix} \begin{pmatrix} L' & 1 & L \\ K' & k & -K \end{pmatrix}.$$

The product of these 3-j symbols is nonvanishing only under certain conditions that provide the rotational selection rules applicable to vibrational lines of symmetric and spherical top molecules.

Both 3-j symbols will vanish unless

L = L' +1, L', or L'-1.

In the special case in which L = L' =0 (and hence with M = M' =0 = K = K', which means that m = 0 = k), these3-j symbols again vanish. Therefore, transitions with

L = L' =0

are again **forbidden.** As usual, the fact that the lab-fixed quantum number m can range over m = 1, 0, -1, requires that

M = M' + 1, M', M'-1.

The selection rules for ΔK depend on the nature of the vibrational transition, in particular, on the component of μ_{trans} along the molecule-fixed axes. For the second 3-j symbol to not vanish, one must have

K = K' + k,

where k = 0, 1, and -1 refer to these molecule-fixed components of the transition dipole. Depending on the nature of the transition, various k values contribute.

1. Symmetric Tops

In a symmetric top molecule such as NH_3, if the transition dipole lies along the molecule's symmetry axis, only k = 0 contributes. Such vibrations preserve the molecule's symmetry relative to this symmetry axis (e.g. the totally symmetric N-H stretching mode in NH_3). The additional selection rule ΔK = 0
is thus obtained. Moreover, for K = K' = 0, all transitions with ΔL = 0 vanish because the second 3-j symbol vanishes. In summary, one has:

ΔK = 0; ΔM = ±1 ,0; ΔL = ±1 ,0 (but L = L' =0 is forbidden and all ΔL = 0 are forbidden for K = K' = 0)

for symmetric tops with vibrations whose transition dipole lies along the symmetry axis.

If the transition dipole lies perpendicular to the symmetry axis, only k = ±1 contribute. In this case, one finds

ΔK = ±1; ΔM = ±1 ,0; ΔL = ±1 ,0 (neither L = L' =0 nor K = K' = 0 can occur for such transitions, so there are no additional constraints).

2. Linear Molecules

When the above analysis is applied to a diatomic species such as HCl, only k = 0 is present since the only vibration present in such a molecule is the bond stretching vibration, which has σ symmetry. Moreover, the rotational functions are spherical harmonics (which can be viewed as $D^*_{L',M',K'}(\theta,\varphi,\chi)$ functions with K' = 0), so the K and K' quantum numbers are identically zero. As a result, the product of 3-j symbols

$$\begin{pmatrix} L' & 1 & L \\ M' & m & -M \end{pmatrix} \begin{pmatrix} L' & 1 & L \\ K' & k & -K \end{pmatrix}$$

reduces to

$$\begin{pmatrix} L' & 1 & L \\ M' & m & -M \end{pmatrix} \begin{pmatrix} L' & 1 & L \\ 0 & 0 & 0 \end{pmatrix},$$

which will vanish unless

$$L = L' + 1,\ L' - 1,$$

but <u>not</u> L = L' (since parity then causes the second 3-j symbol to vanish), and

$$M = M' + 1,\ M',\ M' - 1.$$

The L = L' +1 transitions are termed **R-branch** absorptions and those obeying L = L' -1 are called **P-branch** transitions. Hence, the selection rules

$$\Delta M = \pm 1, 0;\ \Delta L = \pm 1$$

are identical to those for purely rotational transitions.

When applied to linear polyatomic molecules, these same selection rules result if the vibration is of σ symmetry (i.e., has k = 0). If, on the other hand, the transition is of π symmetry (i.e., has k = ±1), so the transition dipole lies perpendicular to the molecule's axis, one obtains:

$$\Delta M = \pm 1, 0;\ \Delta L = \pm 1,\ 0.$$

These selection rules are derived by realizing that in addition to k = ±1, one has:
(i) a linear-molecule rotational wavefunction that in the v = 0 vibrational level is described in terms of a rotation matrix $D_{L',M',0}(\theta,\varphi,\chi)$ with no angular momentum along the molecular axis, K' = 0 ; (ii) a v = 1 molecule whose rotational wavefunction must be given by a rotation matrix $D_{L,M,1}(\theta,\varphi,\chi)$ with one unit of angular momentum about the molecule's axis, K = 1. In the latter case, the angular momentum is produced by the degenerate π vibration itself. As a result, the selection rules above derive from the following product of 3-j symbols:

$$\begin{pmatrix} L' & 1 & L \\ M' & m & -M \end{pmatrix} \begin{pmatrix} L' & 1 & L \\ 0 & 1 & -1 \end{pmatrix}.$$

Because ΔL = 0 transitions are allowed for π vibrations, one says that π vibrations possess **Q- branches** in addition to their R- and P- branches (with ΔL = 1 and -1, respectively).

In the figure shown below, the v = 0 ==> v = 1 (fundamental) vibrational absorption spectrum of HCl is shown. Here the peaks at lower energy (to the right of the figure) belong to P-branch transitions and occur at energies given approximately by:

$$E = \hbar\,\omega_{stretch} + (h^2/8\pi^2 I)\,((L-1)L - L(L+1))$$

$$= \hbar\,\omega_{stretch} - 2\,(h^2/8\pi^2 I)\,L.$$

The R-branch transitions occur at higher energies given approximately by:

$$E = \hbar\,\omega_{stretch} + (h^2/8\pi^2 I)\,((L+1)(L+2) - L(L+1))$$

$$= \hbar\,\omega_{stretch} + 2\,(h^2/8\pi^2 I)\,(L+1).$$

The absorption that is "missing" from the figure below lying slightly below 2900 cm^{-1} is the **Q-branch** transition for which L = L'; it is absent because the selection rules forbid it.

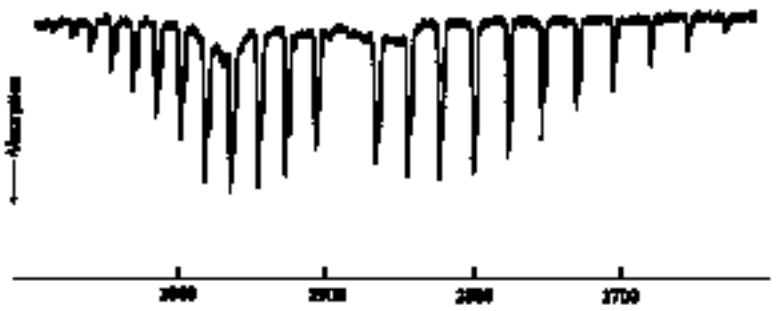

It should be noted that the spacings between the experimentally observed peaks in HCl are not constant as would be expected based on the above P- and R- branch formulas. This is because the moment of inertia appropriate for the v = 1 vibrational level is different than that of the v = 0 level. These effects of vibration-rotation coupling can be modeled by allowing the v = 0 and v = 1 levels to have rotational energies written as

$$E = \hbar\,\omega_{stretch}\,(v + 1/2) + (h^2/8\pi^2 I_v)\,(L\,(L+1))$$

where v and L are the vibrational and rotational quantum numbers. The P- and R- branch transition energies that pertain to these energy levels can then be written as:

$$E_P = \hbar\,\omega_{stretch} - [\,(h^2/8\pi^2 I_1) + (h^2/8\pi^2 I_0)\,]\,L + [\,(h^2/8\pi^2 I_1) - (h^2/8\pi^2 I_0)\,]\,L^2$$

$$E_R = \hbar\,\omega_{stretch} + 2\,(h^2/8\pi^2 I_1)$$

$$+ [\,3(h^2/8\pi^2 I_1) - (h^2/8\pi^2 I_0)\,]\,L + [\,(h^2/8\pi^2 I_1) - (h^2/8\pi^2 I_0)\,]\,L^2\,.$$

Clearly, these formulas reduce to those shown earlier in the $I_1 = I_0$ limit.

If the vibrationally averaged bond length is longer in the v = 1 state than in the v = 0 state, which is to be expected, I_1 will be larger than I_0, and therefore $[\,(h^2/8\pi^2 I_1) - (h^2/8\pi^2 I_0)\,]$ will be negative. In this case, the spacing between neighboring P-branch lines will increase as shown above for HCl. In contrast, the fact that $[\,(h^2/8\pi^2 I_1) - (h^2/8\pi^2 I_0)\,]$ is negative causes the spacing between neighboring R- branch lines to decrease, again as shown for HCl.

III. Electronic-Vibration-Rotation Transitions

When electronic transitions are involved, the initial and final states generally differ in their electronic, vibrational, and rotational energies. Electronic transitions usually require light in the 5000 cm^{-1} to 100,000 cm^{-1} regime, so their study lies within the domain of visible and ultraviolet spectroscopy. Excitations of inner-shell and core orbital electrons may require even higher energy photons, and under these conditions, E2 and M1 transitions may become more important because of the short wavelength of the light involved.

A. The Electronic Transition Dipole and Use of Point Group Symmetry

Returning to the expression

$$R_{i,f} = (2\pi/\hbar^2)\, g(\omega_{f,i})\, |\, \mathbf{E}_0 \cdot \langle \Phi_f \,|\, \mu \,|\, \Phi_i \rangle\, |^2$$

for the rate of photon absorption, we realize that the electronic integral now involves

$$\langle \psi_{ef} \,|\, \mu \,|\, \psi_{ei} \rangle = \mu_{f,i}\,(\mathbf{R}),$$

a transition dipole matrix element between the initial ψ_{ei} and final ψ_{ef} electronic wavefunctions. This element is a function of the internal vibrational coordinates of the molecule, and again is a vector locked to the molecule's internal axis frame.

Molecular point-group symmetry can often be used to determine whether a particular transition's dipole matrix element will vanish and, as a result, the electronic transition will be "forbidden" and thus predicted to have zero intensity. If the direct product of the symmetries of the initial and final electronic states ψ_{ei} and ψ_{ef} do not match the symmetry of the electric dipole operator (which has the symmetry of its x, y, and z components; these symmetries can be read off the right most column of the character tables given in Appendix E), the matrix element will vanish.

For example, the formaldehyde molecule H_2CO has a ground electronic state (see Chapter 11) that has $^1A_1$ symmetry in the C_{2v} point group. Its $\pi \Longrightarrow \pi^*$ singlet excited state also has $^1A_1$ symmetry because both the π and π^* orbitals are of b_1 symmetry. In contrast, the lowest $n \Longrightarrow \pi^*$ singlet excited state is of $^1A_2$ symmetry because the highest energy oxygen centered n orbital is of b_2 symmetry and the π^* orbital is of b_1 symmetry, so the Slater determinant in which both the n and π^* orbitals are singly occupied has its symmetry dictated by the $b_2 \times b_1$ direct product, which is A_2.

The $\pi \Longrightarrow \pi^*$ transition thus involves ground ($^1A_1$) and excited ($^1A_1$) states whose direct product ($A_1 \times A_1$) is of A_1 symmetry. This transition thus requires that the electric dipole operator possess a component of A_1 symmetry. A glance at the C_{2v} point group's character table shows that the molecular z-axis is of A_1 symmetry. Thus, if the light's electric field has a non-zero component along the C_2 symmetry axis (the molecule's z-axis), the $\pi \Longrightarrow \pi^*$ transition is predicted to be allowed. Light polarized along either of the molecule's other two axes cannot induce this transition.

In contrast, the $n \Longrightarrow \pi^*$ transition has a ground-excited state direct product of $B_2 \times B_1 = A_2$ symmetry. The C_{2v} 's point group character table clearly shows that the electric dipole operator (i.e., its x, y, and z components in the molecule-fixed frame) has no component of A_2 symmetry; thus, light of no electric field orientation can induce this $n \Longrightarrow \pi^*$ transition. We thus say that the $n \Longrightarrow \pi^*$ transition is E1 forbidden (although it is M1 allowed).

Beyond such electronic symmetry analysis, it is also possible to derive vibrational and rotational selection rules for electronic transitions that are E1 allowed. As was done in the vibrational spectroscopy case, it is conventional to expand $\mu_{f,i}(\mathbf{R})$ in a power series about the equilibrium geometry of the initial electronic state (since this geometry is more characteristic of the molecular structure prior to photon absorption):

$$\mu_{f,i}(\mathbf{R}) = \mu_{f,i}(\mathbf{R}_e) + \Sigma_a \, \partial\mu_{f,i}/\partial R_a \, (R_a - R_{a,e}) + \ldots.$$

B. The Franck-Condon Factors

The first term in this expansion, when substituted into the integral over the vibrational coordinates, gives $\mu_{f,i}(\mathbf{R}_e) \langle \chi_{vf} | \chi_{vi} \rangle$, which has the form of the electronic transition dipole multiplied by the "overlap integral" between the initial and final vibrational wavefunctions. The $\mu_{f,i}(\mathbf{R}_e)$ factor was discussed above; it is the electronic E1 transition integral evaluated at the equilibrium geometry of the absorbing state. Symmetry can often be used to determine whether this integral vanishes, as a result of which the E1 transition will be "forbidden".

Unlike the vibration-rotation case, the vibrational overlap integrals $\langle \chi_{vf} | \chi_{vi} \rangle$ do not necessarily vanish because χ_{vf} and χ_{vi} are no longer eigenfunctions of the same vibrational Hamiltonian. χ_{vf} is an eigenfunction whose potential energy is the final electronic state's energy surface; χ_{vi} has the initial electronic state's energy surface as its potential. The squares of these $\langle \chi_{vf} | \chi_{vi} \rangle$ integrals, which are what eventually enter into the transition rate expression $R_{i,f} = (2\pi/\hbar^2) \, g(\omega_{f,i}) \, | \, \mathbf{E}_0 \cdot \langle \Phi_f | \mu | \Phi_i \rangle \, |^2$, are called

"**Franck-Condon factors**". Their relative magnitudes play strong roles in determining the relative intensities of various vibrational "bands" (i.e., peaks) within a particular electronic transition's spectrum.

Whenever an electronic transition causes a large change in the geometry (bond lengths or angles) of the molecule, the Franck-Condon factors tend to display the characteristic "broad progression" shown below when considered for one initial-state vibrational level vi and various final-state vibrational levels vf:

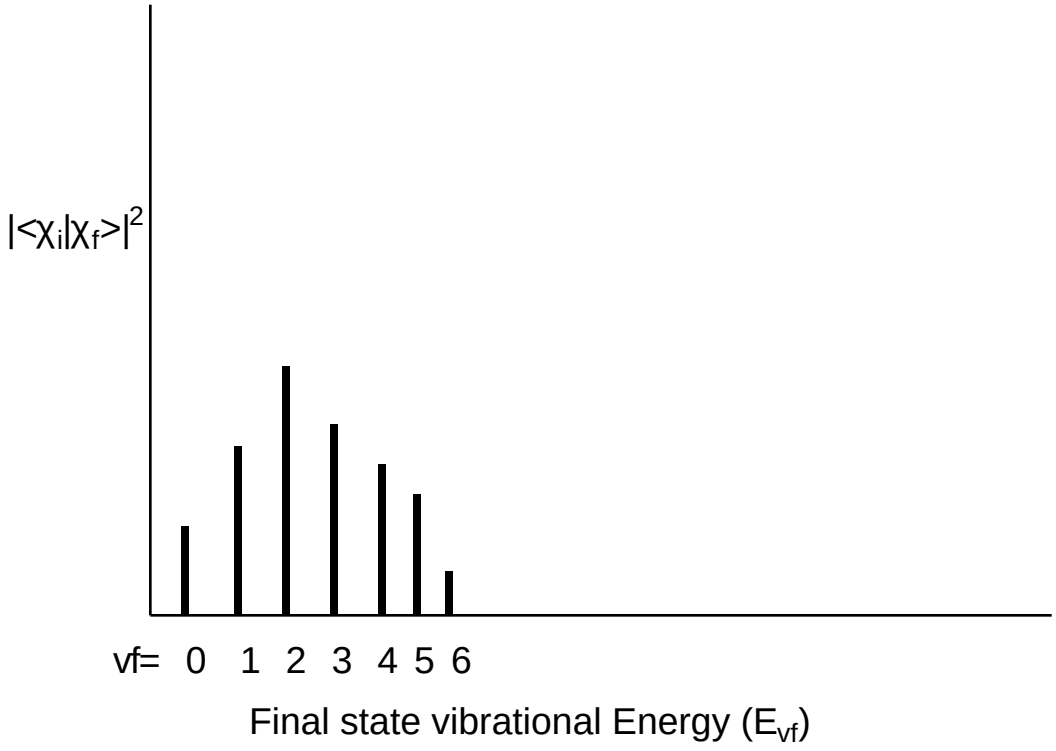

Notice that as one moves to higher vf values, the energy spacing between the states (E_{vf} - E_{vf-1}) decreases; this, of course, reflects the anharmonicity in the excited state vibrational potential. For the above example, the transition to the vf = 2 state has the largest Franck-Condon factor. This means that the overlap of the initial state's vibrational wavefunction χ_{vi} is largest for the final state's χ_{vf} function with vf = 2.

As a qualitative rule of thumb, the larger the geometry difference between the initial and final state potentials, the broader will be the Franck-Condon profile (as shown above) and the larger the vf value for which this profile peaks. Differences in harmonic frequencies between the two states can also broaden the Franck-Condon profile, although not as significantly as do geometry differences.

For example, if the initial and final states have very similar geometries and frequencies along the mode that is excited when the particular electronic excitation is realized, the following type of Franck-Condon profile may result:

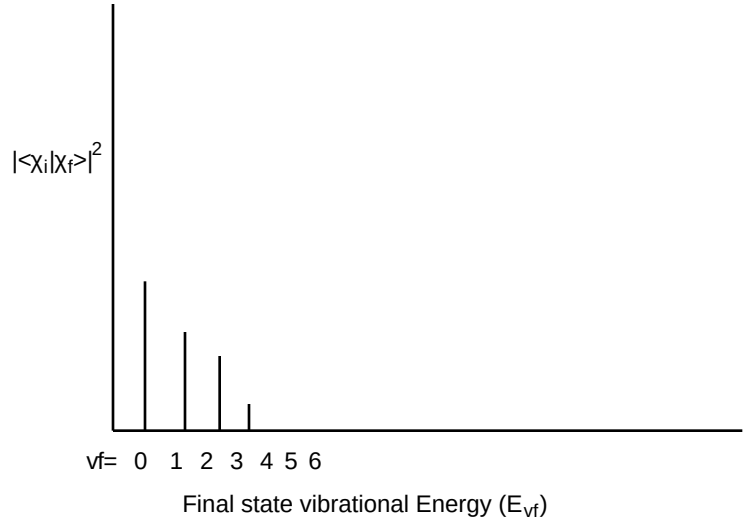

In contrast, if the initial and final electronic states have very different geometries and/or vibrational frequencies along some mode, a very broad Franck-Condon envelope peaked at high-vf will result as shown below:

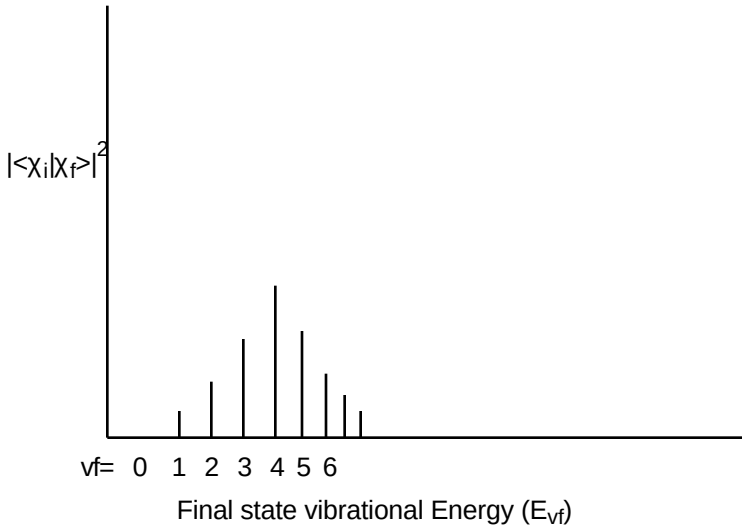

C. Vibronic Effects

The second term in the above expansion of the transition dipole matrix element $\Sigma_a \partial\mu_{f,i}/\partial R_a (R_a - R_{a,e})$ can become important to analyze when the first term $\mu_{fi}(\mathbf{R}_e)$ vanishes (e.g., for reasons of symmetry). This dipole derivative term, when substituted into the integral over vibrational coordinates gives
$\Sigma_a \partial\mu_{f,i}/\partial R_a \langle\chi_{vf} | (R_a - R_{a,e})| \chi_{vi}\rangle$. Transitions for which $\mu_{f,i}(\mathbf{R}_e)$ vanishes but for which $\partial\mu_{f,i}/\partial R_a$ does not for the a^{th} vibrational mode are said to derive intensity through "vibronic coupling" with that mode. The intensities of such modes are dependent on how strongly the electronic dipole integral varies along the mode (i.e, on $\partial\mu_{f,i}/\partial R_a$) as well as on the magnitude of the vibrational integral
$\langle\chi_{vf} | (R_a - R_{a,e})| \chi_{vi}\rangle$.

An example of an E1 forbidden but "vibronically allowed" transition is provided by the singlet n ==> π* transition of H_2CO that was discussed earlier in this section. As detailed there, the ground electronic state has $^1A_1$ symmetry, and the n ==> π* state is of $^1A_2$ symmetry, so the E1 transition integral
$\langle\psi_{ef} | \mu | \psi_{ei}\rangle$ vanishes for all three (x, y, z) components of the electric dipole operator μ . However, vibrations that are of b_2 symmetry (e.g., the H-C-H asymmetric stretch vibration) can induce intensity in the n ==> π* transition as follows:
(i) For such vibrations, the b_2 mode's vi = 0 to vf = 1 vibronic integral
$\langle\chi_{vf} | (R_a - R_{a,e})| \chi_{vi}\rangle$ will be non-zero and probably quite substantial (because, for harmonic oscillator functions these "fundamental" transition integrals are dominant- see earlier);
(ii) Along these same b_2 modes, the electronic transition dipole integral <u>derivative</u> $\partial\mu_{f,i}/\partial R_a$ will be non-zero, even though the integral itself $\mu_{f,i}$ $(\mathbf{R}_e)$ vanishes when evaluated at the initial state's equilibrium geometry.

To understand why the derivative $\partial\mu_{f,i}/\partial R_a$ can be non-zero for distortions (denoted R_a) of b_2 symmetry, consider this quantity in greater detail:

$$\partial\mu_{f,i}/\partial R_a = \partial\langle\psi_{ef} | \mu | \psi_{ei}\rangle/\partial R_a$$

$$= \langle\partial\psi_{ef}/\partial R_a | \mu | \psi_{ei}\rangle + \langle\psi_{ef} | \mu | \partial\psi_{ei}/\partial R_a\rangle + \langle\psi_{ef} | \partial\mu/\partial R_a | \psi_{ei}\rangle.$$

The third integral vanishes because the derivative of the dipole operator itself
$\mu = \Sigma_i\ e\ \mathbf{r}_j + \Sigma_a\ Z_a\, e\ \ \mathbf{R}_a$ with respect to the coordinates of atomic centers, yields an operator that contains only a sum of scalar quantities (the elementary charge e and the

magnitudes of various atomic charges Z_a); as a result and because the integral over the electronic wavefunctions $\langle \psi_{ef} | \psi_{ei} \rangle$ vanishes, this contribution yields zero. The first and second integrals need not vanish by symmetry because the wavefunction derivatives $\partial\psi_{ef}/\partial R_a$ and $\partial\psi_{ei}/\partial R_a$ do not possess the same symmetry as their respective wavefunctions ψ_{ef} and ψ_{ei}. In fact, it can be shown that the symmetry of such a derivative is given by the direct product of the symmetries of its wavefunction and the symmetry of the vibrational mode that gives rise to the $\partial/\partial R_a$. For the H_2CO case at hand, the b_2 mode vibration can induce in the excited $^1A_2$ state a derivative component (i.e., $\partial\psi_{ef}/\partial R_a$) that is of $^1B_1$ symmetry) and this same vibration can induce in the $^1A_1$ ground state a derivative component of $^1B_2$ symmetry.

As a result, the contribution $\langle \partial\psi_{ef}/\partial R_a | \mu | \psi_{ei} \rangle$ to $\partial\mu_{f,i}/\partial R_a$ arising from vibronic coupling within the excited electronic state can be expected to be non-zero for components of the dipole operator μ that are of $(\partial\psi_{ef}/\partial R_a \times \psi_{ei}) = (B_1 \times A_1) = B_1$ symmetry. Light polarized along the molecule's x-axis gives such a b_1 component to μ (see the C_{2v} character table in Appendix E). The second contribution $\langle \psi_{ef} | \mu | \partial\psi_{ei}/\partial R_a \rangle$ can be non-zero for components of μ that are of $(\psi_{ef} \times \partial\psi_{ei}/\partial R_a) = (A_2 \times B_2) = B_1$ symmetry; again, light of x-axis polarization can induce such a transition.

In summary, electronic transitions that are E1 forbidden by symmetry can derive significant (e.g., in H_2CO the singlet n ==> π^* transition is rather intense) intensity through vibronic coupling. In such coupling, one or more vibrations (either in the initial or the final state) cause the respective electronic wavefunction to acquire (through $\partial\psi/\partial R_a$) a symmetry component that is different than that of ψ itself. The symmetry of $\partial\psi/\partial R_a$, which is given as the direct product of the symmetry of ψ and that of the vibration, can then cause the electric dipole integral $\langle \psi' | \mu | \partial\psi/\partial R_a \rangle$ to be non-zero even when $\langle \psi' | \mu | \psi \rangle$ is zero. Such vibronically allowed transitions are said to derive their intensity through vibronic borrowing.

D. Rotational Selection Rules for Electronic Transitions

Each vibrational peak within an electronic transition can also display rotational structure (depending on the spacing of the rotational lines, the resolution of the spectrometer, and the presence or absence of substantial line broadening effects such as

those discussed later in this Chapter). The selection rules for such transitions are derived in a fashion that parallels that given above for the vibration-rotation case. The major difference between this electronic case and the earlier situation is that the vibrational transition dipole moment μ_{trans} appropriate to the former is replaced by $\mu_{f,i}(\mathbf{R}_e)$ for conventional (i.e., non-vibronic) transitions or $\partial\mu_{f,i}/\partial R_a$ (for vibronic transitions).

As before, when $\mu_{f,i}(\mathbf{R}_e)$ (or $\partial\mu_{f,i}/\partial R_a$) lies along the molecular axis of a linear molecule, the transition is denoted σ and k = 0 applies; when this vector lies perpendicular to the axis it is called π and k = ±1 pertains. The resultant **linear-molecule** rotational selection rules are the same as in the vibration-rotation case:

Δ L = ± 1, and Δ M = ± 1,0 (for σ transitions).

Δ L = ± 1,0 and Δ M = ±1,0 (for π transitions).

In the latter case, the L = L' = 0 situation does not arise because a π transition has one unit of angular momentum along the molecular axis which would preclude both L and L' vanishing.

For **non-linear molecules** of the spherical or symmetric top variety, $\mu_{f,i}(\mathbf{R}_e)$ (or $\partial\mu_{f,i}/\partial R_a$) may be aligned along or perdendicular to a symmetry axis of the molecule. The selection rules that result are

Δ L = ± 1,0; Δ M = ± 1,0; and ΔK = 0 (L = L' = 0 is not allowed and all ΔL = 0 are forbidden when K = K' = 0)

which applies when $\mu_{f,i}(\mathbf{R}_e)$ or $\partial\mu_{f,i}/\partial R_a$ lies along the symmetry axis, and

Δ L = ± 1,0; Δ M = ± 1,0; and ΔK = ± 1 (L = L' = 0 is not allowed)

which applies when $\mu_{f,i}(\mathbf{R}_e)$ or $\partial\mu_{f,i}/\partial R_a$ lies perpendicular to the symmetry axis.

IV. Time Correlation Function Expressions for Transition Rates

The first-order E1 "golden-rule" expression for the rates of photon-induced transitions can be recast into a form in which certain specific physical models are easily introduced and insights are easily gained. Moreover, by using so-called equilibrium averaged time correlation functions, it is possible to obtain rate expressions appropriate to a

large number of molecules that exist in a distribution of initial states (e.g., for molecules that occupy many possible rotational and perhaps several vibrational levels at room temperature).

A. State-to-State Rate of Energy Absorption or Emission

To begin, the expression obtained earlier

$$R_{i,f} = (2\pi/\hbar^2)\, g(\omega_{f,i})\, |\, \mathbf{E}_0 \cdot \langle \Phi_f \,|\, \mu \,|\, \Phi_i \rangle\, |^2 ,$$

that is appropriate to transitions between a particular initial state Φ_i and a specific final state Φ_f, is rewritten as

$$R_{i,f} = (2\pi/\hbar^2) \int g(\omega)\, |\, \mathbf{E}_0 \cdot \langle \Phi_f \,|\, \mu \,|\, \Phi_i \rangle\, |^2\, \delta(\omega_{f,i} - \omega)\, d\omega .$$

Here, the $\delta(\omega_{f,i} - \omega)$ function is used to specifically enforce the "resonance condition" that resulted in the time-dependent perturbation treatment given in Chapter 14; it states that the photons' frequency ω must be resonant with the transition frequency $\omega_{f,i}$. It should be noted that by allowing ω to run over positive and negative values, the photon absorption (with $\omega_{f,i}$ positive and hence ω positive) and the stimulated emission case (with $\omega_{f,i}$ negative and hence ω negative) are both included in this expression (as long as $g(\omega)$ is defined as $g(|\omega|)$ so that the negative-ω contributions are multiplied by the light source intensity at the corresponding positive ω value).

The following integral identity can be used to replace the δ-function:

$$\delta(\omega_{f,i} - \omega) = \frac{1}{2\pi} \int_{-\infty}^{\infty} \exp[i(\omega_{f,i} - \omega)t]\, dt$$

by a form that is more amenable to further development. Then, the state-to-state rate of transition becomes:

$$R_{i,f} = (1/\hbar^2) \oint g(\omega) \mid \mathbf{E}_0 \cdot \langle \Phi_f \mid \mu \mid \Phi_i \rangle|^2 \int_{-\infty}^{\infty} \exp[i(\omega_{f,i} - \omega)t]\, dt\, d\omega .$$

B. Averaging Over Equilibrium Boltzmann Population of Initial States

If this expression is then multiplied by the **equilibrium probability** ρ_i that the molecule is found in the state Φ_i and summed over all such initial states and summed over all final states Φ_f that can be reached from Φ_i with photons of energy $\hbar\omega$, the equilibrium averaged rate of photon absorption by the molecular sample is obtained:

$$R_{eq.ave.} = (1/\hbar^2) \sum_{i,\, f} \rho_i$$

$$\oint g(\omega) \mid \mathbf{E}_0 \cdot \langle \Phi_f \mid \mu \mid \Phi_i \rangle|^2 \int_{-\infty}^{\infty} \exp[i(\omega_{f,i} - \omega)t]\, dt\, d\omega .$$

This expression is appropriate for an ensemble of molecules that can be in various initial states Φ_i with probabilities ρ_i. The corresponding result for transitions that originate in a particular state (Φ_i) but end up in any of the "allowed" (by energy and selection rules) final states reads:

$$R_{state\ i.} = (1/\hbar^2) \sum_f \int g(\omega) \mid \mathbf{E}_0 \cdot \langle \Phi_f \mid \mu \mid \Phi_i \rangle|^2$$

$$\int_{-\infty}^{\infty} \exp[i(\omega_{f,i} - \omega)t]\, dt d\omega .$$

For a canonical ensemble, in which the number of molecules, the temperature, and the system volume are specified, ρ_i takes the form:

$$\rho_i = \frac{g_i \exp(-E_i^0/kT)}{Q}$$

where Q is the canonical partition function of the molecules and g_i is the degeneracy of the state Φ_i whose energy is E_i^0.

In the above expression for $R_{eq.ave.}$, a double sum occurs. Writing out the elements that appear in this sum in detail, one finds:

$$\sum_{i,\,f}\ \rho_i\ \mathbf{E}_0 \cdot\ <\Phi_i \mid \mu \mid \Phi_f>\ \mathbf{E}_0 \cdot\ <\Phi_f \mid \mu \mid \Phi_i>\ \exp i(\omega_{f,i})t.$$

In situations in which one is interested in developing an expression for the intensity arising from transitions to <u>all</u> allowed final states, the sum over these final states can be carried out explicitly by first writing

$$<\Phi_f \mid \mu \mid \Phi_i>\ \exp i(\omega_{f,i})t = <\Phi_f \mid \exp(iHt/\hbar)\ \mu\ \exp(-iHt/\hbar) \mid \Phi_i>$$

and then using the fact that the set of states $\{\Phi_k\}$ are complete and hence obey

$$\sum_k |\Phi_k><\Phi_k| = 1.$$

The result of using these identities as well as the **Heisenberg definition** of the time-dependence of the dipole operator

$$\mu(t) = \exp(iHt/\hbar)\ \mu\ \exp(-iHt/\hbar),$$

is:

$$\sum_i \rho_i\ \ <\Phi_i \mid \mathbf{E}_0 \cdot\ \mu\ \ \mathbf{E}_0 \cdot\ \mu\ (t) \mid \Phi_i>\ .$$

In this form, one says that the time dependence has been reduce to that of an equilibrium averaged (n.b., the $\sum_i \rho_i <\Phi_i \mid\ \mid \Phi_i>$) **time correlation function** involving the component of the dipole operator along the external electric field at t = 0 ($\mathbf{E}_0 \cdot\ \mu$) and this component at a different time t ($\mathbf{E}_0 \cdot\ \mu\ (t)$).

C. Photon Emission and Absorption

If $\omega_{f,i}$ is positive (i.e., in the photon absorption case), the above expression will yield a non-zero contribution when multiplied by exp(-i ωt) and integrated over positive ω-values. If $\omega_{f,i}$ is negative (as for stimulated photon emission), this expression will contribute, again when multiplied by exp(-i ωt), for negative ω-values. In the latter situation, ρ_i is the equilibrium probability of finding the molecule in the (excited) state from which emission will occur; this probability can be related to that of the lower state ρ_f by

$$\rho_{excited} = \rho_{lower} \exp[- (E^0_{excited} - E^0_{lower})/kT]$$

$$= \rho_{lower} \exp[- \hbar\omega/kT].$$

In this form, it is important to realize that the excited and lower states are treated as individual states, not as levels that might contain a degenerate set of states.

The absorption and emission cases can be combined into a single net expression for the rate of photon absorption by recognizing that the latter process leads to photon production, and thus must be entered with a negative sign. The resultant expression for the net rate of decrease of photons is:

$$R_{eq.ave.net} = (1/\hbar^2) \sum_i \rho_i (1 - \exp(-\hbar\omega/kT))$$

$$\int\int g(\omega) \, \langle \Phi_i \mid (\mathbf{E}_0 \cdot \mu) \, \mathbf{E}_0 \cdot \mu(t) \mid \Phi_i \rangle \exp(-i\omega t) \, d\omega \, dt.$$

D. The Line Shape and Time Correlation Functions

Now, it is convention to introduce the so-called "line shape" function I (ω):

$$I(\omega) = \sum_i \rho_i \int \langle \Phi_i \mid (\mathbf{E}_0 \cdot \mu) \, \mathbf{E}_0 \cdot \mu(t) \mid \Phi_i \rangle \exp(-i\omega t) \, dt$$

in terms of which the net photon absorption rate is

$$R_{eq.ave.net} = (1/\hbar^2)\,(1 - \exp(-\hbar\omega/kT))\int g(\omega)\, I(\omega)\, d\omega .$$

As stated above, the function

$$C(t) = \sum_i \rho_i \langle \Phi_i | (\mathbf{E}_0 \cdot \mu)\, \mathbf{E}_0 \cdot \mu(t) | \Phi_i \rangle$$

is called the equilibrium averaged **time correlation function** of the component of the electric dipole operator along the direction of the external electric field $\mathbf{E}_0$. Its Fourier transform is I (ω), the **spectral line shape** function. The convolution of I (ω) with the light source's g (ω) function, multiplied by
(1 - exp(-ħ ω/kT)), the correction for stimulated photon emission, gives the net rate of photon absorption.

E. Rotational, Translational, and Vibrational Contributions to the Correlation Function

To apply the time correlation function machinery to each particular kind of spectroscopic transition, one proceeds as follows:

1. For purely **rotational transitions**, the initial and final electronic and vibrational states are the same. Moreover, the electronic and vibrational states are not summed over in the analog of the above development because one is interested in obtaining an expression for a particular $\chi_{iv}\,\psi_{ie} \Longrightarrow \chi_{fv}\,\psi_{fe}$ electronic-vibrational transition's lineshape. As a result, the sum over final states contained in the expression (see earlier) $\sum_{i,f} \rho_i\, \mathbf{E}_0 \cdot \langle \Phi_i | \mu | \Phi_f \rangle\, \mathbf{E}_0 \cdot \langle \Phi_f | \mu(t) | \Phi_i \rangle \exp(i\omega_{f,i})t$ applies only to summing over final rotational states. In more detail, this can be shown as follows:

$$\sum_{i,f} \rho_i\, \mathbf{E}_0 \cdot \langle \Phi_i | \mu | \Phi_f \rangle\, \mathbf{E}_0 \cdot \langle \Phi_f | \mu(t) | \Phi_i \rangle$$

$$= \sum_{i,f} \rho_i\, \mathbf{E}_0 \cdot \langle \varphi_{ir}\chi_{iv}\psi_{ie} | \mu | \varphi_{fr}\chi_{iv}\psi_{ie} \rangle\, \mathbf{E}_0 \cdot \langle \varphi_{fr}\chi_{iv}\psi_{ie} | \mu(t) | \varphi_{ir}\chi_{iv}\psi_{ie} \rangle$$

$$= \sum_{i,f} \rho_{ir}\rho_{iv}\rho_{ie}\, \mathbf{E}_0 \cdot \langle \varphi_{ir}\chi_{iv} | \mu(\mathbf{R}) | \varphi_{fr}\chi_{iv} \rangle\, \mathbf{E}_0 \cdot \langle \varphi_{fr}\chi_{iv} | \mu(\mathbf{R},t) | \varphi_{ir}\chi_{iv} \rangle$$

$$= \sum_{i,f} \rho_{ir}\rho_{iv}\rho_{ie}\, \mathbf{E}_0 \cdot \langle \varphi_{ir} | \mu_{ave.iv} | \varphi_{fr} \rangle\, \mathbf{E}_0 \cdot \langle \varphi_{fr} | \mu_{ave.iv}(t) | \varphi_{ir} \rangle$$

$$= \sum_i \rho_{ir}\,\rho_{iv}\,\rho_{ie}\,\mathbf{E}_0 \cdot \langle \varphi_{ir} | \mu_{ave.iv}\ \mathbf{E}_0 \cdot \ \mu_{ave.iv}(t) | \varphi_{ir} \rangle .$$

In moving from the second to the third lines of this derivation, the following identity was used:

$$\langle \varphi_{fr}\,\chi_{iv}\,\psi_{ie} | \mu(t) | \varphi_{ir}\,\chi_{iv}\,\psi_{ie} \rangle = \langle \varphi_{fr}\,\chi_{iv}\,\psi_{ie} | \exp(iHt/\hbar)$$

$$\mu \exp(-iHt/\hbar) | \varphi_{ir}\,\chi_{iv}\,\psi_{ie} \rangle$$

$$= \langle \varphi_{fr}\,\chi_{iv}\,\psi_{ie} | \exp(iH_{v,r}t/\hbar)\,\mu(\mathbf{R})\,\exp(-iH_{v,r}t/\hbar) | \varphi_{ir}\,\chi_{iv}\,\psi_{ie} \rangle ,$$

where H is the full (electronic plus vibrational plus rotational) Hamiltonian and $H_{v,r}$ is the vibrational and rotational Hamiltonian for motion on the electronic surface of the state ψ_{ie} whose dipole moment is $\mu(\mathbf{R})$. From the third line to the fourth, the (approximate) separation of rotational and vibrational motions in $H_{v,r}$

$$H_{v,r} = H_v + H_r$$

has been used along with the fact that χ_{iv} is an eigenfunction of H_v:

$$H_v\,\chi_{iv} = E_{iv}\,\chi_{iv}$$

to write

$$\langle \chi_{iv} | \mu(\mathbf{R},t) | \chi_{iv} \rangle = \exp(i H_r t/\hbar) \langle \chi_{iv} | \exp(iH_v t/\hbar)$$

$$\mu(\mathbf{R}) \exp(-iH_v t/\hbar) | \chi_{iv} \rangle \exp(-iH_r t/\hbar)$$

$$= \exp(i H_r t/\hbar) \langle \chi_{iv} | \exp(iE_{iv} t/\hbar)$$

$$\mu(\mathbf{R}) \exp(-iE_{iv} t/\hbar) | \chi_{iv} \rangle \exp(-iH_r t/\hbar)$$

$$= \exp(i H_r t/\hbar) \langle \chi_{iv} | \mu(\mathbf{R}) | \chi_{iv} \rangle \exp(-iH_r t/\hbar)$$

$= \mu_{ave.iv}(t)$.

In effect, μ is replaced by the vibrationally averaged electronic dipole moment $\mu_{ave,iv}$ for each initial vibrational state that can be involved, and the time correlation function thus becomes:

$$C(t) = \sum_i \rho_{ir}\,\rho_{iv}\;\rho_{ie} \langle \varphi_{ir} \,|\, (\mathbf{E}_0 \cdot \mu_{ave,iv})\, \mathbf{E}_0 \cdot \mu_{ave,iv}(t) \,|\, \varphi_{ir} \rangle ,$$

where $\mu_{ave,iv}(t)$ is the averaged dipole moment for the vibrational state χ_{iv} at time t, given that it was $\mu_{ave,iv}$ at time t = 0. The time dependence of $\mu_{ave,iv}(t)$ is induced by the rotational Hamiltonian H_r, as shown clearly in the steps detailed above:

$$\mu_{ave,iv}(t) = \exp(i H_r t/\hbar) \langle \chi_{iv} \,|\, \mu(\mathbf{R}) \,|\, \chi_{iv} \rangle \exp(-iH_r t/\hbar).$$

In this particular case, the equilibrium average is taken over the initial rotational states whose probabilities are denoted ρ_{ir} , any initial vibrational states that may be populated, with probabilities ρ_{iv}, and any populated electronic states, with probabilities ρ_{ie}.

2. For **vibration-rotation transitions** within a single electronic state, the initial and final electronic states are the same, but the initial and final vibrational and rotational states differ. As a result, the sum over final states contained in the expression $\sum_{i,\,f}\, \rho_i\, \mathbf{E}_0 \cdot \langle \Phi_i \,|\, \mu \,|\, \Phi_f \rangle\, \mathbf{E}_0 \cdot \langle \Phi_f \,|\, \mu \,|\, \Phi_i \rangle \exp i(\omega_{f,i})t$ applies only to summing over final vibrational and rotational states. Paralleling the development made in the pure rotation case given above, this can be shown as follows:

$$\sum_{i,\,f}\, \rho_i\, \mathbf{E}_0 \cdot \langle \Phi_i \,|\, \mu \,|\, \Phi_f \rangle\, \mathbf{E}_0 \cdot \langle \Phi_f \,|\, \mu(t) \,|\, \Phi_i \rangle$$

$$= \sum_{i,\,f}\, \rho_i\, \mathbf{E}_0 \cdot \langle \varphi_{ir}\, \chi_{iv}\, \psi_{ie} \,|\, \mu \,|\, \varphi_{fr}\, \chi_{fv}\, \psi_{ie} \rangle\, \mathbf{E}_0 \cdot \langle \varphi_{fr}\, \chi_{fv}\, \psi_{ie} \,|\, \mu(t) \,|\, \varphi_{ir}\, \chi_{iv}\, \psi_{ie} \rangle$$

$$= \sum_{i,\,f}\, \rho_{ir}\, \rho_{iv}\, \rho_{ie}\, \mathbf{E}_0 \cdot \langle \varphi_{ir}\, \chi_{iv} \,|\, \mu(\mathbf{R}) \,|\, \varphi_{fr}\, \chi_{fv} \rangle\, \mathbf{E}_0 \cdot \langle \varphi_{fr}\, \chi_{fv} \,|\, \mu(\mathbf{R},t) \,|\, \varphi_{ir}\, \chi_{iv} \rangle$$

$$= \sum_{i,\,f}\, \rho_{ir}\, \rho_{iv}\, \rho_{ie}\, \mathbf{E}_0 \cdot \langle \varphi_{ir}\, \chi_{iv} \,|\, \mu(\mathbf{R}_e) + \sum_a (R_a - R_{a,eq}) \partial\mu/\partial R_a \,|\, \varphi_{fr}\, \chi_{fv} \rangle$$

$$\mathbf{E}_0 \cdot \langle \varphi_{fr}\, \chi_{fv} | \exp(iH_r t/\hbar)(\mu(\mathbf{R}_e) + \sum_a (R_a - R_{a,eq})\partial\mu/\partial R_a)$$

$$\exp(-iH_r t/\hbar) | \varphi_{ir}\chi_{iv} \rangle \exp(i\omega_{fv,iv} t)$$

$$= \sum_{ir,\, iv,\, ie} \rho_{ir}\, \rho_{iv}\, \rho_{ie} \sum_{fv,fr} \sum_a \langle \chi_{iv} | (R_a - R_{a,eq}) | \chi_{fv} \rangle$$

$$\sum_{a'} \langle \chi_{fv} | (R_{a'} - R_{a',eq}) | \chi_{iv} \rangle \exp(i\omega_{fv,iv} t)$$

$$\mathbf{E}_0 \cdot \langle \varphi_{ir} | \partial\mu/\partial R_a \;\; \mathbf{E}_0 \cdot \exp(iH_r t/\hbar) \partial\mu/\partial R_{a'} \exp(-iH_r t/\hbar) | \varphi_{ir} \rangle$$

$$= \sum_{ir,\, iv,\, ie} \rho_{ir}\, \rho_{iv}\, \rho_{ie} \sum_{fv,fr} \exp(i\omega_{fv,iv} t)$$

$$\langle \varphi_{ir} | (\mathbf{E}_0 \cdot \mu_{trans})\, \mathbf{E}_0 \cdot \exp(iH_r t/\hbar)\, \mu_{trans} \exp(-iH_r t/\hbar) | \varphi_{ir} \rangle,$$

where the vibrational transition dipole matrix element is defined as before

$$\mu_{trans} = \sum_a \langle \chi_{iv} | (R_a - R_{a,eq}) | \chi_{fv} \rangle \, \partial\mu/\partial R_a \,,$$

and derives its time dependence above from the rotational Hamiltonian:

$$\mu_{trans}(t) = \exp(iH_r t/\hbar)\, \mu_{trans} \exp(-iH_r t/\hbar).$$

The corresponding final expression for the time correlation function C(t) becomes:

$$C(t) = \sum_i \rho_{ir}\, \rho_{iv}\, \rho_{ie} \langle \varphi_{ir} | (\mathbf{E}_0 \cdot \mu_{trans})\, \mathbf{E}_0 \cdot \mu_{trans}(t) | \varphi_{ir} \rangle \exp(i\omega_{fv,iv} t).$$

The net rate of photon absorption remains:

$$R_{eq.ave.net} = (1/\hbar^2)(1 - \exp(-\hbar\omega)) \int g(\omega)\, I(\omega)\, d\omega \,,$$

where $I(\omega)$ is the Fourier transform of $C(t)$.

The expression for $C(t)$ clearly contains two types of time dependences: (i) the $\exp(i\omega_{fv,iv} t)$, upon Fourier transforming to obtain $I(\omega)$, produces δ-function "spikes" at

frequencies $\omega = \omega_{fv,iv}$ equal to the spacings between the initial and final vibrational states, and (ii) rotational motion time dependence that causes $\mu_{trans}(t)$ to change with time. The latter appears in the form of a correlation function for the component of μ_{trans} along $\mathbf{E}_0$ at time t = 0 and this component at another time t. The convolution of both these time dependences determines the from of $I(\omega)$.

3. For **electronic-vibration-rotation transitions**, the initial and final electronic states are different as are the initial and final vibrational and rotational states. As a result, the sum over final states contained in the expression $\sum_{i,f} \rho_i \mathbf{E}_0 \cdot \langle\Phi_i|\mu|\Phi_f\rangle \mathbf{E}_0 \cdot \langle\Phi_f|\mu|\Phi_i\rangle \exp i(\omega_{f,i})t$ applies to summing over final electronic, vibrational, and rotational states. Paralleling the development made in the pure rotation case given above, this can be shown as follows:

$$\sum_{i,f} \rho_i \mathbf{E}_0 \cdot \langle\Phi_i|\mu|\Phi_f\rangle \mathbf{E}_0 \cdot \langle\Phi_f|\mu(t)|\Phi_i\rangle$$

$$= \sum_{i,f} \rho_i \mathbf{E}_0 \cdot \langle\varphi_{ir}\chi_{iv}\psi_{ie}|\mu|\varphi_{fr}\chi_{fv}\psi_{fe}\rangle \mathbf{E}_0 \cdot \langle\varphi_{fr}\chi_{fv}\psi_{fe}|\mu(t)|\varphi_{ir}\chi_{iv}\psi_{ie}\rangle$$

$$= \sum_{i,f} \rho_{ir}\rho_{iv}\rho_{ie} \mathbf{E}_0 \cdot \langle\varphi_{ir}\chi_{iv}|\mu_{i,f}(\mathbf{R})|\varphi_{fr}\chi_{fv}\rangle \mathbf{E}_0 \cdot \langle\varphi_{fr}\chi_{fv}|\mu_{i,f}(\mathbf{R},t)|\varphi_{ir}\chi_{iv}\rangle$$

$$= \sum_{i,f} \rho_{ir}\rho_{iv}\rho_{ie} \mathbf{E}_0 \cdot \langle\varphi_{ir}|\mu_{i,f}(\mathbf{R}_e)|\varphi_{fr}\rangle |\langle\chi_{iv}|\chi_{fv}\rangle|^2$$

$$\mathbf{E}_0 \cdot \langle\varphi_{fr}|\exp(iH_rt/\hbar)\,\mu_{i,f}(\mathbf{R}_e)\exp(-iH_rt/\hbar)|\varphi_{ir}\rangle \exp(i\omega_{fv,iv}t + i\Delta E_{i,f}t/\hbar)$$

$$= \sum_{i,f} \rho_{ir}\rho_{iv}\rho_{ie} \langle\varphi_{ir}|\mathbf{E}_0 \cdot \mu_{i,f}(\mathbf{R}_e)\,\mathbf{E}_0 \cdot \mu_{i,f}(\mathbf{R}_e,t)|\varphi_{ir}\rangle |\langle\chi_{iv}|\chi_{fv}\rangle|^2$$

$$\exp(i\omega_{fv,iv}t + i\Delta E_{i,f}t/\hbar),$$

where

$$\mu_{i,f}(\mathbf{R}_e,t) = \exp(iH_rt/\hbar)\,\mu_{i,f}(\mathbf{R}_e)\exp(-iH_rt/\hbar)$$

is the electronic transition dipole matrix element, evaluated at the equilibrium geometry of the absorbing state, that derives its time dependence from the rotational Hamiltonian H_r as in the time correlation functions treated earlier.

This development thus leads to the following definition of C(t) for the electronic, vibration, and rotation case:

$$C(t) = \sum_{i,\,f} \rho_{ir}\,\rho_{iv}\,\rho_{ie}\; \langle \varphi_{ir} \,|\, \mathbf{E}_0 \cdot \mu_{i,f}(\mathbf{R}_e)\, \mathbf{E}_0 \cdot \mu_{i,f}(\mathbf{R}_e,t) \,|\varphi_{ir}\rangle \, |\langle \chi_{iv} \,|\, \chi_{fv}\rangle|^2$$

$$\exp(i\omega_{fv,iv}t + i\Delta E_{i,f}t/\hbar)$$

but the net rate of photon absorption remains:

$$R_{eq.ave.net} = (1/\hbar^2)\,(1 - \exp(-\hbar\omega/kT))\int g(\omega)\, I\,(\omega)\, d\omega .$$

Here, $I(\omega)$ is the Fourier transform of the above C(t) and $\Delta E_{i,f}$ is the adiabatic electronic energy difference (i.e., the energy difference between the v = 0 level in the final electronic state and the v = 0 level in the initial electronic state) for the electronic transition of interest. The above C(t) clearly contains Franck-Condon factors as well as time dependence $\exp(i\omega_{fv,iv}t + i\Delta E_{i,f}t/\hbar)$ that produces δ-function spikes at each electronic-vibrational transition frequency and rotational time dependence contained in the time correlation function quantity $\langle \varphi_{ir} \,|\, \mathbf{E}_0 \cdot \mu_{i,f}(\mathbf{R}_e)\, \mathbf{E}_0 \cdot \mu_{i,f}(\mathbf{R}_e,t) \,|\varphi_{ir}\rangle$.

To summarize, the line shape function $I(\omega)$ produces the net rate of photon absorption

$$R_{eq.ave.net} = (1/\hbar^2)\,(1 - \exp(-\hbar\omega/kT))\int g(\omega)\, I\,(\omega)\, d\omega$$

in all of the above cases, and $I(\omega)$ is the Fourier transform of a corresponding time-dependent C(t) function in all cases. However, the pure rotation, vibration-rotation, and electronic-vibration-rotation cases differ in the form of their respective C(t)'s. Specifically,

$$C\,(t) = \sum_i \rho_{ir}\,\rho_{iv}\;\rho_{ie}\,\langle \varphi_{ir} \,|\, (\mathbf{E}_0 \cdot \mu_{ave,iv})\, \mathbf{E}_0 \cdot \mu_{ave,iv}\,(t) \,|\, \varphi_{ir}\rangle$$

in the pure rotational case,

$$C(t) = \sum_i \rho_{ir}\,\rho_{iv}\,\rho_{ie} \langle \varphi_{ir} | (\mathbf{E}_0 \cdot \mu_{trans})\, \mathbf{E}_0 \cdot \mu_{trans}(t) | \varphi_{ir} \rangle \exp(i\omega_{fv,iv} t)$$

in the vibration-rotation case, and

$$C(t) = \sum_{i,f} \rho_{ir}\,\rho_{iv}\,\rho_{ie} \langle \varphi_{ir} | \mathbf{E}_0 \cdot \mu_{i,f}(\mathbf{R}_e)\, \mathbf{E}_0 \cdot \mu_{i,f}(\mathbf{R}_e,t) | \varphi_{ir} \rangle |\langle \chi_{iv} | \chi_{fv} \rangle|^2$$

$$\exp(i\omega_{fv,iv} t + \Delta E_{i,f} t/\hbar)$$

in the electronic-vibration-rotation case.

All of these time correlation functions contain time dependences that arise from rotational motion of a dipole-related vector (i.e., the vibrationally averaged dipole $\mu_{ave,iv}(t)$, the vibrational transition dipole $\mu_{trans}(t)$, or the electronic transition dipole $\mu_{i,f}(\mathbf{R}_e,t)$) and the latter two also contain oscillatory time dependences (i.e., $\exp(i\omega_{fv,iv}t)$ or $\exp(i\omega_{fv,iv}t + i\Delta E_{i,f}t/\hbar)$) that arise from vibrational or electronic-vibrational energy level differences. In the treatments of the following sections, consideration is given to the rotational contributions under circumstances that characterize, for example, dilute gaseous samples where the collision frequency is low and liquid-phase samples where rotational motion is better described in terms of diffusional motion.

F. Line Broadening Mechanisms

If the rotational motion of the molecules is assumed to be entirely unhindered (e.g., by any environment or by collisions with other molecules), it is appropriate to express the time dependence of each of the dipole time correlation functions listed above in terms of a "free rotation" model. For example, when dealing with diatomic molecules, the electronic-vibrational-rotational C(t) appropriate to a specific electronic-vibrational transition becomes:

$$C(t) = (q_r\, q_v\, q_e\, q_t)^{-1} \sum_J (2J+1) \exp(-h^2 J(J+1)/(8\pi^2 I k T)) \exp(-h\nu_{vib} v i / kT)$$

$$g_{ie} \langle \varphi_J | \mathbf{E}_0 \cdot \mu_{i,f}(\mathbf{R}_e)\, \mathbf{E}_0 \cdot \mu_{i,f}(\mathbf{R}_e,t) | \varphi_J \rangle |\langle \chi_{iv} | \chi_{fv} \rangle|^2$$

$$\exp(i\,[h\nu_{vib}]\, t + i\Delta E_{i,f}\, t/\hbar).$$

Here,

$$q_r = (8\pi^2 IkT/h^2)$$

is the rotational partition function (I being the molecule's moment of inertia $I = \mu R_e^2$, and $h^2J(J+1)/(8\pi^2 I)$ the molecule's rotational energy for the state with quantum number J and degeneracy 2J+1)

$$q_v = \exp(-h\nu_{vib}/2kT)\ (1-\exp(-h\nu_{vib}/kT))^{-1}$$

is the vibrational partition function (ν_{vib} being the vibrational frequency), g_{ie} is the degeneracy of the initial electronic state,

$$q_t = (2\pi mkT/h^2)^{3/2}\ V$$

is the translational partition function for the molecules of mass m moving in volume V, and $\Delta E_{i,f}$ is the adiabatic electronic energy spacing.

The functions $\langle\varphi_J \mid \mathbf{E}_0 \cdot \mu_{i,f}(\mathbf{R}_e)\ \mathbf{E}_0 \cdot \mu_{i,f}(\mathbf{R}_e,t) \mid\varphi_J\rangle$ describe the time evolution of the dipole-related vector (the electronic transition dipole in this case) for the rotational state J. In a "free-rotation" model, this function is taken to be of the form:

$$\langle\varphi_J \mid \mathbf{E}_0 \cdot \mu_{i,f}(\mathbf{R}_e)\ \mathbf{E}_0 \cdot \mu_{i,f}(\mathbf{R}_e,t) \mid\varphi_J\rangle$$

$$= \langle\varphi_J \mid \mathbf{E}_0 \cdot \mu_{i,f}(\mathbf{R}_e)\ \mathbf{E}_0 \cdot \mu_{i,f}(\mathbf{R}_e,0) \mid\varphi_J\rangle\ \mathrm{Cos}\frac{h\ J(J+1)\ t}{4\pi I}\ ,$$

where

$$\frac{h\ J(J+1)}{4\pi I} = \omega_J$$

is the rotational frequency (in cycles per second) for rotation of the molecule in the state labeled by J. This oscillatory time dependence, combined with the $\exp(i\omega_{fv,iv}t + i\Delta E_{i,f}t/\hbar)$ time dependence arising from the electronic and vibrational factors, produce, when this C(t) function is Fourier transformed to generate $I(\omega)$ a series of δ-function "peaks" whenever

$$\omega = \omega_{fv,iv} + \Delta E_{i,f}/\hbar \pm \omega_J\ .$$

The intensities of these peaks are governed by the

$$(q_r\, q_v\, q_e\, q_t)^{-1} \sum_J (2J+1) \exp(- h^2 J(J+1)/(8\pi^2 IkT)) \exp(- h\nu_{vib} vi /kT)\, g_{ie}$$

Boltzmann population factors as well as by the $|\langle\chi_{iv} | \chi_{fv}\rangle|^2$ Franck-Condon factors and the $\langle\varphi_J | \mathbf{E}_0 \cdot \mu_{i,f}(\mathbf{R}_e)\, \mathbf{E}_0 \cdot \mu_{i,f}(\mathbf{R}_e,0) |\varphi_J\rangle$ terms.

This same analysis can be applied to the pure rotation and vibration-rotation C(t) time dependences with analogous results. In the former, δ-function peaks are predicted to occur at

$$\omega = \pm \omega_J$$

and in the latter at

$$\omega = \omega_{fv,iv} \pm \omega_J ;$$

with the intensities governed by the time independent factors in the corresponding expressions for C(t).

In experimental measurements, such sharp δ-function peaks are, of course, not observed. Even when very narrow band width laser light sources are used (i.e., for which g(ω) is an extremely narrowly peaked function), spectral lines are found to possess finite widths. Let us now discuss several sources of line broadening, some of which will relate to deviations from the "unhindered" rotational motion model introduced above.

1. Doppler Broadening

In the above expressions for C(t), the averaging over initial rotational, vibrational, and electronic states is explicitly shown. There is also an average over the translational motion implicit in all of these expressions. Its role has not (yet) been emphasized because the molecular energy levels, whose spacings yield the characteristic frequencies at which light can be absorbed or emitted, do not depend on translational motion. However, the frequency of the electromagnetic field experienced by moving molecules does depend on the velocities of the molecules, so this issue must now be addressed.

Elementary physics classes express the so-called **Doppler shift** of a wave's frequency induced by movement either of the light source or of the molecule (Einstein tells us these two points of view must give identical results) as follows:

$$\omega_{observed} = \omega_{nominal} (1 + v_z/c)^{-1} \approx \omega_{nominal} (1 - v_z/c + ...).$$

Here, $\omega_{nominal}$ is the frequency of the unmoving light source seen by unmoving molecules, v_z is the velocity of relative motion of the light source and molecules, c is the speed of light, and $\omega_{observed}$ is the Doppler shifted frequency (i.e., the frequency seen by the molecules). The second identity is obtained by expanding, in a power series, the $(1 + v_z/c)^{-1}$ factor, and is valid in truncated form when the molecules are moving with speeds significantly below the speed of light.

For all of the cases considered earlier, a C(t) function is subjected to Fourier transformation to obtain a spectral lineshape function $I(\omega)$, which then provides the essential ingredient for computing the net rate of photon absorption. In this Fourier transform process, the variable ω is assumed to be the frequency of the electromagnetic field experienced by the molecules. The above considerations of Doppler shifting then leads one to realize that the correct functional form to use in converting C(t) to $I(\omega)$ is:

$$I(\omega) = \int C(t) \exp(-it\omega(1-v_z/c)) \, dt \, ,$$

where ω is the nominal frequency of the light source.

As stated earlier, within C(t) there is also an equilibrium average over translational motion of the molecules. For a gas-phase sample undergoing random collisions and at thermal equilibrium, this average is characterized by the well known Maxwell-Boltzmann velocity distribution:

$$(m/2\pi kT)^{3/2} \exp(-m (v_x^2+v_y^2+v_z^2)/2kT) \, dv_x \, dv_y \, dv_z.$$

Here m is the mass of the molecules and v_x, v_y, and v_z label the velocities along the lab-fixed cartesian coordinates.

Defining the z-axis as the direction of propagation of the light's photons and carrying out the averaging of the Doppler factor over such a velocity distribution, one obtains:

$$\int_{-\infty}^{\infty} \exp(-it\omega(1-v_z/c)) \, (m/2\pi kT)^{3/2} \exp(-m (v_x^2+v_y^2+v_z^2)/2kT) \, dv_x \, dv_y \, dv_z$$

$$= \exp(-i\omega t) \int_{-\infty}^{\infty} (m/2\pi kT)^{1/2} \exp(i\omega t v_z/c) \exp(-mv_z^2/2kT)\, dv_z$$

$$= \exp(-i\omega t) \exp(-\omega^2 t^2 kT/(2mc^2)).$$

This result, when substituted into the expressions for C(t), yields expressions identical to those given for the three cases treated above but with one modification. The translational motion average need no longer be considered in each C(t); instead, the earlier expressions for C(t) must each be multiplied by a factor $\exp(-\omega^2 t^2 kT/(2mc^2))$ that embodies the translationally averaged Doppler shift. The spectral line shape function I(ω) can then be obtained for each C(t) by simply Fourier transforming:

$$I(\omega) = \int_{-\infty}^{\infty} \exp(-i\omega t)\, C(t)\, dt\ .$$

When applied to the rotation, vibration-rotation, or electronic-vibration-rotation cases within the "unhindered" rotation model treated earlier, the Fourier transform involves integrals of the form:

$$I(\omega) = \int_{-\infty}^{\infty} \exp(-i\omega t)\, \exp(-\omega^2 t^2 kT/(2mc^2)) \exp(i(\omega_{fv,iv} + \Delta E_{i,f}/\hbar \pm \omega_J)t)\, dt\ .$$

This integral would arise in the electronic-vibration-rotation case; the other two cases would involve integrals of the same form but with the $\Delta E_{i,f}/\hbar$ absent in the vibration-rotation situation and with $\omega_{fv,iv} + \Delta E_{i,f}/\hbar$ missing for pure rotation transitions. All such integrals can be carried out analytically and yield:

$$I(\omega) = \sqrt{\frac{2mc^2\pi}{\omega^2 kT}}\ \exp[\ -(\omega - \omega_{fv,iv} - \Delta E_{i,f}/\hbar \pm \omega_J)^2\, mc^2/(2\omega^2 kT)].$$

The result is a series of **Gaussian** "peaks" in ω-space, centered at:

$$\omega = \omega_{fv,iv} + \Delta E_{i,f}/\hbar \pm \omega_J$$

with widths (σ) determined by

$$\sigma^2 = \omega^2 kT/(mc^2),$$

given the temperature T and the mass of the molecules m. The hotter the sample, the faster the molecules are moving on average, and the broader is the distribution of Doppler shifted frequencies experienced by these molecules. The net result then of the Doppler effect is to produce a line shape function that is similar to the "unhindered" rotation model's series of δ-functions but with each δ-function peak broadened into a Gaussian shape.

2. Pressure Broadening

To include the effects of collisions on the rotational motion part of any of the above C(t) functions, one must introduce a model for how such collisions change the dipole-related vectors that enter into C(t). The most elementary model used to address collisions applies to gaseous samples which are assumed to undergo unhindered rotational motion until struck by another molecule at which time a randomizing "kick" is applied to the dipole vector and after which the molecule returns to its unhindered rotational movement.

The effects of such collisionally induced kicks are treated within the so-called **pressure broadening** (sometimes called collisional broadening) model by modifying the free-rotation correlation function through the introduction of an exponential damping factor $\exp(-|t|/\tau)$:

$$<\varphi_J | \mathbf{E}_0 \cdot \mu_{i,f}(\mathbf{R}_e) \mathbf{E}_0 \cdot \mu_{i,f}(\mathbf{R}_e,0) |\varphi_J> \mathrm{Cos} \frac{h\ J(J+1)\ t}{4\pi I}$$

$$<\varphi_J | \mathbf{E}_0 \cdot \mu_{i,f}(\mathbf{R}_e) \mathbf{E}_0 \cdot \mu_{i,f}(\mathbf{R}_e,0) |\varphi_J> \mathrm{Cos} \frac{h\ J(J+1)\ t}{4\pi I} \exp(-|t|/\tau).$$

This damping function's time scale parameter τ is assumed to characterize the average time between collisions and thus should be inversely proportional to the collision frequency. Its magnitude is also related to the effectiveness with which collisions cause the dipole function to deviate from its unhindered rotational motion (i.e., related to the collision strength). In effect, the exponential damping causes the time correlation function $<\varphi_J | \mathbf{E}_0 \cdot$

$\mu_{i,f}(\mathbf{R}_e)\,\mathbf{E}_0 \cdot \mu_{i,f}(\mathbf{R}_e,t)\,|\varphi_J\rangle$ to "lose its memory" and to decay to zero; this "memory" point of view is based on viewing $\langle\varphi_J|\,\mathbf{E}_0 \cdot \mu_{i,f}(\mathbf{R}_e)\,\mathbf{E}_0 \cdot \mu_{i,f}(\mathbf{R}_e,t)\,|\varphi_J\rangle$ as the projection of $\mathbf{E}_0 \cdot \mu_{i,f}(\mathbf{R}_e,t)$ along its t = 0 value $\mathbf{E}_0 \cdot \mu_{i,f}(\mathbf{R}_e,0)$ as a function of time t.

Introducing this additional $\exp(-|t|/\tau)$ time dependence into C(t) produces, when C(t) is Fourier transformed to generate I(ω),

$$I(\omega) = \int_{-\infty}^{\infty} \exp(-i\omega t)\exp(-|t|/\tau)\exp(-\omega^2 t^2 kT/(2mc^2))\exp(i(\omega_{fv,iv}+\Delta E_{i,f}/\hbar \pm \omega_J)t)dt\ .$$

In the limit of very small Doppler broadening, the $(\omega^2 t^2 kT/(2mc^2))$ factor can be ignored (i.e., $\exp(-\omega^2 t^2 kT/(2mc^2))$ set equal to unity), and

$$I(\omega) = \int_{-\infty}^{\infty} \exp(-i\omega t)\exp(-|t|/\tau)\exp(i(\omega_{fv,iv}+\Delta E_{i,f}/\hbar \pm \omega_J)t)dt$$

results. This integral can be performed analytically and generates:

$$I(\omega) = \frac{1}{4\pi}\left\{\frac{1/\tau}{(1/\tau)^2+(\omega-\omega_{fv,iv}-\Delta E_{i,f}/\hbar \pm \omega_J)^2} + \frac{1/\tau}{(1/\tau)^2+(\omega+\omega_{fv,iv}+\Delta E_{i,f}/\hbar \pm \omega_J)^2}\right\},$$

a pair of **Lorentzian** peaks in ω-space centered again at

$$\omega = \pm\,[\omega_{fv,iv}+\Delta E_{i,f}/\hbar \pm \omega_J].$$

The full width at half height of these Lorentzian peaks is $2/\tau$. One says that the individual peaks have been pressure or collisionally broadened.

When the Doppler broadening can not be neglected relative to the collisional broadening, the above integral

$$I(\omega) = \int_{-\infty}^{\infty} \exp(-i\omega t)\exp(-|t|/\tau)\exp(-\omega^2 t^2 kT/(2mc^2))\exp(i(\omega_{fv,iv}+\Delta E_{i,f}/\hbar \pm \omega_J)t)dt$$

is more difficult to perform. Nevertheless, it can be carried out and again produces a series of peaks centered at

$$\omega = \omega_{fv,iv} + \Delta E_{i,f}/\hbar \pm \omega_J$$

but whose widths are determined both by Doppler and pressure broadening effects. The resultant line shapes are thus no longer purely Lorentzian nor Gaussian (which are compared in the figure below for both functions having the same full width at half height and the same integrated area), but have a shape that is called a **Voight** shape.

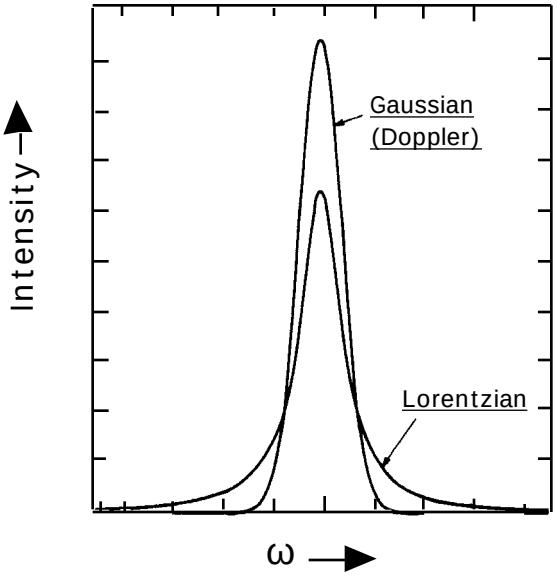

3. Rotational Diffusion Broadening

Molecules in liquids and very dense gases undergo frequent collisions with the other molecules; that is, the mean time between collisions is short compared to the rotational period for their unhindered rotation. As a result, the time dependence of the dipole related correlation function can no longer be modeled in terms of free rotation that is interrupted by (infrequent) collisions and Dopler shifted. Instead, a model that describes the incessant buffeting of the molecule's dipole by surrounding molecules becomes appropriate. For liquid samples in which these frequent collisions cause the molecule's dipole to undergo angular motions that cover all angles (i.e., in contrast to a frozen glass or

solid in which the molecule's dipole would undergo strongly perturbed pendular motion about some favored orientation), the so-called **rotational diffusion** model is often used.

In this picture, the rotation-dependent part of C(t) is expressed as:

$$<\varphi_J \mid \mathbf{E}_0 \cdot \mu_{i,f}(\mathbf{R}_e)\, \mathbf{E}_0 \cdot \mu_{i,f}(\mathbf{R}_e,t) \mid \varphi_J>$$

$$= <\varphi_J \mid \mathbf{E}_0 \cdot \mu_{i,f}(\mathbf{R}_e)\, \mathbf{E}_0 \cdot \mu_{i,f}(\mathbf{R}_e,0) \mid \varphi_J>\ \exp(-2D_{rot}|t|),$$

where D_{rot} is the rotational diffusion constant whose magnitude details the time decay in the averaged value of $\mathbf{E}_0 \cdot \mu_{i,f}(\mathbf{R}_e,t)$ at time t with respect to its value at time t = 0; the larger D_{rot}, the faster is this decay.

As with pressure broadening, this exponential time dependence, when subjected to Fourier transformation, yields:

$$I(\omega) = \int_{-\infty}^{\infty} \exp(-i\omega t)\exp(-2D_{rot}|t|)\exp(-\omega^2 t^2 kT/(2mc^2))\exp(i(\omega_{fv,iv}+\Delta E_{i,f}/\hbar \pm \omega_J)t)dt\ .$$

Again, in the limit of very small Doppler broadening, the $(\omega^2 t^2 kT/(2mc^2))$ factor can be ignored (i.e., $\exp(-\omega^2 t^2 kT/(2mc^2))$ set equal to unity), and

$$I(\omega) = \int_{-\infty}^{\infty} \exp(-i\omega t)\exp(-2D_{rot}|t|)\exp(i(\omega_{fv,iv}+\Delta E_{i,f}/\hbar \pm \omega_J)t)dt$$

results. This integral can be evaluated analytically and generates:

$$I(\omega) = \frac{1}{4\pi}\ \{\ \frac{2D_{rot}}{(2D_{rot})^2 + (\omega-\omega_{fv,iv}-\Delta E_{i,f}/\hbar \pm \omega_J)^2}$$

$$+\ \frac{2D_{rot}}{(2D_{rot})^2 + (\omega+\omega_{fv,iv}+\Delta E_{i,f}/\hbar \pm \omega_J)^2}\ \},$$

a pair of **Lorentzian** peaks in ω-space centered again at

$$\omega = \pm[\omega_{fv,iv}+\Delta E_{i,f}/\hbar \pm \omega_J].$$

The full width at half height of these Lorentzian peaks is $4D_{rot}$. In this case, one says that the individual peaks have been broadened via rotational diffusion. When the Doppler broadening can not be neglected relative to the collisional broadening, the above integral

$$I(\omega) = \int_{-\infty}^{\infty} \exp(-i\omega t)\exp(-2D_{rot}|t|)\exp(-\omega^2 t^2 kT/(2mc^2))\exp(i(\omega_{fv,iv}+\Delta E_{i,f}/\hbar \pm \omega_J)t)dt .$$

is more difficult to perform. Nevertheless, it can be carried out and again produces a series of peaks centered at

$$\omega = \pm[\omega_{fv,iv}+\Delta E_{i,f}/\hbar \pm \omega_J]$$

but whose widths are determined both by Doppler and rotational diffusion effects.

4. Lifetime or Heisenberg Homogeneous Broadening

Whenever the absorbing species undergoes one or more processes that depletes its numbers, we say that it has a finite lifetime. For example, a species that undergoes unimolecular dissociation has a finite lifetime, as does an excited state of a molecule that decays by spontaneous emission of a photon. Any process that depletes the absorbing species contributes another source of time dependence for the dipole time correlation functions C(t) discussed above. This time dependence is usually modeled by appending, in a multiplicative manner, a factor $\exp(-|t|/\tau)$. This, in turn modifies the line shape function $I(\omega)$ in a manner much like that discussed when treating the rotational diffusion case:

$$I(\omega) = \int_{-\infty}^{\infty} \exp(-i\omega t)\exp(-|t|/\tau)\exp(-\omega^2 t^2 kT/(2mc^2))\exp(i(\omega_{fv,iv}+\Delta E_{i,f}/\hbar \pm \omega_J)t)dt .$$

Not surprisingly, when the Doppler contribution is small, one obtains:

$$I(\omega) = \frac{1}{4\pi} \{ \frac{1/\tau}{(1/\tau)^2 + (\omega-\omega_{fv,iv}-\Delta E_{i,f}/\hbar \pm \omega_J)^2}$$

$$+ \frac{1/\tau}{(1/\tau)^2 + (\omega+\omega_{fv,iv}+\Delta E_{i,f}/\hbar \pm \omega_J)^2} \}.$$

In these Lorentzian lines, the parameter τ describes the kinetic decay lifetime of the molecule. One says that the spectral lines have been **lifetime or Heisenberg broadened** by an amount proportional to 1/τ. The latter terminology arises because the finite lifetime of the molecular states can be viewed as producing, via the Heisenberg uncertainty relation $\Delta E \Delta t > \hbar$, states whose energy is "uncertain" to within an amount ΔE.

5. Site Inhomogeneous Broadening

Among the above line broadening mechanisms, the pressure, rotational diffusion, and lifetime broadenings are all of the **homogeneous** variety. This means that each molecule in the sample is affected in exactly the same manner by the broadening process. For example, one does not find some molecules with short lifetimes and others with long lifetimes, in the Heisenberg case; the entire ensemble of molecules is characterized by a single lifetime.

In contrast, Doppler broadening is **inhomogeneous** in nature because each molecule experiences a broadening that is characteristic of its particular nature (velocity v_z in this case). That is, the fast molecules have their lines broadened more than do the slower molecules. Another important example of inhomogeneous broadening is provided by so-called **site broadening**. Molecules imbedded in a liquid, solid, or glass do not, at the instant of photon absorption, all experience exactly the same interactions with their surroundings. The distribution of instantaneous "solvation" environments may be rather "narrow" (e.g., in a highly ordered solid matrix) or quite "broad" (e.g., in a liquid at high temperature). Different environments produce different energy level splittings $\omega = \omega_{fv,iv} + \Delta E_{i,f}/\hbar \pm \omega_J$ (because the initial and final states are "solvated" differently by the surroundings) and thus different frequencies at which photon absorption can occur. The distribution of energy level splittings causes the sample to absorb at a range of frequencies as illustrated in the figure below where homogeneous and inhomogeneous line shapes are compared.

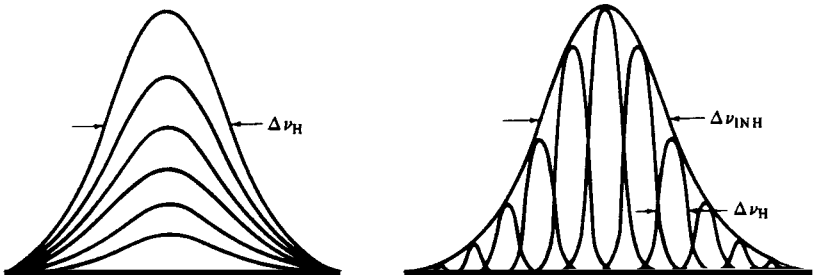

Homogeneous (a) and inhomogeneous (b) band shapes having inhomogeneous width $\Delta\nu_{INH}$, and homogeneous width $\Delta\nu_H$.

The spectral line shape function $I(\omega)$ is further broadened when site inhomogeneity is present and significant. These effects can be modeled by convolving the kind of $I(\omega)$ function that results from Doppler, lifetime, rotational diffusion, and pressure broadening with a Gaussian distribution $P(\Delta E)$ that describes the inhomogeneous distribution of energy level splittings:

$$I(\omega) = \int I^0(\omega;\Delta E)\ P(\Delta E)\ d\Delta E\ .$$

Here $I^0(\omega;\Delta E)$ is a line shape function such as those described earlier each of which contains a set of frequencies (e.g., $\omega = \omega_{fv,iv} + \Delta E_{i,f}/\hbar \pm \omega_J = \omega + \Delta E/\hbar$) at which absorption or emission occurs.

A common experimental test for inhomogeneous broadening involves **hole burning**. In such experiments, an intense light source (often a laser) is tuned to a frequency ω_{burn} that lies within the spectral line being probed for inhomogeneous broadening. Then, a second tunable light source is used to scan through the profile of the spectral line, and, for example, an absorption spectrum is recorded. Given an absorption profile as shown below in the absence of the intense burning light source:

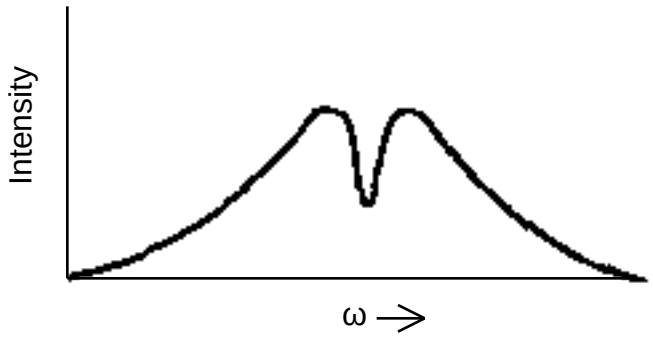

one expects to see a profile such as that shown below:

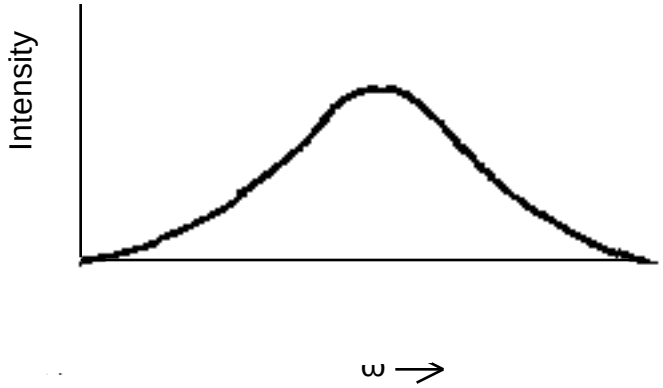

if inhomogeneous broadening is operative.

The interpretation of the change in the absorption profile caused by the bright light source proceeds as follows:

(i) In the ensemble of molecules contained in the sample, some molecules will absorb at or near the frequency of the bright light source ω_{burn}; other molecules (those whose environments do not produce energy level splittings that match ω_{burn}) will not absorb at this frequency.

(ii) Those molecules that do absorb at ω_{burn} will have their transition saturated by the intense light source, thereby rendering this frequency region of the line profile transparent to further absorption.

(iii) When the "probe" light source is scanned over the line profile, it will induce absorptions for those molecules whose local environments did not allow them to be saturated by the ω_{burn} light. The absorption profile recorded by this probe light source's detector thus will match that of the original line profile, until

(iv) the probe light source's frequency matches ω_{burn}, upon which no absorption of the probe source's photons will be recorded because molecules that absorb in this frequency regime have had their transition saturated.
(v) Hence, a "**hole**" will appear in the spectrum recorded by the probe light source's detector in the region of ω_{burn}.

Unfortunately, the technique of hole burning does not provide a fully reliable method for identifying inhomogeneously broadened lines. If a hole is observed in such a burning experiment, this provides ample evidence, but if one is not seen, the result is not definitive. In the latter case, the transition may not be strong enough (i.e., may not have a large enough "rate of photon absorption") for the intense light source to saturate the transition to the extent needed to form a hole.

This completes our introduction to the subject of molecular spectroscopy. More advanced treatments of many of the subjects treated here as well as many aspects of modern experimental spectroscopy can be found in the text by Zare on angular momentum as well as in Steinfeld's text Molecules and Radiation, 2nd Edition, by J. I. Steinfeld, MIT Press (1985).

Chapter 16

Collisions among molecules can also be viewed as a problem in time-dependent quantum mechanics. The perturbation is the "interaction potential", and the time dependence arises from the movement of the nuclear positions.

The simplest and most widely studied problems in chemical reaction dynamics involve describing the unimolecular motion or bimolecular collision of a system in a well characterized electronic state. Referring back to the discussion of Chapter 3, we recall that the motion of the nuclei are governed by a Schrödinger equation

$$[E_j(R)\ \ \Xi_j^0 (R) + T\ \Xi_j^0(R)] = E\ \Xi_j^0 (R)$$

in which the electronic energy E_j (R) assumes the role of the potential upon which movement occurs. This treatment of the nuclear motion is based on the Born-Oppenheimer approximation (see Chapter 3 for details) which assumes that coupling to nearby electronic states can be ignored. These assumptions are valid only when the energy surface of interest $E_j(R)$ is not crossed or closely approached by another electronic energy surface $E_k(R)$. When the electronic states are so widely spaced, it is proper to speak of the movement of the molecule(s) on the electronic surface $E_j(R)$, and to use either classical or quantum mechanical methods to follow such movements.

To simplify the notation throughout this Chapter, the above Schrödinger equation appropriate to movement on a single electronic energy surface will be written as follows:

$$[T + V(R)]\ \Xi (R) = E\ \Xi (R),$$

where T denotes the kinetic energy operator for all 3N of the geometrical coordinates (collectively denoted R) needed to specify the location of the N nuclei, V(R) is the electronic energy as a function of these coordinates, and
Ξ (R) is the nuclear-motion wavefunction.

For example, when diatomic species are considered, V is a function of the radial coordinate describing the distance between the two nuclei, T contains derivatives with respect to radial as well as two angular coordinates (those pertaining to rotation or relative angular motion of the two nuclei), and R refers to these radial and angular coordinates. For a triatomic species such as H_2O, V is a function of two O-H bond lengths and the H-O-H angle, and R refers to these three internal coordinates as well as the three angle coordinates needed to specify the orientation of the H_2O molecule in space relative to a space-fixed

coordinate system (e.g., three Euler angles used in Chapter 3 to treat rotation of spherical and symmetric top molecules).

In Chapters 1 and 3 and in all of Section 4, such nuclear-motion Schrödinger equations were used to treat the bound vibrational motions of molecules (i.e., the movement of the nuclei when the energy available is not adequate to rupture one or more of the bonds in the molecule). These same Schrödinger equations also apply to the scattering of the constituent nuclei (e.g., the vibration-rotation motion of HCl is treated by the same Schrödinger equation as the scattering of an H atom and a Cl atom). The primary difference between these two situations lies in the total energy (E) available: in the former, E lies below the dissociation asymptote of the ground-state HCl electronic potential energy; in the latter E is higher than this asymptote (e.g., see the potential curve shown below with some of its bound state energies and a state in the continuum).

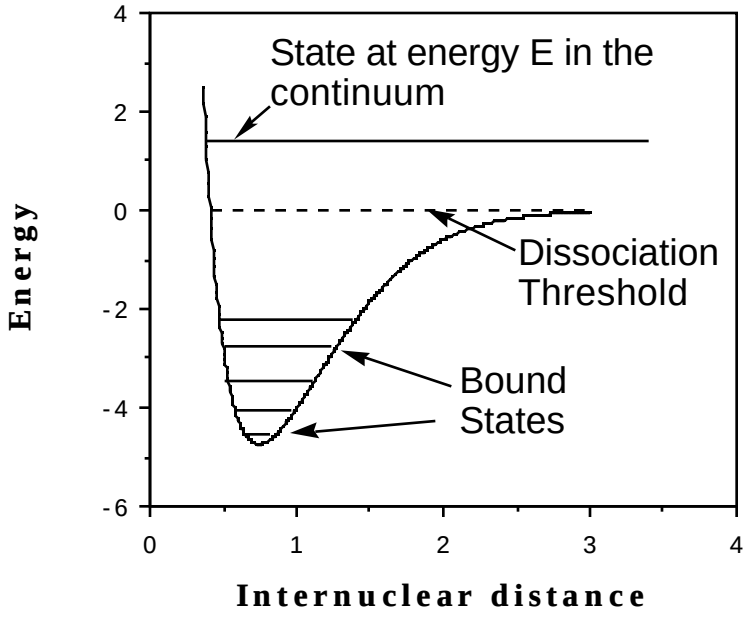

The different energies appropriate to bound-state and scattering situations affect the boundary conditions appropriate to the nuclear-motion wavefunctions in the large internuclear distance region. For the HCl example at hand, the bound-state vibrational wavefunctions $\Xi(R,\theta,\varphi)$ decay exponentially (see Chapter 1) for large R because such R-values lie in the classically forbidden region of R-space where E - V(R) is negative. In contrast, the scattering wavefunctions for this same V(R) potential and the same HCl molecule need not decay in the large-E region. As illustrated explicitly below for a model problem, this difference in large-R boundary conditions causes major differences in the eigenvalue spectrum of the Hamiltonian in these two cases. In particular, the bound-state

energy levels of HCl are discrete (i.e., quantized) but the scattering states are not (i.e., an H atom and a Cl atom may collide with arbitrary relative translational energy).

Let us now examine how the Schrödinger equation is solved for cases in which E lies above the dissociation energy of V(R) by considering a few simple model problems that can be solved exactly.

I. One Dimensional Scattering

Atom-atom scattering on a single Born-Oppenheimer energy surface can be reduced to a one-dimensional Schrödinger equation by separating the radial and angular parts of the three-dimensional Schrödinger equation in the same fashion as used for the Hydrogen atom in Chapter 1. The resultant equation for the radial part $\psi(R)$ of the wavefunction can be written as:

$$- (\hbar^2/2\mu)\, R^{-2}\, \partial/\partial R\, (R^2 \partial\psi/\partial R) + L\,(L+1)\hbar^2/(2\mu R^2)\, \psi + V(R)\, \psi = E\, \psi,$$

where L is the quantum number that labels the angular momentum of the colliding particles whose reduced mass is μ.

Defining $\Psi(R) = R\, \psi(R)$ and substituting into the above equation gives the following equation for Ψ:

$$- (\hbar^2/2\mu)\, \partial^2\Psi/\partial R^2 + L\,(L+1)\hbar^2/(2\mu R^2)\, \Psi + V(R)\, \Psi = E\, \Psi.$$

The combination of the "centrifugal potential" $L\,(L+1)\hbar^2/(2\mu R^2)$ and the electronic potential V(R) thus produce a total "effective potential" for describing the radial motion of the system.

The simplest reasonable model for such an effective potential is provided by the "square well" potential illustrated below. This model V(R) could, for example, be applied to the L = 0 scattering of two atoms whose bond dissociation energy is D_e and whose equilibrium bond length for this electronic surface lies somewhere between R = 0 and R = R_{max}.

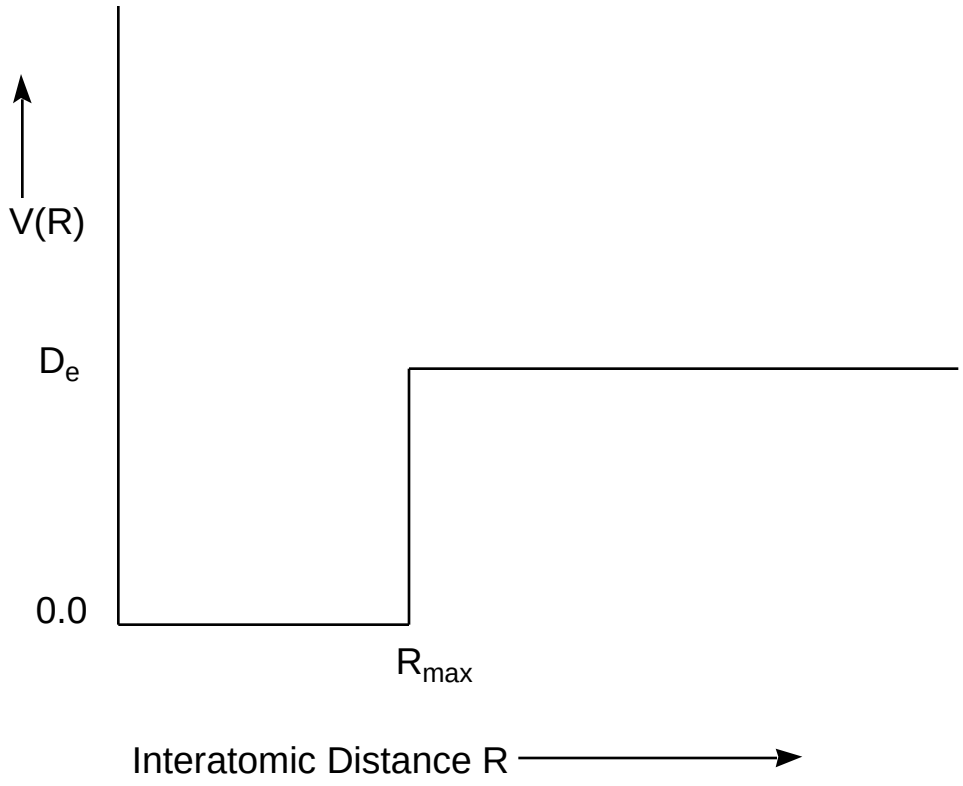

The piecewise constant nature of this particular V(R) allows exact solutions to be written both for bound and scattering states because the Schrödinger equation

$$- (\hbar^2/2\mu)\, d^2\Psi/dR^2 = E\,\Psi \qquad (\text{for } 0 \le R \le R_{max})$$

$$- (\hbar^2/2\mu)\, d^2\Psi/dR^2 + D_e\,\Psi = E\,\Psi \qquad (R_{max} \le R < \infty)$$

admits simple sinusoidal solutions.

A. Bound States

The **bound states** are characterized by having $E < D_e$. For the inner region, the two solutions to the above equation are

$$\Psi_1(R) = A \sin(kR)$$

and

$$\Psi_2(R) = B \cos(kR)$$

where

$$k = \sqrt{2\mu E/\hbar^2}$$

is termed the "local wave number" because it is related to the momentum values for the $\exp(\pm i k R)$ components of such a function:

$$- i \hbar \partial \exp(\pm i k R)/\partial R = \hbar k \exp(\pm i k R).$$

The cos(kR) solution must be excluded (i.e., its amplitude B in the general solution of the Schrödinger equation must be chosen equal to 0.0) because this function does not vanish at R = 0, where the potential moves to infinity and thus the wavefunction must vanish. This means that only the

$$\Psi = A \sin(kR)$$

term remains for this inner region.

Within the asymptotic region ($R > R_{max}$) there are also two solutions to the Schrödinger equation:

$$\Psi_3 = C \exp(-\kappa R)$$

and

$$\Psi_4 = D \exp(\kappa R)$$

where

$$\kappa = \sqrt{2\mu(D_e - E)/\hbar^2} \ .$$

Clearly, one of these functions is a decaying function of R for large R and the other Ψ_4 grows exponentially for large R. The latter's amplitude D must be set to zero because this

function generates a probability density that grows larger and larger as R penetrates deeper and deeper into the classically forbidden region (where E < V(R)).

To connect Ψ_1 in the inner region to Ψ_3 in the outer region, we use the fact that Ψ and $d\Psi/dR$ must be continuous except at points R where V(R) undergoes an infinite discontinuity (see Chapter 1). Continuity of Ψ at R_{max} gives:

$$A \sin(kR_{max}) = C \exp(-\kappa R_{max}),$$

and continuity of $d\Psi/dR$ at R_{max} yields

$$A\, k \cos(kR_{max}) = -\kappa C \exp(-\kappa R_{max}).$$

These two equations allow the ratio C/A as well as the energy E (which appears in κ and in k) to be determined:

$$A/C = -\kappa/k \exp(-\kappa R_{max})/\cos(kR_{max}).$$

The condition that determines E is based on the well known requirement that the determinant of coefficients must vanish for homogeneous linear equations to have no-trivial solutions (i.e., not A = C = 0):

$$\det \begin{pmatrix} \sin(kR_{max}) & -\exp(-\kappa R_{max}) \\ k\cos(kR_{max}) & \kappa\exp(-\kappa R_{max}) \end{pmatrix} = 0$$

The vanishing of this determinant can be rewritten as

$$\kappa \sin(kR_{max}) \exp(-\kappa R_{max}) + k \cos(kR_{max}) \exp(-\kappa R_{max}) = 0$$

or

$$\tan(kR_{max}) = -k/\kappa \ .$$

When employed in the expression for A/C, this result gives

$$A/C = \exp(-\kappa R_{max})/\sin(kR_{max}).$$

For very large D_e compared to E, the above equation for E reduces to the familiar "particle in a box" energy level result since k/κ vanishes in this limit, and thus $\tan(kR_{max}) = 0$, which is equivalent to $\sin(kR_{max}) = 0$, which yields the familiar $E = n^2h^2/(8\mu R^2_{max})$ and $C/A = 0$, so $\Psi = A \sin(kR)$.

When D_e is not large compared to E, the full transcendental equation $\tan(kR_{max}) = - k/\kappa$ must be solved numerically or graphically for the eigenvalues E_n, n = 1, 2, 3, ... These energy levels, when substituted into the definitions for k and κ give the wavefunctions:

$$\Psi = A \sin(kR) \qquad (\text{for } 0 \le R \le R_{max})$$

$$\Psi = A \sin(kR_{max}) \exp(\kappa R_{max}) \exp(-\kappa R) \qquad (\text{for } R_{max} \le R < \infty).$$

The one remaining unknown A can be determined by requiring that the modulus squared of the wavefunction describe a probability density that is normalized to unity when integrated over all space:

$$\int_0^\infty |\Psi|^2 \, dR = 1.$$

Note that this condition is equivalent to

$$\int_0^\infty |\psi|^2 \, R^2 dR = 1$$

which would pertain to the original radial wavefunction. In the case of an infinitely deep potential well, this normalization condition reduces to

$$\int_0^{R_{max}} A^2 \sin^2(kR) dR = 1$$

which produces

$$A = \sqrt{\frac{2}{R_{max}}} \ .$$

B. Scattering States

The **scattering states** are treated in much the same manner. The functions Ψ_1 and Ψ_2 arise as above, and the amplitude of Ψ_2 must again be chosen to vanish because Ψ must vanish at R = 0 where the potential moves to infinity. However, in the exterior region ($R > R_{max}$), the two solutions are now written as:

$$\Psi_3 = C \exp(ik'R)$$

$$\Psi_4 = D \exp(-ik'R)$$

where the large-R local wavenumber

$$k' = \sqrt{2\mu(E - D_e)/\hbar^2}$$

arises because $E > D_e$ for scattering states.

The conditions that Ψ and $d\Psi/dR$ be continuous at R_{max} still apply:

$$A \sin(kR_{max}) = C \exp(i\, k'R_{max}) + D \exp(-i\, k'R_{max})$$

and

$$k\, A \cos(kR_{max}) = i\, k'C \exp(i\, k'R_{max}) - ik'\, D \exp(-i\, k'R_{max}).$$

However, these two equations (in three unknowns A, C, and D) can no longer be solved to generate eigenvalues E and amplitude ratios. There are now three amplitudes as well as the E value but only these two equations plus a normalization condition to be used. The result is that the energy no longer is specified by a boundary condition; it can take on any value. We thus speak of scattering states as being "in the continuum" because the allowed values of E form a continuum beginning at $E = D_e$ (since the zero of energy is defined in this example as at the bottom of the potential well).

The $R > R_{max}$ components of Ψ are commonly referred to as "incoming"

$$\Psi_{in} = D \exp(-ik'R)$$

and "outgoing"

$$\Psi_{out} = C \exp(ik'R)$$

because their radial momentum eigenvalues are $-\hbar k'$ and $\hbar k'$, respectively. It is a common convention to define the amplitude D so that the **flux** of incoming particles is unity. Choosing

$$D = \sqrt{\frac{\mu}{\hbar k'}}$$

produces an incoming wavefunction whose current density is:

$$S(R) = -i\hbar/2\mu \left[\Psi_{in}^* (d/dR\ \Psi_{in}) - (d\Psi_{in}/dR)^* \Psi_{in}\right]$$

$$= |D|^2 (-i\hbar/2\mu) [-2ik']$$

$$= -1.$$

This means that there is one unit of current density moving inward (this produces the minus sign) for all values of R at which Ψ_{in} is an appropriate wavefunction (i.e., $R > R_{max}$). This condition takes the place of the probability normalization condition specified in the bound-state case when the modulus squared of the total wavefunction is required to be normalized to unity over all space. Scattering wavefunctions can not be so normalized because they do not decay at large R; for this reason, the flux normalization condition is usually employed. The magnitudes of the outgoing (C) and short range (A) wavefunctions relative to that of the incoming function (D) then provide information about the scattering and "trapping" of incident flux by the interaction potential.

Once D is so specified, the above two boundary matching equations are written as a set of two inhomogeneous linear equations in two unknowns (A and C):

$$A \sin(kR_{max}) - C \exp(i\ k'R_{max}) = D \exp(-i\ k'R_{max})$$

and

$$k\,A\cos(kR_{max}) - i\,k'C\exp(i\,k'R_{max}) = -\,ik'\,D\exp(-i\,k'R_{max})$$

or

$$\begin{pmatrix} \sin(kR_{max}) & -\exp(i\,k'R_{max}) \\ k\cos(kR_{max}) & -i\,k'\exp(i\,k'R_{max}) \end{pmatrix} \begin{pmatrix} A \\ C \end{pmatrix} = \begin{pmatrix} D\exp(-i\,k'R_{max}) \\ -ik'\,D\exp(-i\,k'R_{max}) \end{pmatrix}.$$

Non-trivial solutions for A and C will exist except when the determinant of the matrix on the left side vanishes:

$$-i\,k'\sin(kR_{max}) + k\cos(kR_{max}) = 0,$$

which can be true only if

$$\tan(kR_{max}) = ik'/k.$$

This equation is not obeyed for any (real) value of the energy E, so solutions for A and C in terms of the specified D can always be found.

In summary, specification of unit incident flux is made by choosing D as indicated above. For any collision energy $E > D_e$, the 2x1 array on the right hand side of the set of linear equations written above can be formed, as can the 2x2 matrix on the left side. These linear equations can then be solved for A and C. The overall wavefunction for this E is then given by:

$$\Psi = A\sin(kR) \qquad (\text{for } 0 \le R \le R_{max})$$

$$\Psi = C\exp(ik'R) + D\exp(-ik'R) \qquad (\text{for } R_{max} \le R < \infty).$$

C. Shape Resonance States

If the angular momentum quantum number L in the effective potential introduced earlier is non-zero, this potential has a repulsive component at large R. This repulsion can combine with short-range attractive interactions due, for example, to chemical bond forces,

to produce an effective potential that one can model in terms of simple piecewise functions shown below.

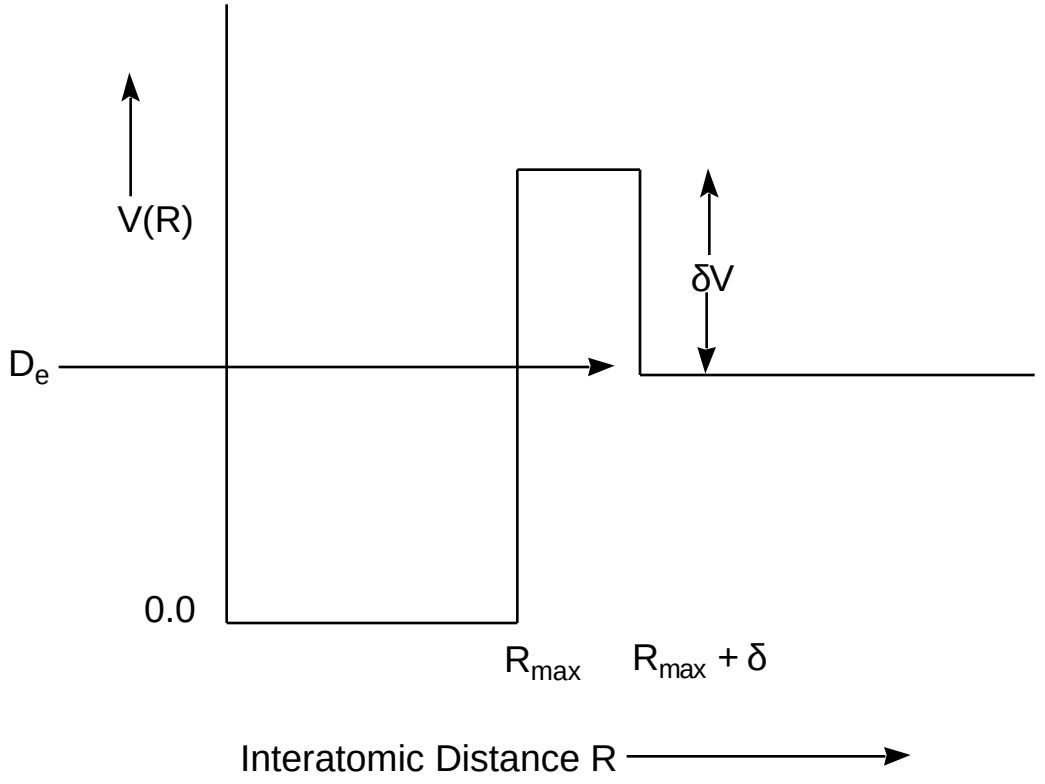

Again, the piecewise nature of the potential allows the one-dimensional Schrödinger equation to be solved analytically. For energies below D_e, one again finds bound states in much the same way as illustrated above (but with the exponentially decaying function exp(-κ'R) used in the region $R_{max} \le R \le R_{max} + \delta$, with $\kappa' = \sqrt{2\mu(D_e + \delta V - E)/\hbar^2}$).

For energies lying above $D_e + \delta V$, scattering states occur and the four amplitudes of the functions (sin(kR), exp(±i k'''R) with $k''' = \sqrt{2\mu(-D_e - \delta V + E)/\hbar^2}$, and exp(i k'R)) appropriate to each R-region are determined in terms of the amplitude of the incoming asymptotic function D exp(-ik'R) from the four equations obtained by matching Ψ and dΨ/dR at R_{max} and at $R_{max} + \delta$.

For energies lying in the range $D_e < E < D_e + \delta V$, a qualitatively different class of scattering function exists. These so-called **shape resonance** states occur at energies that are determined by the condition that the amplitude of the wavefunction within the barrier (i.e., for $0 \le R \le R_{max}$) be large so that incident flux successfully tunnels through the

barrier and builds up, through constructive interference, large probability amplitude there. Let us now turn our attention to this specific energy regime.

The piecewise solutions to the Schrödinger equation appropriate to the shape-resonance case are easily written down:

$$\Psi = A\sin(kR) \qquad (\text{for } 0 \le R \le R_{max})$$

$$\Psi = B_+ \exp(\kappa' R) + B_- \exp(-\kappa' R) \qquad (\text{for } R_{max} \le R \le R_{max} + \delta)$$

$$\Psi = C \exp(ik' R) + D \exp(-ik' R) \qquad (\text{for } R_{max} + \delta \le R < \infty).$$

Note that both exponentially growing and decaying functions are acceptable in the $R_{max} \le R \le R_{max} + \delta$ region because this region does not extend to $R = \infty$. There are four amplitudes (A, B_+, B_-, and C) that must be expressed in terms of the specified amplitude D of the incoming flux. Four equations that can be used to achieve this goal result when Ψ and $d\Psi/dR$ are matched at R_{max} and at $R_{max} + \delta$:

$$A\sin(kR_{max}) = B_+ \exp(\kappa' R_{max}) + B_- \exp(-\kappa' R_{max}),$$

$$A k\cos(kR_{max}) = \kappa' B_+ \exp(\kappa' R_{max}) - \kappa' B_- \exp(-\kappa' R_{max}),$$

$$B_+ \exp(\kappa'(R_{max} + \delta)) + B_- \exp(-\kappa'(R_{max} + \delta))$$

$$= C \exp(ik'(R_{max} + \delta)) + D \exp(-ik'(R_{max} + \delta)),$$

$$\kappa' B_+ \exp(\kappa'(R_{max} + \delta)) - \kappa' B_- \exp(-\kappa'(R_{max} + \delta))$$

$$= ik' C \exp(ik'(R_{max} + \delta)) - ik' D \exp(-ik'(R_{max} + \delta)).$$

It is especially instructive to consider the value of A/D that results from solving this set of four equations in four unknowns because the modulus of this ratio provides information about the relative amount of amplitude that exists inside the centrifugal barrier in the attractive region of the potential compared to that existing in the asymptotic region as incoming flux.

The result of solving for A/D is:

$$A/D = 4\,\kappa' \exp(-ik'(R_{max}+\delta))$$

$$\{\exp(\kappa'\delta)(ik'-\kappa')(\kappa'\sin(kR_{max})+k\cos(kR_{max}))/ik'$$

$$+ \exp(-\kappa'\delta)(ik'+\kappa')(\kappa'\sin(kR_{max})-k\cos(kR_{max}))/ik' \}^{-1}.$$

Further, it is instructive to consider this result under conditions of a high (large $D_e + \delta V - E$) and thick (large δ) barrier. In such a case, the "tunnelling factor" $\exp(-\kappa'\delta)$ will be very small compared to its counterpart $\exp(\kappa'\delta)$, and so

$$A/D = 4\,\frac{ik'\kappa'}{ik'-\kappa'} \exp(-ik'(R_{max}+\delta)) \exp(-\kappa'\delta)\,\{\kappa'\sin(kR_{max})+k\cos(kR_{max})\}^{-1}.$$

The $\exp(-\kappa'\delta)$ factor in A/D causes the magnitude of the wavefunction inside the barrier to be small in most circumstances; we say that incident flux must tunnel through the barrier to reach the inner region and that $\exp(-\kappa'\delta)$ gives the probability of this tunnelling. The magnitude of the A/D factor could become large if the collision energy E is such that

$$\kappa'\sin(kR_{max})+k\cos(kR_{max})$$

is small. In fact, if

$$\tan(kR_{max}) = -\,k/\kappa'$$

this denominator factor in A/D will vanish and A/D will become infinite. Note that the above condition is similar to the energy quantization condition

$$\tan(kR_{max}) = -\,k/\kappa$$

that arose when bound states of a finite potential well were examined earlier in this Chapter. There is, however, an important difference. In the bound-state situation

$$k = \sqrt{2\mu E/\hbar^2}$$

and

$$\kappa = \sqrt{2\mu(D_e - E)/\hbar^2}\ ;$$

in this shape-resonance case, k is the same, but

$$\kappa' = \sqrt{2\mu(D_e + \delta V - E)/\hbar^2}\ )$$

rather than κ occurs, so the two $\tan(kR_{max})$ equations are not identical.

However, in the case of a very high barrier (so that κ' is much larger than k), the denominator

$$\kappa'\sin(kR_{max})+k\cos(kR_{max}) \quad \kappa' \sin(kR_{max})$$

in A/D can become small if

$$\sin(kR_{max}) \quad 0.$$

This condition is nothing but the energy quantization condition that would occur for the particle-in-a-box potential shown below.

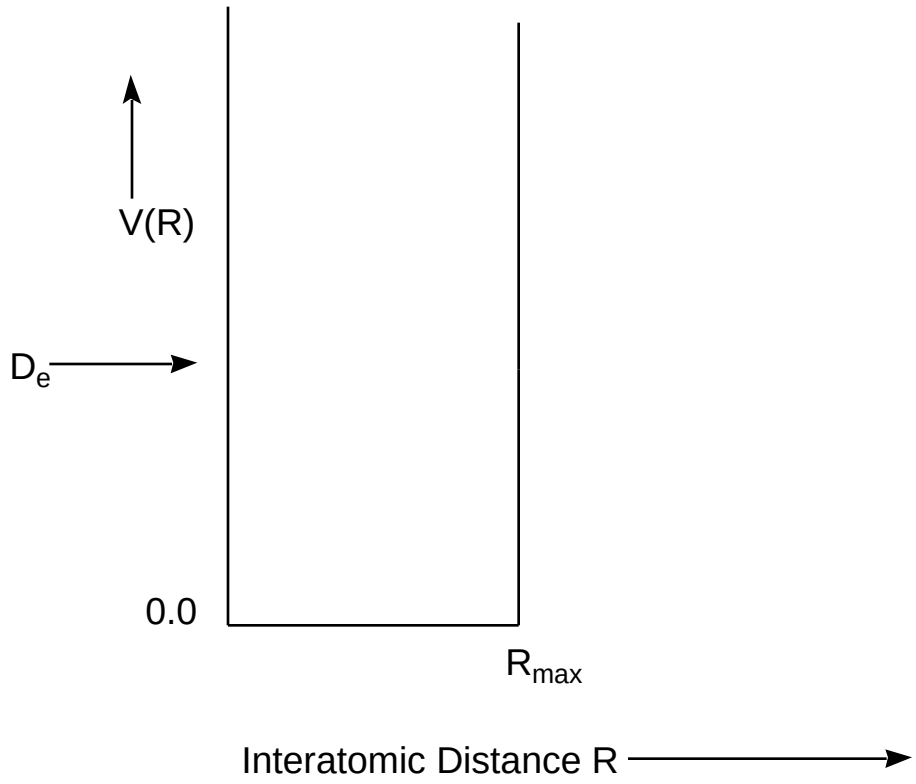

This potential is identical to the true effective potential for $0 \leq R \leq R_{max}$, but extends to infinity beyond R_{max} ; the barrier and the dissociation asymptote displayed by the true potential are absent.

In summary, when a barrier is present on a potential energy surface, at energies above the dissociation asymptote D_e but below the top of the barrier ($D_e + \delta V$ here), one can expect shape-resonance states to occur at "special" scattering energies E. These so-called resonance energies can often be approximated by the bound-state energies of a potential that is identical to the potential of interest in the inner region ($0 \leq R \leq R_{max}$ here) but that extends to infinity beyond the top of the barrier (i.e., beyond the barrier, it does not fall back to values below E).

The chemical significance of shape resonances is great. Highly rotationally excited molecules may have more than enough total energy to dissociate (D_e), but this energy may be "stored" in the rotational motion, and the vibrational energy may be less than D_e. In terms of the above model, high angular momentum may produce a significant barrier in the effective potential, but the system's vibrational energy may lie significantly below D_e. In such a case, and when viewed in terms of motion on an angular momentum modified effective potential, the lifetime of the molecule with respect to dissociation is determined by the rate of tunnelling through the barrier.

For the case at hand, one speaks of "rotational predissociation" of the molecule. The lifetime τ can be estimated by computing the frequency ν at which flux existing inside R_{max} strikes the barrier at R_{max}

$$\nu = \frac{\hbar k}{2\mu R_{max}} \quad (sec^{-1})$$

and then multiplying by the probability P that flux tunnels through the barrier from R_{max} to $R_{max} + \delta$:

$$P = \exp(-2\kappa' \delta).$$

The result is that

$$\tau^{-1} = \frac{\hbar k}{2\mu R_{max}} \exp(-2\kappa' \delta)$$

with the energy E entering into k and κ' being determined by the resonance condition: $(\kappa' \sin(kR_{max}) + k\cos(kR_{max}))$ = minimum.

Although the examples treated above involved piecewise constant potentials (so the Schrödinger equation and the boundary matching conditions could be solved exactly), many of the characteristics observed carry over to more chemically realistic situations. As discussed, for example, in Energetic Principles of Chemical Reactions, J. Simons, Jones and Bartlett, Portola Valley, Calif. (1983), one can often model chemical reaction processes in terms of:

(i) motion along a "reaction coordinate" (s) from a region characteristic of reactant materials where the potential surface is positively curved in all direction and all forces (i.e., gradients of the potential along all internal coordinates) vanish,

(ii) to a transition state at which the potential surface's curvature along s is negative while all other curvatures are positive and all forces vanish,

(iii) onward to product materials where again all curvatures are positive and all forces vanish.

Within such a "reaction path" point of view, motion transverse to the reaction coordinate s is often modelled in terms of local harmonic motion although more sophisticated treatments of the dynamics is possible. In any event, this picture leads one to consider motion along a single degree of freedom (s), with respect to which much of the above treatment can be carried over, coupled to transverse motion along all other internal degrees of freedom taking place under an entirely positively curved potential (which therefore produces restoring forces to movement away from the "streambed" traced out by the reaction path s).

II. Multichannel Problems

When excited electronic states are involved, couplings between two or more electronic surfaces may arise. Dynamics occuring on an excited-state surface may evolve in a way that produces flux on another surface. For example, collisions between an electronically excited 1s2s (^{3}S) He atom and a ground-state $1s^2$ (^{1}S) He atom occur on a potential energy surface that is repulsive at large R (due to the repulsive interaction between the closed-shell $1s^2$ He and the large 2s orbital) but attractive at smaller R (due to the $\sigma^2\sigma^{*1}$ orbital occupancy arising from the three 1s-derived electrons). The ground-state potential energy surface for this system (pertaining to two $1s^2$ (^{1}S) He atoms is repulsive at small R values (because of the $\sigma^2\sigma^{*2}$ nature of the electronic state). In this case, there are two Born-Oppenheimer electronic-nuclear motion states that are degenerate and thus need to be combined to achieve a proper description of the dynamics:

$$\Psi_1 = |\sigma^2\sigma^{*2}|\ \Psi_{grnd.}(R,\theta,\varphi)$$

pertaining to the ground electronic state and the scattering state $\Psi_{grnd.}$ on this energy surface, and

$$\Psi_2 = |\sigma^2\sigma^{*1}2\sigma^1|\ \Psi_{ex.}(R,\theta,\varphi)$$

pertaining to the excited electronic state and the nuclear-motion state $\Psi_{ex.}$ on this energy surface. Both of these wavefunctions can have the same energy E; the former has high nuclear-motion energy and low electronic energy, while the latter has higher electronic energy and lower nuclear-motion energy.

A simple model that can be used to illustrate the two-state couplings that arise in such cases is introduced through the two one-dimensional piecewise potential surfaces shown below.

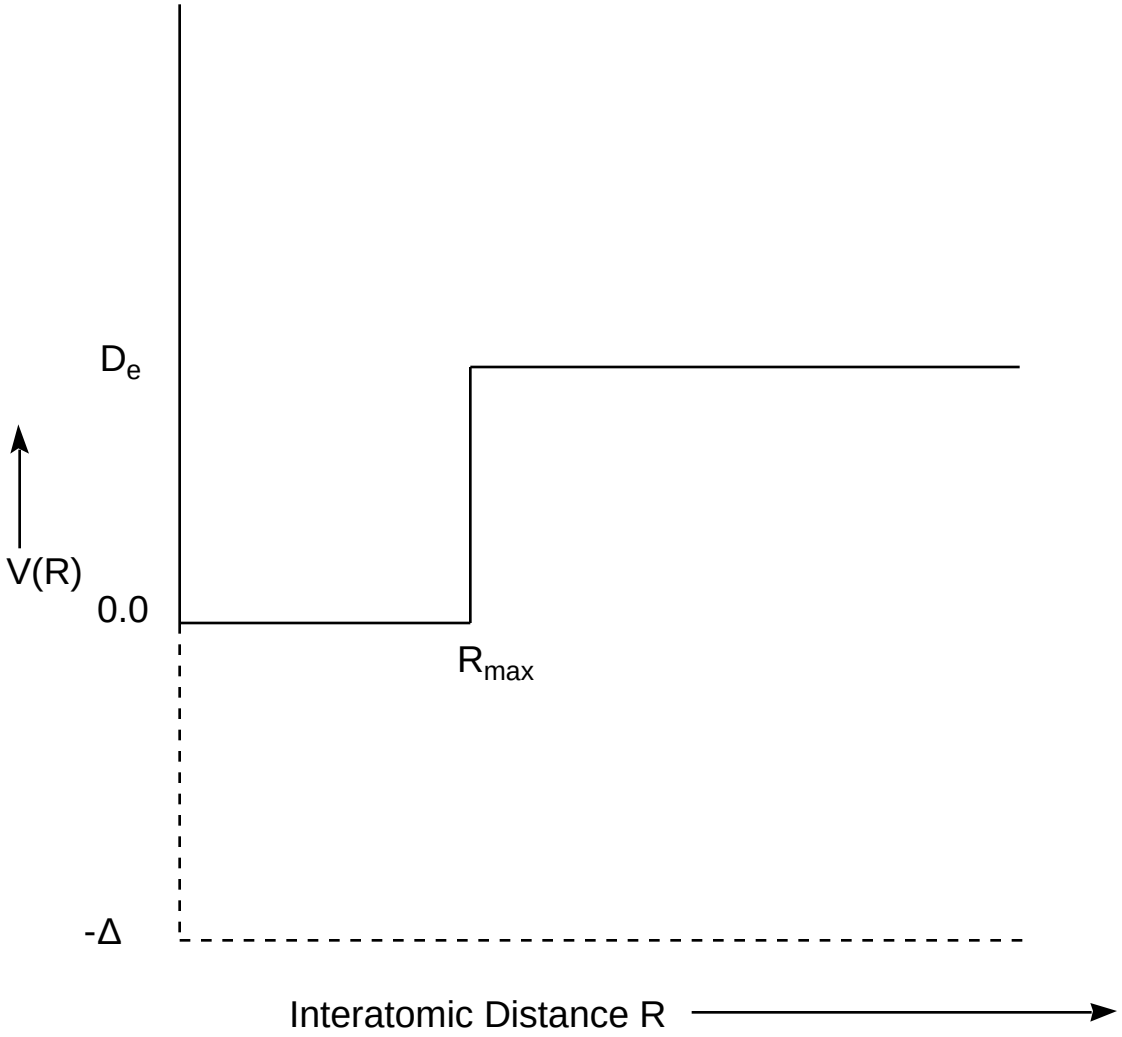

The dashed energy surface

$$V(R) = -\Delta \qquad (\text{for } 0 \leq R < \infty)$$

provides a simple representation of a repulsive lower-energy surface, and the solid-line plot represents the excited-state surface that has a well of depth D_e and whose well lies Δ above the ground-state surface.

In this case, and for energies lying above zero (for $E < 0$, only nuclear motion on the lower energy dashed surface is "open" (i.e., accessible)) yet below D_e, the nuclear-

motion wavefunction can have amplitudes belonging to both surfaces. That is, the total (electronic and nuclear) wavefunction consists of two portions that can be written as:

$$\Psi = A\,\varphi \sin(kR) + \varphi' A'' \sin(k''R) \qquad (\text{for } 0 \le R \le R_{max})$$

and

$$\Psi = A\,\varphi \sin(kR_{max}) \exp(\kappa R_{max}) \exp(-\kappa R) + \varphi' A'' \sin(k''R)$$

$$(\text{for } R_{max} \le R < \infty),$$

where φ and φ' denote the electronic functions belonging to the upper and lower energy surfaces, respectively. The wavenumbers k and k" are defined as:

$$k = \sqrt{2\mu E/\hbar^2}$$

$$k'' = \sqrt{2\mu(E + \Delta)/\hbar^2}$$

and κ is as before

$$\kappa = \sqrt{2\mu(D_e - E)/\hbar^2} \ .$$

For the lower-energy surface, only the sin(k"R) function is allowed because the cos(k"R) function does not vanish at R = 0.

A. The Coupled Channel Equations

In such cases, the relative amplitudes (A and A") of the nuclear motion wavefunctions on each surface must be determined by substituting the above "two-channel" wavefunction (the word channel is used to denote separate asymptotic states of the system; in this case, the φ and φ' electronic states) into the full Schrödinger equation. In Chapter 3,

the couplings among Born-Oppenheimer states were so treated and resulted in the following equation:

$$[\,(E_j(R) - E)\,\Xi_j(R) + T\,\Xi_j(R)\,] = -\,\Sigma_i\,\{\,<\Psi_j \mid T \mid \Psi_i>(R)\,\Xi_i(R)$$

$$+\,\Sigma_{a=1,M}\,(-\hbar^2/m_a)\,<\Psi_j \mid \nabla_a \mid \Psi_i>(R)\cdot \nabla_a\,\Xi_i(R)\,\}$$

where $E_j(R)$ and $\Xi_j(R)$ denote the electronic energy surfaces and nuclear-motion wavefunctions, Ψ_j denote the corresponding electronic wavefunctions, and the ∇_a represent derivatives with respect to the various coordinates of the nuclei. Changing to the notation used in the one-dimensional model problem introduced above, these so-called **coupled-channel** equations read:

$$[(-\Delta - E) - \hbar^2/2\mu\, d^2/dR^2\,]\, A''\sin(k''R)$$

$$= -\,\{<\varphi'|\,-\,\hbar^2/2\mu\, d^2/dR^2|\varphi'>\, A''\sin(k''R)$$

$$+\,(-\,\hbar^2/\mu)\,<\varphi'|d/dR|\varphi>\, d/dR\, A\sin(kR)\,\}\qquad (\text{for } 0 \le R \le R_{max}),$$

$$[(-\Delta - E) - \hbar^2/2\mu\, d^2/dR^2\,]\, A''\sin(k''R)$$

$$= -\,\{<\varphi'|-\,\hbar^2/2\mu\, d^2/dR^2|\varphi'>\, A''\sin(k''R)$$

$$+\,(-\,\hbar^2/\mu)\,<\varphi'|d/dR|\varphi>\, d/dR\, A\,\varphi\sin(kR_{max})\exp(\kappa R_{max})\exp(-\kappa R)\,\}$$

$$(\text{for } R_{max} \le R < \infty\,);$$

when the index j refers to the ground-state surface ($V(R) = -\Delta$, for $0 < R < \infty$), and

$$[(0 - E) - \hbar^2/2\mu\, d^2/dR^2\,]\, A\sin(kR) = -\,\{<\varphi|\,-\,\hbar^2/2\mu\, d^2/dR^2|\varphi>\, A\sin(kR)$$

$$+\,(-\,\hbar^2/\mu)\,<\varphi|d/dR|\varphi'>\, d/dR\, A''\sin(k''R)\,\}(\text{for } 0 \le R \le R_{max}),$$

$$[(D_e - E) - \hbar^2/2\mu\, d^2/dR^2\,]\, A\sin(kR_{max})\exp(\kappa R_{max})\exp(-\kappa R)$$

$$= - \{ \langle \varphi | - \hbar^2/2\mu \, d^2/dR^2 | \varphi \rangle \, A\sin(kR_{max}) \exp(\kappa R_{max}) \exp(-\kappa R)$$

$$+ (- \hbar^2/\mu) \langle \varphi | d/dR | \varphi' \rangle \, d/dR \; A''\sin(k''R) \; \} \quad (\text{for } R_{max} \leq R < \infty)$$

when the index j refers to the excited-state surface (where V(R) = 0, for $0 < R \leq R_{max}$ and $V(R) = D_e$ for $R_{max} \leq R < \infty$).

Clearly, if the right-hand sides of the above equations are ignored, one simply recaptures the Schrödinger equations describing motion on the separate potential energy surfaces:

$$[(-\Delta - E) - \hbar^2/2\mu \, d^2/dR^2 \,] \, A''\sin(k''R) = 0 \qquad (\text{for } 0 \leq R \leq R_{max}),$$

$$[(-\Delta - E) - \hbar^2/2\mu \, d^2/dR^2 \,] \, A''\sin(k''R) = 0 \qquad (\text{for } R_{max} \leq R < \infty);$$

that describe motion on the lower-energy surface, and

$$[(0 - E) - \hbar^2/2\mu \, d^2/dR^2 \,] \, A\sin(kR) = 0 \qquad (\text{for } 0 \leq R \leq R_{max}),$$

$$[(D_e - E) - \hbar^2/2\mu \, d^2/dR^2 \,] \, A\sin(kR_{max}) \exp(\kappa R_{max}) \exp(-\kappa R) = 0$$

$$(\text{for } R_{max} \leq R < \infty)$$

describing motion on the upper surface on which the bonding interaction occurs. The terms on the right-hand sides provide the couplings that cause the true solutions to the Schrödinger equation to be combinations of solutions for the two separate surfaces.

In applications of the coupled-channel approach illustrated above, coupled sets of second order differential equations (two in the above example) are solved by starting with a specified flux in one of the channels and a chosen energy E. For example, one might specify the amplitude A to be unity to represent preparation of the system in a bound vibrational level (with $E < D_e$) of the excited electronic-state potential. One would then choose E to be one of the eigenenergies of that potential. Propagation methods could be used to solve the coupled differential equations subject to these choices of E and A. The

result would be the determination of the amplitude A' of the wavefunction on the ground-state surface. The ratio A'/A provides a measure of the strength of coupling between the two Born-Oppenheimer states.

B. Perturbative Treatment

Alternatively, one can treat the coupling between the two states via time dependent perturbation theory. For example, by taking A = 1.0 and choosing E to be one of the eigenenergies of the excited-state potential, one is specifying that the system is initially (just prior to t = 0) prepared in a state whose wavefunction is:

$$\Psi^0_{ex} = \varphi \sin(kR) \qquad (\text{for } 0 \le R \le R_{max})$$

$$\Psi^0_{ex} = \varphi \sin(kR_{max}) \exp(\kappa R_{max}) \exp(-\kappa R) \quad (\text{for } R_{max} \le R < \infty).$$

From t = 0 on, the coupling to the other state

$$\Psi^0_{grnd} = \varphi' \sin(k'R) \qquad (\text{for } 0 \le R < \infty)$$

is induced by the "perturbation" embodied in the terms on the right-hand side of the coupled-channel equations.

Within this time dependent perturbation theory framework, the rate of transition of probability amplitude from the initially prepared state (on the excited state surface) to the ground-state surface is proportional to the square of the perturbation matrix elements between these two states:

$$\text{Rate} \propto \left| \int_0^{R_{max}} \sin(kR) \langle\varphi|d/dR|\varphi'\rangle \, (d/dR \sin(k''R))dR \right.$$

$$\left. + \int_{R_{max}}^{\infty} \sin(kR_{max}) \exp(\kappa R_{max}) \exp(-\kappa R) \langle\varphi|d/dR|\varphi'\rangle (d/dR \sin(k''R))dR \right|^2$$

The matrix elements occurring here contain two distinct parts:

$\langle \varphi | d/dR | \varphi' \rangle$

has to do with the electronic state couplings that are induced by radial movement of the nuclei; and both

$$\sin(kR) \; d/dR \sin(k''R)$$

and

$$\sin(kR_{max}) \exp(\kappa R_{max}) \exp(-\kappa R) \; d/dR \; \sin(k''R)$$

relate to couplings between the two nuclear-motion wavefunctions induced by these same radial motions. For a transition to occur, both the electronic and nuclear-motion states must undergo changes. The initially prepared state (the bound state on the upper electronic surface) has high electronic and low nuclear-motion energy, while the state to which transitions may occur (the scattering state on the lower electronic surface) has low electronic energy and higher nuclear-motion energy.

Of course, in the above example, the integrals over R can be carried out if the electronic matrix elements $\langle \varphi | d/dR | \varphi' \rangle$ can be handled. In practical chemical applications (for an introductory treatment see Energetic Principles of Chemical Reactions, J. Simons, Jones and Bartlett, Portola Valley, Calif. (1983)), the evaluation of these electronic matrix elements is a formidable task that often requires computation intensive techniques such as those discussed in Section 6.

Even when the electronic coupling elements are available (or are modelled or parameterized in some reasonable manner), the solution of the coupled-channel equations that govern the nuclear motion is a demanding task. For the purposes of this text, it suffices to note that:

(i) couplings between motion on two or more electronic states can and do occur;

(ii) these couplings are essential to treat whenever the electronic energy difference (i.e., the spacing between pairs of Born-Oppenheimer potential surfaces) is small (i.e., comparable to vibrational or rotational energy level spacings);

(iii) there exists a rigorous theoretical framework in terms of which one can evaluate the rates of so-called **radiationless transitions** between pairs of such electronic,

vibrational, rotational states. Expressions for such transitions involve (a) electronic matrix elements $\langle\varphi|d/dR|\varphi'\rangle$ that depend on how strongly the electronic states are modulated by movement (hence the d/dR) of the nuclei, and (b) nuclear-motion integrals connecting the initial and final nuclear-motion wavefunctions, which also contain d/dR because they describe the "recoil" of the nuclei induced by the electronic transition.

C. Chemical Relevance

As presented above, the most obvious situation of multichannel dynamics arises when electronically excited molecules undergo radiationless relaxation (e.g., internal conversion when the spin symmetry of the two states is the same or intersystem crossing when the two states differ in spin symmetry). These subjects are treated in some detail in the text Energetic Principles of Chemical Reactions, J. Simons, Jones and Bartlett, Portola Valley, Calif. (1983)) where radiationless transitions arising in photochemistry and polyatomic molecule reactivity are discussed.

Let us consider an example involving the chemical reactivity of electronically excited alkaline earth or $d^{10}s^2$ transition metal atoms with H_2 molecules. The particular case for $Cd^* + H_2 \rightarrow CdH + H$ has been studied experimentally and theoretically. In such systems, the potential energy surface connecting to ground-state Cd (^1S) + H_2 becomes highly repulsive as the collision partners approach (see the depiction provided in the Figure shown below). The three surfaces that correlate with the Cd (^1P) + H_2 species prepared by photo-excitation of Cd (^1S) behave quite differently as functions of the Cd-to-H_2 distance because in each the singly occupied 6p orbital assumes a different orientation relative to the H_2 molecule's bond axis. For (near) C_{2v} orientations, these states are labeled $^1B_2$, $^1B_1$, and $^1A_1$; they have the 6p orbital directed as shown in the second Figure, respectively. The corresponding triplet surfaces that derive from Cd (^3P) + H_2 behave, as functions of the Cd-to-H_2 distance (R) in similar manner, except they are shifted to lower energy because Cd (^3P) lies below Cd (^1P) by ca. 37 kcal/mol.

Collisions between Cd (^1P) and H_2 can occur on any of the three surfaces mentioned above. Flus on the $^1A_1$ surface is primarily reflected (at low collision energies characteristic of the thermal experiments) because this surface is quite repulsive at large R. Flux on the $^1B_1$ surface can proceed in to quite small R (ca. 2.4 Å) before repulsive forces on this surface reflect it. At geometries near R = 2.0Å and r_{HH} = 0.88 Å, the highly repulsive $^3A_1$ surface intersects this $^1B_1$ surface from below. At and near this intersection, a combination of spin-orbit coupling (which is large for Cd) and non-adiabatic coupling

may induce flux to evolve onto the $^3A_1$ surface, after which fragmentation to Cd (^3P) + H_2 could occur.

In contrast, flux on the $^1B_2$ surface propogates inward under attractive forces to R = 2.25 Å and r_{HH} = 0.79 Å where it may evolve onto the $^3A_1$ surface which intersects from below. At and near this intersection, a combination of spin-orbit coupling (which is large for Cd) and non-adiabatic coupling may induce flux to evolve onto the $^3A_1$ surface, after which fragmentation to Cd (^3P) + H_2 could occur. Flux that continues to propogate inward to smaller R values experiences even stronger attractive forces that lead, near R = 1.69 Å and r_{HH} = 1.54 Å, to an intersection with the $^1A_1$ surface that connects to Cd (^1S) + H_2. Here, non-adiabatic couplings may cause flux to evolve onto the $^1A_1$ surface which may then lead to formation of ground state Cd (^1S) + H_2 or Cd (^1S) + H + H, both of which are energetically possible. Processes in which electronically excited atoms produce ground-state atoms through such collisions and surface hopping are termed "electronic quenching".

The nature of the non-adiabatic couplings that arise in the two examples given above are quite different. In the former case, when the $^1B_1$ and $^3A_1$ surfaces are in close proximity to one another, the first-order coupling element:

$$<\Psi(^1B_1)| \quad _j |\Psi(^3A_1)>$$

is non-zero only for nuclear motions (i.e., $_j$) of $b_1 x a_1 = b_1$ symmetry. For the CdH_2 collision complex being considered in (or near) C_{2v} symmetry, such a motion corresponds to rotational motion of the nuclei about an axis lying parallel to the H-H bond axis. In contrast, to couple the $^3A_1$ and $^1B_2$ electronic states through an element of the form

$$<\Psi(^1B_2)| \quad _j |\Psi(^3A_1)> ,$$

the motion must be of $b_2 x a_1 = b_2$ symmetry. This movement corresponds to asymmetric vibrational motion of the two Cd-H interatomic coordinates.

The implications of these observations are clear. For example, in so-called half-collision experiments in which a van der Waals CdH_2 complex is probed, internal rotational motion would be expected to enhance $^1B_1 \rightarrow {}^3A_1$ quenching, whereas asymmetric vibrational motion should enhance the $^1B_2 \rightarrow {}^3A_1$ process.

Moreover, the production of ground-state Cd (^1S) +H_2 via $^1B_2 \rightarrow {}^1A_1$ surface hopping (near R = 1.69 Å and r_{HH} = 1.54 Å) should also be enhanced by asymmetric vibrational excitation. The $^1B_2$ and $^1A_1$ surfaces also provide, through their non-adiabatic couplings, a "gateway" to formation of the asymmetric bond cleavage products CdH ($^2\Sigma$) +

H. It can be shown that the curvature (i.e., second energy derivative) of a potential energy surface consists of two parts: (i) one part that in always positive, and (ii) a second that can be represented in terms of the non-adiabatic coupling elements between the two surfaces and the energy gap ΔE between the two surfaces. Applied to the two states at hand, this second contributor to the curvature of the $^1B_2$ surface is:

$$\frac{|\langle \Psi(^1B_2) | \quad_j | \Psi(^1A_1)\rangle|^2}{E(^1B_2) - E(^1A_1)} .$$

Clearly, when the $^1A_1$ state is higher in energy but strongly non-adiabatically coupled to the $^1B_2$ state, negative curvature along the asymmetric b_2 vibrational mode is expected for the $^1B_2$ state. When the $^1A_1$ state is lower in energy, negative curvature along the b_2 vibrational mode is expected for the $^1A_1$ state (because the above expression also expresses the curvature of the $^1A_1$ state).

Therefore, in the region of close-approach of these two states, state-to-state surface hopping can be facile. Moreover, one of the two states (the lower lying at each geometry) will likely possess negative curvature along the b_2 vibrational mode. It is this negative curvature that causes movement away from C_{2v} symmetry to occur spontaneously, thus leading to the CdH ($^2\Sigma$) + H reaction products.

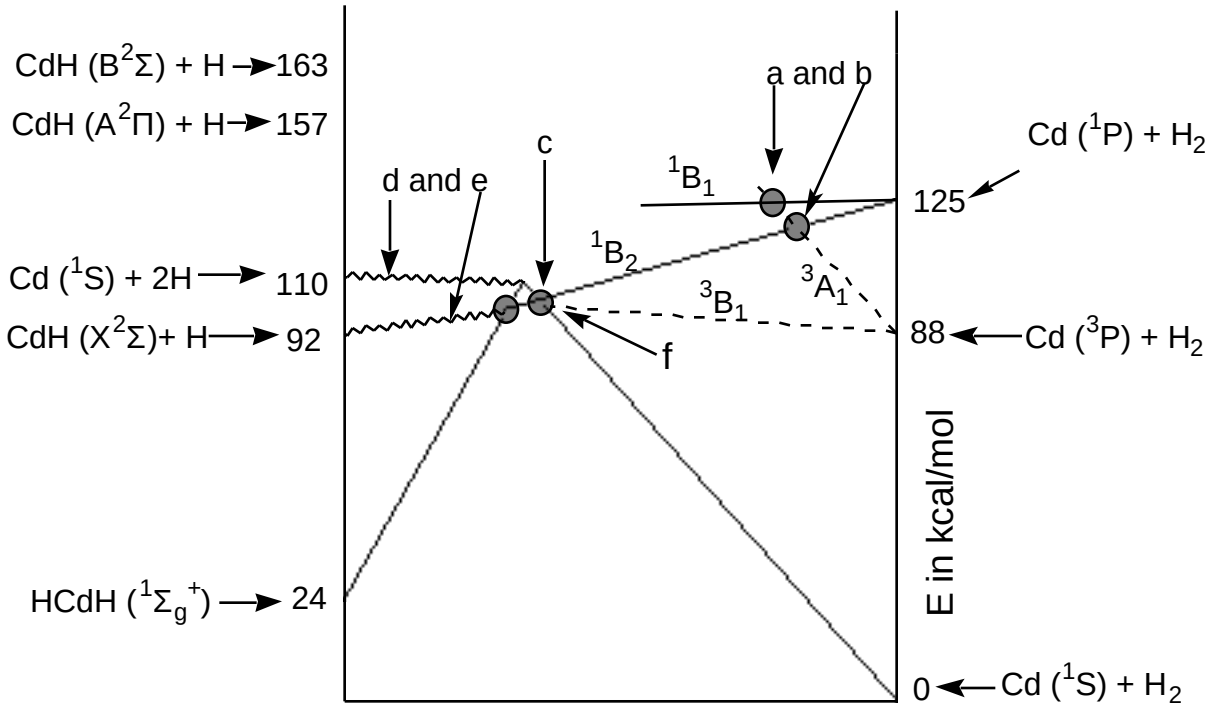

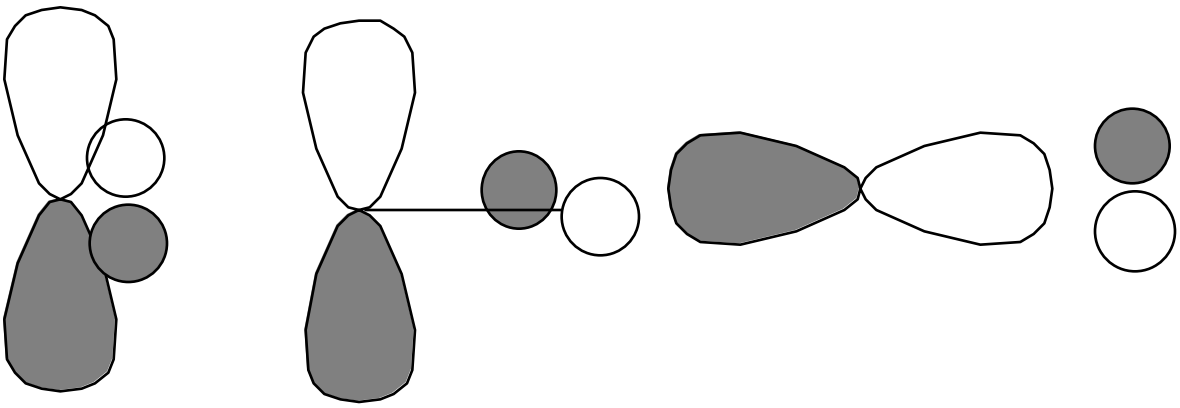

b_2 overlap of Cd 6p orbital and H_2 σ_g orbital

b_1 overlap of Cd 6p orbital and H_2 σ_g orbital

a_1 overlap of Cd 6p orbital and H_2 σ_g orbital

Coupled-state dynamics can also be used to describe situations in which vibrational rather than electronic-state transitions occur. For example, when van der Waals complexes such as HCl···Ar undergo so-called vibrational predissociation, one thinks in terms of movement of the Ar atom relative to the center of mass of the HCl molecule playing the role of the R coordinate above, and the vibrational state of HCl as playing the role of the quantized (electronic) state in the above example.

In such cases, a vibrationally excited HCl molecule (e.g., in v = 1) to which an Ar atom is attached via weak van der Waals attraction transfers its vibrational energy to the Ar atom, subsequently dropping to a lower (e.g., v = 0) vibrational level. Within the two-coupled-state model introduced above, the upper energy surface pertains to Ar in a bound vibrational level (having dissociation energy D_e) with HCl in an excited vibrational state (Δ being the v = 0 to v = 1 vibrational energy gap), and the lower surface describes an Ar atom that is free from the HCl molecule that is itself in its v = 0 vibrational state. In this case, the coordinate R is the Ar-to-HCl distance.

In analogy with the electronic-nuclear coupling example discussed earlier, the rate of transition from HCl (v=1) bound to Ar to HCl(v=0) plus a free Ar atom depends on the strength of coupling between the Ar···HCl relative motion coordinate (R) and the HCl internal vibrational coordinate. The $\langle\varphi|d/dR|\varphi'\rangle$ coupling elements in this case are integrals over the HCl vibrational coordinate x involving the v = 0 (φ) and v = 1 (φ') vibrational functions. The integrals over the R coordinate in the earlier expression for the rate of radiationless transitions now involve integration over the distance R between the Ar atom and the center of mass of the HCl molecule.

This completes our discussion of dynamical processes in which more than one Born-Oppenheimer state is involved. There are many situations in molecular spectroscopy and chemical dynamics where consideration of such coupled-state dynamics is essential. These cases are characterized by

(i) total energies E which may be partitioned in two or more ways among the internal degrees of freedom (e.g., electronic and nuclear motion or vibrational and ad-atom in the above examples),

(ii) Born-Oppenheimer potentials that differ in energy by a small amount (so that energy transfer from the other degree(s) of freedom is facile).

III. Classical Treatment of Nuclear Motion

For all but very elementary chemical reactions (e.g., D + HH → HD + H or F + HH → FH + H) or scattering processes (e.g., CO (v,J) + He → CO (v',J') + He), the

above fully quantal coupled channel equations simply can not be solved even when modern supercomputers are employed. Fortunately, the Schrödinger equation can be replaced by a simple classical mechanics treatment of nuclear motions under certain circumstances.

For motion of a particle of mass μ along a direction R, the primary condition under which a classical treatment of nuclear motion is valid

$$\frac{\lambda}{4\pi}\frac{1}{p}\left|\frac{dp}{dR}\right| << 1$$

relates to the fractional change in the local momentum defined as:

$$p = \sqrt{2\mu(E - E_j(R))}$$

along R within the 3N - 5 or 3N - 6 dimensional internal coordinate space of the molecule, as well as to the local de Broglie wavelength

$$\lambda = \frac{2\pi\hbar}{|p|} .$$

The inverse of the quantity $\frac{1}{p}\left|\frac{dp}{dR}\right|$ can be thought of as the length over which the momentum changes by 100%. The above condition then states that the local de Broglie wavelength must be short with respect to the distance over which the potential changes appreciably. Clearly, whenever one is dealing with heavy nuclei that are moving fast (so |p| is large), one should anticipate that the local de Broglie wavelength of those particles may be short enough to meet the above criteria for classical treatment.

It has been determined that for potentials characteristic of typical chemical bonding (whose depths and dynamic range of interatomic distances are well known), and for all but low-energy motions (e.g., zero-point vibrations) of light particles such as Hydrogen and Deuterium nuclei or electrons, the local de Broglie wavelengths are often short enough for the above condition to be met (because of the large masses μ of non-Hydrogenic species) except when their velocities approach zero (e.g., near classical turning points). It is therefore common to treat the nuclear-motion dynamics of molecules that do not contain H or D atoms in a purely classical manner, and to apply so-called semi-classical corrections

near classical turning points. The motions of H and D atomic centers usually require quantal treatment except when their kinetic energies are quite high.

A. Classical Trajectories

To apply classical mechanics to the treatment of nuclear-motion dynamics, one solves Newtonian equations

$$m_k \frac{d^2 X_k}{dt^2} = - \frac{dE_j}{dX_k}$$

where X_k denotes one of the 3N cartesian coordinates of the atomic centers in the molecule, m_k is the mass of the atom associated with this coordinate, and $\frac{dE_j}{dX_k}$ is the derivative of the potential, which is the electronic energy $E_j(R)$, along the k^{th} coordinate's direction. Starting with coordinates $\{X_k(0)\}$ and corresponding momenta $\{P_k(0)\}$ at some initial time t = 0, and given the ability to compute the force $- \frac{dE_j}{dX_k}$ at any location of the nuclei, the Newton equations can be solved (usually on a computer) using finite-difference methods:

$$X_k(t+\delta t) = X_k(t) + P_k(t)\, \delta t/m_k$$

$$P_k(t+\delta t) = P_k(t) - \frac{dE_j}{dX_k}(t)\ \delta t.$$

In so doing, one generates a sequence of coordinates $\{X_k(t_n)\}$ and momenta $\{P_k(t_n)\}$, one for each "time step" t_n. The histories of these coordinates and momenta as functions of time are called "**classical trajectories**". Following them from early times, characteristic of the molecule(s) at "reactant" geometries, through to late times, perhaps characteristic of "product" geometries, allows one to monitor and predict the fate of the time evolution of the nuclear dynamics. Even for large molecules with many atomic centers, propagation of such classical trajectories is feasible on modern computers <u>if</u> the forces $- \frac{dE_j}{dX_k}$ can be computed in a manner that does not consume inordinate amounts of computer time.

In Section 6, methods by which such force calculations are performed using first-principles quantum mechanical methods (i.e., so-called <u>ab initio</u> methods) are discussed. Suffice it to say that these calculations are often the rate limiting step in carrying out

classical trajectory simulations of molecular dynamics. The large effort involved in the ab initio determination of electronic energies and their gradients $-\frac{dE_j}{dX_k}$ motivate one to consider using empirical "force field" functions $V_j(R)$ in place of the ab initio electronic energy $E_j(R)$. Such model potentials $V_j(R)$, are usually constructed in terms of easy to compute and to differentiate functions of the interatomic distances and valence angles that appear in the molecule. The parameters that appear in the attractive and repulsive parts of these potentials are usually chosen so the potential is consistent with certain experimental data (e.g., bond dissociation energies, bond lengths, vibrational energies, torsion energy barriers).

For a large polyatomic molecule, the potential function V usually contains several distinct contributions:

$$V = V_{bond} + V_{bend} + V_{vanderWaals} + V_{torsion} + V_{electrostatic}.$$

Here V_{bond} gives the dependence of V on stretching displacements of the bonds (i.e., interatomic distances between pairs of bonded atoms) and is usually modeled as a harmonic or Morse function for each bond in the molecule:

$$V_{bond} = \sum_J 1/2\ k_J\ (R_J - R_{eq,J})^2$$

or

$$V_{bond} = \sum_J D_{e,J}\ (1-\exp(-a_J(R_J - R_{eq,J})))^2$$

where the index J labels the bonds and the k_J, a_J and $R_{eq,J}$ are the force constant and equilibrium bond length parameters for the J^{th} bond.

V_{bend} describes the bending potentials for each triplet of atoms (ABC) that are bonded in a A-B-C manner; it is usually modeled in terms of a harmonic potential for each such bend:

$$V_{bend} = \sum_J 1/2\ k^{\theta}_J\ (\theta_J - \theta_{eq,J})^2\ .$$

The $\theta_{eq,J}$ and k^{θ}_J are the equilibrium angles and force constants for the J^{th} angle.

$V_{vanderWaals}$ represents the van der Waals interactions between all pairs of atoms that are not bonded to one another. It is usually written as a sum over all pairs of such atoms (labeled J and K) of a Lennard-Jones 6,12 potential:

$$V_{vanderWaals} = \sum_{J<K} [a_{J,K} (R_{J,K})^{-12} - b_{J,K} (R_{J,K})^{-6}]$$

where $a_{J,K}$ and $b_{J,K}$ are parameters relating to the repulsive and dispersion attraction forces, respectively for the J^{th} and K^{th} atoms.

$V_{torsion}$ contributions describe the dependence of V on angles of rotation about single bonds. For example, rotation of a CH_3 group around the single bond connecting the carbon atom to another group may have an angle dependence of the form:

$$V_{torsion} = V_0 (1 - \cos(3\theta))$$

where θ is the torsion rotation angle, and V_0 is the magnitude of the interaction between the C-H bonds and the group on the atom bonded to carbon.

$V_{electrostatic}$ contains the interactions among polar bonds or other polar groups (including any charged groups). It is usually written as a sum over pairs of atomic centers (J and K) of Coulombic interactions between fractional charges $\{Q_J\}$ (chosen to represent the bond polarity) on these atoms:

$$V_{electrostatic} = \sum_{J<K} Q_J Q_K / R_{J,K}$$

Although the total potential V as written above contains many components, each is a relatively simple function of the Cartesian positions of the atomic centers. Therefore, it is relatively straightforward to evaluate V and its gradient along all 3N Cartesian directions in a computationally efficient manner. For this reason, the use of such empirical force fields in so-called **molecular mechanics** simulations of classical dynamics is widely used for treating large organic and biological molecules.

B. Initial Conditions

No single trajectory can be used to simulate chemical reaction or collisions that relate to realistic experiments. To generate classical trajectories that are characteristic of particular experiments, one must choose many initial conditions (coordinates and momenta)

the collection of which is representative of the experiment. For example, to use an **ensemble** of trajectories to simulate a molecular beam collision between H and Cl atoms at a collision energy E, one must follow many classical trajectories that have a range of "impact parameters" (b) from zero up to some maximum value b_{max} beyond which the H ····Cl interaction potential vanishes. The figure shown below describes the impact parameter as the distance of closest approach that a trajectory would have if no attractive or repulsive forces were operative.

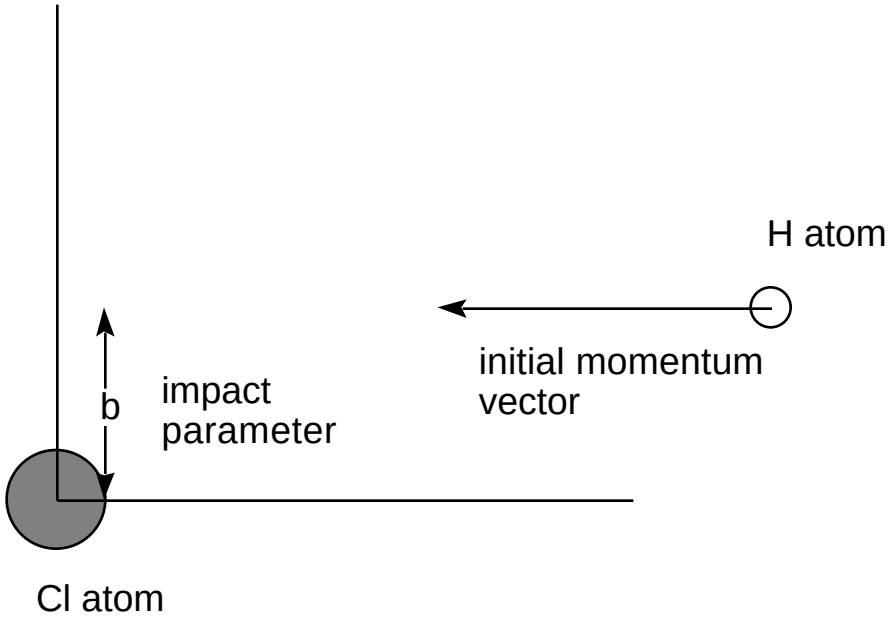

Moreover, if the energy resolution of the experiment makes it impossible to fix the collision energy closer than an amount δE, one must run collections of trajectories for values of E lying within this range.

If, in contrast, one wishes to simulate thermal reaction rates, one needs to follow trajectories with various E values and various impact parameters b from initiation at t = 0 to their conclusion (at which time the chemical outcome is interrogated). Each of these trajectories must have their outcome weighted by an amount proportional to a Boltzmann factor exp(-E/RT), where R is the ideal gas constant and T is the temperature because this factor specifies the probability that a collision occurs with kinetic energy E.

As the complexity of the molecule under study increases, the number of parameters needed to specify the initial conditions also grows. For example, classical trajectories that relate to $F + H_2 \rightarrow HF + H$ need to be specified by providing (i) an impact parameter for the F to the center of mass of H_2, (ii) the relative translational energy of the F and H_2, (iii)

the radial momentum and coordinate of the H_2 molecule's bond length, and (iv) the angular momentum of the H_2 molecule as well as the angle of the H-H bond axis relative to the line connecting the F atom to the center of mass of the H_2 molecule. Many such sets of initial conditions must be chosen and the resultant classical trajectories followed to generate an ensemble of trajectories pertinent to an experimental situation.

It should be clear that even the classical mechanical simulation of chemical experiments involves considerable effort because no single trajectory can represent the experimental situation. Many trajectories, each with different initial conditions selected so they represent, as an ensemble, the experimental conditions, must be followed and the outcome of all such trajectories must be averaged over the probability of realizing each specific initial condition.

C. Analyzing Final Conditions

Even after classical trajectories have been followed from t = 0 until the outcomes of the collisions are clear, one needs to properly relate the fate of each trajectory to the experimental situation. For the $F + H_2 \rightarrow HF + H$ example used above, one needs to examine each trajectory to determine, for example, (i) whether HF + H products are formed or non-reactive collision to produce $F + H_2$ has occurred, (ii) the amount of rotational energy and angular momentum that is contained in the HF product molecule, (iii) the amount of relative translational energy that remains in the H + FH products, and (iv) the amount of vibrational energy that ends up in the HF product molecule.

Because classical rather than quantum mechanical equations are used to follow the time evolution of the molecular system, there is no guarantee that the amount of energy or angular momentum found in degrees of freedom for which these quantities should be quantized will be so. For example, $F + H_2 \rightarrow HF + H$ trajectories may produce HF molecules with internal vibrational energy that is not a half integral multiple of the fundamental vibrational frequency ω of the HF bond. Also, the rotational angular momentum of the HF molecule may not fit the formula $J(J+1)\, h^2/(8\pi^2 I)$, where I is HF's moment of inertia.

To connect such purely classical mechanical results more closely to the world of quantized energy levels, a method know as "binning" is often used. In this technique, one assigns the outcome of a classical trajectory to the particular quantum state (e.g., to a vibrational state v or a rotational state J of the HF molecule in the above example) whose quantum energy is closest to the classically determined energy. For the HF example at

hand, the classical vibrational energy $E_{cl.vib}$ is simply used to define, as the closest integer, a vibrational quantum number v according to:

$$v = \frac{(E_{cl,vib})}{\hbar\omega} - 1/2.$$

Likewise, a rotational quantum number J can be assigned as the closest integer to that determined by using the classical rotational energy $E_{cl,rot}$ in the formula:

$$J = 1/2 \{ (1+32\pi^2 I E_{cl,rot}/h^2)^{1/2} - 1\}$$

which is the solution of the quadratic equation $J(J+1)\, h^2/8\pi^2 I = E_{cl,rot}$. By following many trajectories and assigning vibrational and rotational quantum numbers to the product molecules formed in each trajectory, one can generate histograms giving the frequency with which each product molecule quantum state is observed for the ensemble of trajectories used to simulate the experiment of interest. In this way, one can approximately extract product-channel quantum state distributions from classical trajectory simulations.

IV. Wavepackets

In an attempt to combine the attributes and stregths of classical trajectories, which allow us to "watch" the motions that molecules undergo, and quantum mechanical wavefunctions, which are needed if interference phenomena are to be treated, a hybrid approach is sometimes used. A popular and rather successful such point of view is provided by so called **coherent state wavepackets**.

A quantum mechanical wavefunction $\psi(\mathbf{x}|\,\mathbf{X},\,\mathbf{P})$ that is a function of all pertinent degrees of freedom (denoted collectively by $\mathbf{x}$) and that depends on two sets of parameters (denoted $\mathbf{X}$ and $\mathbf{P}$, respectively) is defined as follows:

$$\psi(\mathbf{x}|\,\mathbf{X},\,\mathbf{P}) = \prod_{k=1}^{N} (2\pi<\Delta x_k>^2)^{-1/2} \exp\{iP_k x_k/\hbar - (x_k - X_k)^2/(4<\Delta x_k>^2)\}\,.$$

Here, $<\Delta x_k>^2$ is the uncertainty

$$<\Delta x_k>^2 = \int |\psi|^2 (x_k - X_k)^2 d\mathbf{x}$$

along the k^{th} degree of freedom for this wavefunction, defined as the mean squared displacement away from the average coordinate

$$\int |\psi|^2 x_k d\mathbf{x} = X_k.$$

So, the parameter X_k specifies the average value of the coordiate x_k. In like fashion, it can be shown that the parameter P_k is equal to the average value of the momentum along the k^{th} coordinate:

$$\int \psi^*(-i\hbar\partial/\partial x_k \psi) d\mathbf{x} = P_k.$$

The uncertainty in the momentum along each coordinate:

$$<\Delta p_k>^2 = \int \psi^*(-i\hbar\partial/\partial x_k - P_k)^2 \psi d\mathbf{x}$$

is given, for functions of the coherent state form, in terms of the coordinate uncertainty as

$$<\Delta p_k>^2 <\Delta x_k>^2 = \hbar^2/4.$$

Of course, the general Heisenberg uncertainty condition

$$<\Delta p_k>^2 <\Delta x_k>^2 \geq \hbar^2/4$$

limits the coordinate and momentum uncertainty products for arbitrary wavefunctions. The coherent state wave packet functions are those for which this uncertainty product is minimum. In this sense, coherent state wave packets are seen to be as close to classical as possible since in classical mechanics there are no limits placed on the resolution with which one can observe coordinates and momenta.

These wavepacket functions are employed as follows in the most straightforward treatements of combined quantal/classical mechanics:

1. Classical trajectories are used, as discribed in greater detail above, to generate a series of coordinates $X_k(t_n)$ and momenta $P_k(t_n)$ at a sequence of times denoted $\{t_n\}$.

2. These classical coordinates and momenta are used to define a wavepacket function as written above, whose X_k and P_k parameters are taken to be the coordinates and momenta of the classical trajectory. In effect, the wavepacket moves around "riding" the classical trajectory's coordiates and momenta as time evolves.

3. At any time t_n, the quantum mechanical properties of the system are computed by forming the expectation values of the corresponding quantum operators for a wavepacket wavefunction of the form given above with X_k and P_k given by the classical coordinates and momenta at that time t_n.

Such wavepackets are, of course, simple approximations to the true quantum mechanical functions of the system because they do not obey the Schrödinger equation appropriate to the system. The should be expected to provide accurate representations to the true wavefunctions for systems that are more classical in nature (i.e., when the local de Broglie wave lengths are short compared to the range over which the potentials vary appreciably). For species containing light particles (e.g., electrons or H atoms) or for low kinetic energies, the local de Broglie wave lengths will not satisfy such criteria, and these approaches can be expected to be less reliable. For further information about the use of coherent state wavepackets in molecular dynamics and molecular spectroscopy, see E. J. Heller, Acc. Chem. Res. 14, 368 (1981).

This completes our treatment of the subjects of molecular dynamics and molecular collisions. Neither its depth not its level was at the research level; rather, we intended to provide the reader with an introduction to many of the theoretical concepts and methods that arise when applying either the quantum Schrödinger equation or classical Newtonian mechanics to chemical reaction dynamics. Essentially none of the experimental aspects of this subject (e.g., molecular beam methods for preparing "cold" molecules, laser pump-probe methods for preparing reagents in specified quantum states and observing products in such states) have been discussed. An excellent introduction to both the experimental and theoretical foundations of modern chemical and collision dynamics is provided by the text Molecular Reaction Dynamics and Chemical Reactivity by R. D. Levine and R. B. Bernstein, Oxford Univ. Press (1987).